Maura Harumi Sugai Guérios

UNDERSTANDING THE GROWTH OF HYPHAE OF FILAMENTOUS FUNGI ON THE SURFACES OF SOLID MEDIA THROUGH COMPUTATIONAL MODELS AND CONFOCAL MICROSCOPY

Thesis for the degree of Doctor in Chemical Engineer presented to the Postgraduate Program in Chemical Engineering at the Federal University of Santa Catarina
Supervisor: Prof. Dr. Agenor Furigo Jr
Co-supervisor: Prof. Dr. David Alexander Mitchell

Florianópolis, Brazil
2016

Ficha de identificação da obra elaborada pelo autor através do Programa de Geração Automática da Biblioteca Universitária da UFSC.

Maura Harumi Sugai Guérios

UNDERSTANDING THE GROWTH OF HYPHAE OF FILAMENTOUS FUNGI ON THE SURFACES OF SOLID MEDIA THROUGH COMPUTATIONAL MODELS AND CONFOCAL MICROSCOPY

This thesis was considered adequate for the title of Doctor and was approved in its final form by the Postgraduate Program in Chemical Engineering at the Federal University of Santa Catarina.

Florianópolis, August 26th of 2016.

_____
Prof. Cíntia Soares, Dr.
Program Coordinator

Examiners:

_____
Prof. Agenor Furigo Jr, Dr.
Supervisor, Federal University
of Santa Catarina

_____
Prof. David Alexander
Mitchell, Dr.
Co-supervisor, Federal
University of Paraná

_____
Prof. Suraia Said, Dr.
University of São Paulo
(retired)

_____
Prof. Sonia Couri, Dr.
State University of Rio de
Janeiro

_____
Prof. Glaucia Maria Falcão de
Aragão, Dr.
Federal University of Santa
Catarina

_____
Prof. Leonel Teixeira Pinto, Dr.
Federal University of Santa
Catarina

_____
Prof. Fernanda Vieira Berti, Dr.
Federal University of Santa
Catarina

This thesis is dedicated to my mother,

for her strength and perseverance.

ACKNOWLEDGEMENTS

ABSTRACT

This thesis was developed in the context of citrus waste biorefineries. Within such biorefineries, it has been proposed that the pectinases to be used for hydrolysis of pectin be produced by solid-state fermentation, using the filamentous fungus *Aspergillus niger*. During solid-state fermentation, aerial hyphae occupy the interparticle spaces, binding adjacent particles together, while surface, biofilm and penetrative hyphae secrete a pool of hydrolytic enzymes that decrease the firmness of the solid particle. The resulting morphology of the mycelium, namely the spatial distributions of these hyphae, is related to mass and heat transfer within the fermentation bed and, apparently, to the production of hydrolytic enzymes. However, more studies are necessary to understand the factors that determine the morphology of the mycelium. A useful tool for guiding such studies is a 3D phenomenological model that describes the morphology of the mycelium formed by the filamentous fungus and relates this morphology with intra- and extracellular phenomena, such as, for example, intracellular flow of substrate through the fungal network. The aim of the thesis was to provide theoretical and experimental foundations for the development of such a model. This objective was achieved in two main steps: development of a computational model for penetrative and aerial hyphae and time-lapse visualization of mycelial growth. The computational model was developed to explore the factors affecting the distribution of aerial hyphae with height above the surface and of penetrative hyphae with depth below the surface, with rules of branching and inactivation that were different for each type of hypha. These rules were adjusted to data from the literature for the growth of *Rhizopus oligosporus* and *Aspergillus oryzae* on solid media. The adjusted rules lead to the hypothesis that penetrative hypha extend mainly downwards, with their maximum length being determined by the firmness of the solid particle and the pressure drop inside the hypha. Meanwhile, aerial hyphae grow in any direction, as though their tips move in a random walk, and there is no limitation of maximum height. Aerial hyphae seem to stop extending due to steric impediments, resulting in a maximum local biomass concentration. In order to study the growth of penetrative hyphae and expression of hydrolytic enzymes, fluorescent strains of *Aspergillus niger* were constructed. The mode of growth of penetrative hyphae was characterized with various different inoculum density and the types of carbon sources in the medium. These results indicated that penetrative hyphae differentiate around the same time reproductive hyphae begin to grow: extension of leading hyphae is interrupted and intense branching

starts. In addition, expression of exopolygalacturonase B in penetrative hyphae also changes with differentiation: from apical and limited to few hyphae to subapical and present in the majority of hyphae.

RESUMO EXPANDIDO

Esta tese foi desenvolvida no contexto de biorrefinarias de polpa cítrica. Para estas biorrefinarias, propõe-se que as pectinases a serem usadas na hidrólise da pectina sejam produzidas por fermentação em estado sólido, utilizando o fungo filamentoso *Aspergillus niger*. Na fermentação em estado sólido, hifas aéreas ocupam o espaço entre as partículas, entrelaçando partículas adjacentes, enquanto que hifas superficiais, de biofilme e penetrantes secretam enzimas hidrolíticas que modificam a consistência das partículas. A morfologia do micélio formado, ou seja, a distribuição espacial das hifas, está relacionada com a eficiência de transferência de massa e de calor através do leito de fermentação e, aparentemente, com a produção de enzimas hidrolíticas. No entanto, faltam estudos sobre os fatores que determinam a morfologia do micélio. Uma ferramenta útil para guiar estes estudos é um modelo fenomenológico 3D que descreve a morfologia adotada pelo fungo filamentoso e relaciona esta morfologia a fenômenos intra e extracelulares, como, por exemplo, fluxo intracelular de substrato através do micélio. O objetivo desta tese foi obter fundamentação teórica e experimental para o desenvolvimento deste modelo. Para este fim, o trabalho foi conduzido em duas partes: desenvolvimento de um modelo matemático para hifas penetrantes e aéreas e visualização do crescimento do micélio em *time-lapse*. O modelo matemático foi desenvolvido para investigar os fatores que afetam a distribuição de hifas aéreas em função da altura acima da superfície do meio e de hifas penetrantes em função da profundidade abaixo da superfície. Neste modelo, o espaço acima e abaixo da superfície é dividido em andares e a extensão das hifas é descrita pela adição de segmentos de hifa, de tamanho fixo, em cada andar. O modelo inicia-se com pontas de hifa na superfície, a partir das quais segmentos de hifa podem estender e cada segmento formado pode continuar estendendo, ramificar ou inativar, de acordo com regras de probabilidade, que são diferentes para cada tipo de hifa. Estas regras, e os parâmetros correspondentes, foram ajustadas aos dados de distribuição de biomassa de *Rhizopus oligosporus* e *Aspergillus oryzae*, em diferentes meios sólidos. Com base nestas regras, foram propostas hipóteses de que as hifas penetrantes estendem principalmente para baixo e o comprimento máximo delas é determinado pela consistência da partícula sólida e pela perda de carga no interior da hifa. Enquanto isso, as hifas aéreas crescem em qualquer direção, como se suas pontas se movimentassem seguindo o passeio aleatório, e não há limitação de altura máxima para o crescimento. As hifas aéreas param de estender devido ao impedimento estérico,

resultante de uma máxima concentração local de biomassa. A fim de investigar o crescimento de hifas penetrantes e a expressão de pectinases ao longo do micélio, duas cepas fluorescentes de *Aspergillus niger* foram desenvolvidas: as duas cepas expressam o gene *eGFP* (proteína fluorescente verde melhorada) sob um promotor constitutivo e um gene de fusão de uma poligalacturonase e mCherry, que é uma proteína fluorescente vermelha, sob o promotor nativo da poligalacturonase. A poligalacturonase escolhida para a cepa pgaRed foi a endopoligalacturonase B, codificada no gene *pgaB*, cujo promotor é constitutivo, ao passo que a poligalacturonase escolhida para a cepa pgxRed foi a exopoligalacturonase B, codificada no gene *pgxB*, cujo promotor é induzido por galacturonato presente no meio. Através destas cepas, o modo de crescimento das hifas penetrantes foi caracterizado: se a densidade de esporos é baixa, hifas penetrantes podem ser formadas diretamente do tubo germinativo, caso contrário, as hifas penetrantes são formadas apenas depois que as hifas superficiais atingirem uma densidade mínima; as ramificações são subapicais e bem distribuídas ao longo da hifa parental, exceto quando a densidade de hifas dentro do sólido é alta e, neste caso, as ramificações ocorrem nas regiões de menor densidade de hifas, que geralmente são próximas às pontas das hifas parentais. As hifas penetrantes diferenciam-se no mesmo momento em que surgem as hifas reprodutivas e, a partir deste momento, as hifas parentais param de estender e ocorre intensa formação de ramificações. Além disso, a expressão de *pgxB* nas hifas penetrantes muda de apical, e limitada a poucas hifas, para subapical e presente na maioria das hifas. O tipo de fonte de carbono afeta o tempo de germinação, a profundidade máxima atingida pelas hifas penetrantes e a frequência de ramificação por hifa. Por fim, o conhecimento adquirido com as cepas fluorescentes foi utilizado para delinear como o modelo fenomenológico 3D deve ser desenvolvido no futuro.

Palavras-chave: Fermentação em Estado Sólido. Modelagem. Fungos Filamentosos. Morfologia. Pectinase. Microscopia Confocal.

LIST OF FIGURES

LIST OF TABLES

LIST OF ABREVIATIONS

AmyR – transcription activator for some genes encoding amylolytic enzymes
CAT – Conidial Anastomosis Tubes
CreA – transcription repressor for some genes involved in carbon catabolism
eGFP – Enhanced Green Fluorescent Protein
Eq. – Equation
FRAP – Fluorescence Recovery After Bleaching
GaaR – transcription activator for some genes involved in polygalacturonate hydrolysis
HGU – Hyphal Growth Unit
mRNA – messenger RNA
ORF – Open Reading Frame
PCR – Polymerase Chain Reaction
PDA – Potato Dextrose Agar
PET – Polyethylene Terephthalate
pgaA – endopolygalacturonase B
pgaB – endopolygalacturonase B
pgaD – endopolygalacturonase B
pgxB – exopolygalacturonase B
SC – Synthetic Complete Media
SCD – Synthetic Complete Media supplemented with glucose
SCGal – Synthetic Complete Media supplemented with galacturonate
SCPga – Synthetic Complete Media supplemented with polygalacturonate
SCSta – Synthetic Complete Media supplemented with starch
SSF – Solid-State Fermentation
XlnR – transcription activator for some genes encoding xylanolytic enzymes

LIST OF SYMBOLS

A	Cross-sectional area of the hypha (μm^2)
A_L	Area of contact of the plasma membrane with the extracellular medium (μm^2)
Area	Area of study (mm²)
c_1	Proportionality constant (L^3 s^{-1} g-nutrient^{-1} g-biomass^{-1})
c_2	Proportionality constant (L g-transporter g-biomass^{-1})
c_3	Proportionality constant (g-nutrient g-transporter-substrate-complex^{-1} s^{-1})
$\left. C_{o_2} \right|_j$	O_2 concentration around tank j (g-O_2 L^{-1})
$C_{o_2}^f$	O_2 concentration in the biofilm (g-O_2 L^{-1})
d	Current depth of the hyphal tip (μm)
D_E	Effective diffusivity of the enzyme in the solid particle (μm^2 s^{-1})
d_{lim}	Limiting depth for growth of short penetrative hyphae (μm)
d_n	Number of the horizontal plane at which the new segment is added in subapical branches, expressed in "number of layers"
D_S	Diffusivity of maltose inside the hypha (μm^2 s^{-1})
$D_{o_2}^f$	Effective diffusivity of O_2 in the biofilm layer (μm^2 s^{-1})
D_S^e	Effective diffusivity of the soluble nutrient or hydrolysis product in the solid particle (μm^2 s^{-1})
E	Enzyme concentration (g-enzyme L^{-1})
E^2	Average of the squares of the absolute errors (g^2 L^{-2})
h	Height above the surface (mm)
$H(x)$	Heaviside function
h_{layer}	Height of each layer (μm)
$h_{\text{lim,RH}}$	Limiting height for growth of reproductive hyphae (mm)
I	Inoculation rate (spores mm⁻²)
j	Number of the tank
$\left. J_E \right|_{z=0}$	Flux of enzyme across the surface of the particle (g-enzyme μm^{-2} s^{-1})
k	Exponent of Eq. (3.1)
k_c	Maximum rate of vesicle consumption (g-vesicles s^{-1})
K_C	Saturation constant for vesicle consumption (g-vesicles L^{-1})

k_{cat}	Catalytic constant of the enzyme (g-polymeric-nutrient g-enzyme^{-1} s^{-1})
K_m	Saturation constant for the hydrolysis of the polymeric carbon and energy source (g-polymeric-nutrient L^{-1})
k_{max}	Maximum specific transport rate of soluble nutrient or hydrolysis product across the plasma membrane (g-nutrient g-transporter^{-1} s^{-1})
K_{O_2}	Saturation constant for O$_2$ (g-O$_2$ L^{-1})
k_p	Maximum rate of vesicle production (g-vesicles L^{-1} s^{-1})
K_P	Saturation constant for vesicle production (g-nutrient L^{-1})
K_s	Saturation constant for glucose in growth rate expression (g-nutrient L^{-1})
K_t	Saturation constant for the absorption of soluble nutrient or hydrolysis product across the membrane (g-nutrient L^{-1})
L	Length of the tip-tank (μm)
m	Maintenance coefficient (g-nutrient g-biomass^{-1} s^{-1})
m_e	Exponent of Eq. (4.4)
n	Tank number of the tip-tank
n_e	Exponent of Eq. (4.5)
N_0	Number of hyphal tips located immediately under the solid surface at 0 h (tips)
N_h	Number of hyphal tips added per hour immediately under the solid surface (tips h^{-1})
n_L	Length of the hypha that will receive a subapical branch, expressed in "number of layers"
n_p	Number of experimental data points
n_R	Random number
N_{rep}	Percentage of germinated spores that form two reproductive hyphae
P_B	Probability of branching for long penetrative hyphae
P_{base}	Turgor pressure at the base of a penetrative hypha (bar)
P_E	Probability of penetrative hyphae extending,
$P_{E,max}$	Maximum probability of penetrative hyphae extending,
P_G	Probability of germination for each spore
P_I	Probability of inactivation of tips of vegetative aerial hyphae
$P_{I,RH}$	Probability of inactivation of tips of reproductive aerial hyphae
P_{min}	Limiting turgor pressure at the tip for penetration (bar)

P_{tip}	Turgor pressure at the tip of a penetrative hypha (bar)
r	Radial position in the biofilm (µm)
r_a	Rate of absorption across the plasma membrane (g-nutrient s^{-1})
r_E	Rate of secretion of enzyme (g-enzyme µm^{-2} s^{-1})
r_{EP}	Rate of production of extracellular products (g-extracellular-products s^{-1})
r_{IP}	Rate of production of intracellular products (g-intracellular-products s^{-1})
r_{LI}	Rate of production of lipids (g-lipids s^{-1})
r_N	Rate of consumption of alanine (g-alanine s^{-1})
r_{O_2}	Rate of consumption of O_2 (g-O_2 s^{-1})
r_S	Rate of consumption of glucose (g-glucose s^{-1})
r_X	Rate of biomass growth (g-biomass L^{-1} s^{-1} for Eq. (2.12); g-biomass s^{-1} for Eq. (2.15))
S^f	Concentration of soluble nutrient or hydrolysis product in the biofilm (g L^{-1})
S_e	Concentration of extracellular soluble nutrient or hydrolysis product (g L^{-1})
S_i	Concentration of intracellular soluble nutrient or hydrolysis product (g L^{-1})
$S_i\big|_j$	Concentration of maltose in tank j (g-maltose L^{-1})
S_p	Concentration of polymeric nutrient (g-polymeric-nutrient L^{-1})
t	Cultivation time (s)
T	Transporter concentration per area of the plasma membrane (g-transporter µm^{-2})
t_D	Time at which differentiation of aerial hyphae occurs
t_E	Time when the secretion of enzyme ceases (s)
v	Velocity of cytoplasmic flow (µm s^{-1})
X	Concentration of biomass (g-biomass L^{-1})
$X_{exp,i}$	Experimental value for layer i (g-biomass L^{-1})
X_{LP}	Concentration of long penetrative hyphae (g-biomass L^{-1})
X_{max}	Maximum biomass concentration for each layer (g-biomass L^{-1})
$X_{pred,i}$	Average value predicted by the layer model for layer i (g-biomass L^{-1})

X_{R0}	Area under the entire half-normal distribution curve for reproductive aerial hyphae (g-biomass mm L^{-1})
X_{V0}	Area under the entire half-normal distribution curve for vegetative aerial hyphae (g-biomass mm L^{-1})
Y_E	Yield of glucose from starch (g-glucose g-polymeric-nutrient^{-1})
Y_L	Extension of hyphal length per mass of vesicle consumed (μm g-vesicle^{-1})
Y_{X/O_2}	Yield of biomass for O$_2$ (g-biomass g-O$_2$ $^{-1}$)
Y_ϕ	Yield coefficient for production of vesicles from maltose (g-vesicles g-nutrient^{-1})
z	Depth within the solid particle (μm)
$\Delta P/L$	Pressure gradient inside the hypha (bar μm^{-1})
Δt_{RH}	Duration of each iteration for the phase during which reproductive aerial hyphae grow
Δt_S	Duration of each iteration for the phase during which vegetative penetrative hyphae grow
Δt_{VH}	Duration of each iteration for the phase during which vegetative aerial hyphae grow
Δz	Length of a "normal" tank (μm)
$\phi\big|_j$	Concentration of vesicles in tank j (g-vesicles L^{-1})
η	Membrane coordinate (μm)
$\mu_{\max}$	Maximum specific growth rate constant (s^{-1})
θ	Concentration of the transporter-substrate complex (g-transporter-substrate-complex L^{-1})
ρ_X	Biomass dry weight per volume (g-biomass L^{-1})
σ_R	Standard deviation for the concentration of reproductive aerial hyphae in the half-normal distribution curve (mm)
σ_V	Standard deviation for the concentration of vegetative aerial hyphae in the half-normal distribution curve (mm)
ψ	Velocity of active transport of vesicles (μm s^{-1})

CONTENTS

1 INTRODUCTION

This project is part of the bilateral project CNPq/AKA-Finlândia (process number 490236/2012-0), which aims to develop and improve processes involved in a biorefinery of citrus waste. In this biorefinary, the pectin fraction of the citrus waste would be hydrolysed enzymatically, yielding mostly galacturonate, which, in turn, could be converted to ethanol, ascorbic acid, mucic acid or galactonic acid (BIZ, 2015). The pectinases used in this hydrolysis step would be produced by filamentous fungi through a process called solid-state fermentation (SSF), which is defined as the growth of microorganisms on moist particles with a continuous gas phase around the particles. The present work focuses on understanding the growth of filamentous fungi and pectinase expression in SSF.

Aspergillus niger is one of the fungi indicated for pectinase production because it secretes all the enzymes required for the complete hydrolysis of pectin and it has already been used in pilot scale production of pectinolytic enzymes (NIU et al., 2015; PITOL et al., 2016). For this reason, the present work focuses on growth of *Aspergillus niger*. Since there were not enough data on growth of *Aspergillus niger* initially, literature data for the growth of *Rhizopus oligosporus*, commonly used in the production of oriental food products through SSF, has also been used in this work. Therefore, some specific characteristics of both fungi are detailed in this chapter.

1.1 GROWTH OF FILAMENTOUS FUNGI ON SOLID MEDIA

Filamentous fungi such as *Aspergillus niger* and *Rhizopus oligosporus* colonize solid particles by forming tubular structures named hyphae, with radii between 1 and 10 μm (TINDEMANS; KERN; MULDER, 2006). When hyphae grow, they extend their length by expanding the membranes and cell walls of their tips, while their radius remains almost constant. They may also form new tips through branching. Branches may be formed at the tip, classified as apical branches, or elsewhere in the hypha, classified as subapical or lateral branches. As hyphae continue to extend at their tips and branch, a network of connected hyphae is formed, which is called a mycelium. Interchange of nutrients and organelles may occur throughout the mycelium.

Growth of filamentous fungi on solid particles is the basis of the industrial process called solid-state fermentation. The oldest applications of SSF are in the production of oriental food products, such as tempeh,

which consists of soybeans colonized by *Rhizopus oligosporus*, and soy sauce, which is produced using a mixture of soybeans and wheat grains colonized by *Aspergillus oryzae*. Recently, SSF has been used industrially for the production of enzymes, biopesticides, pigments and organic acids, among other products (THOMAS et al., 2013).

The inoculum used in SSF is usually a spore suspension. The spore germinates by, first, absorbing water and swelling, and, then, by forming an unbranched hypha. Until this hypha forms its first branch, it is named germ tube. Eventually, four types of hyphae are formed, classified based on where they grow: surface hyphae, biofilm hyphae, penetrative hyphae and aerial hyphae (Figure 1.1).

Figure 1.1 Schematic representation of the four types of hyphae formed when filamentous fungi grow on solid surfaces.
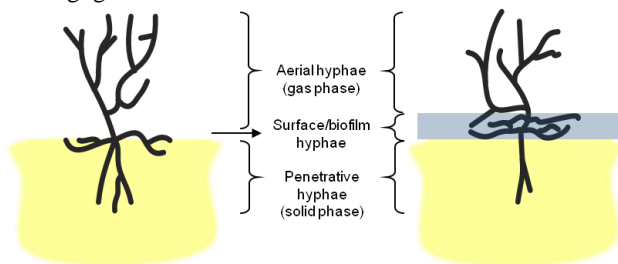
In order for hyphae to be able to penetrate solid media, they need turgor pressure at their tips. Turgor pressure is the difference between the internal and external osmotic pressures. Hyphae control their turgor pressure by maintaining a higher concentration of osmolytes in the cytosol than in the extracellular space, through synthesis or absorption of osmolytes (LEW, 2011). Chapter 2 presents a more detailed explanation about how hyphae grow.

Towards the end of its development, the mycelium differentiates, forming reproductive aerial hyphae. The role of these hyphae is to form spores above the biomass layer, to be dispersed for the dispersal of the species. The reproductive hypha of *Aspergillus niger* is also called a conidiophore and its spore is called a conidium. Conidiophores may be formed from penetrative hyphae or from surface hyphae, in which a hyphal segment differentiates into a "foot cell", which serves as the base of the conidiophore (Figure 1.2). From the foot cell, a thick and unbranched hypha, called a stalk, extends. After this stalk reaches a predetermined height, its tip enlarges, resulting in a structure that is called

a vesicle. This vesicle undergoes a series of cellular divisions, resulting in the formation of chains of conidia.

Figure 1.2 Schematic representation of the formation of a reproductive hypha of *Aspergillus niger*, the conidiophore (adapted from Boyce and Andrianopoulos, 2006).
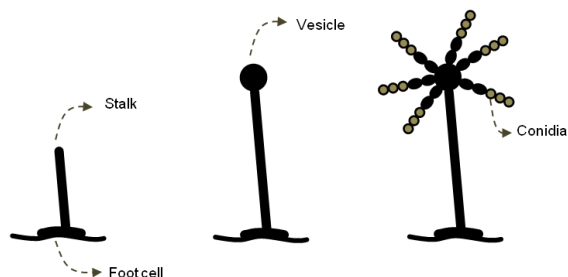
The formation of spores by *Rhizopus oligosporus* involves different structures (Figure 1.3). First of all, species of *Rhizopus* typically produce an aerial hypha called a stolon, which extends away from the colony in order to start a new colony (SHURTLEFF; AOYAGI, 1979). When the stolon touches the solid surface, it forms a node from which penetrative hyphae and reproductive hyphae are formed. In this case, penetrative hyphae are also called rhizoids and reproductive hyphae, sporangiophores. These sporangiophores extend upwards and eventually form a structure at their tips called a sporangium, in which the spores, named sporangiospores, are formed.

Another difference between *Aspergillus niger* and *Rhizopus oligosporus* is that the first is a septate fungus while the latter is aseptate. The septum is an invagination of the cell wall and cellular membrane of the hypha, forming internal walls that are perpendicular to the lateral membrane. In *Aspergillus*, septa divide the hypha into segments of regular lengths, but the presence of a single pore in the middle of these septa allows the exchange of organelles and cytosol (BARRY; WILLIAMS, 2011). The hypha is able to close this pore when needed, for example, in order to avoid excessive loss of intracellular material when a hyphal segment is damaged and, possibly, to regulate the cytoplasmic flow (MARKHAM, 1995; LEW, 2011).

Depending on the fungus and substrate particles used in SSF, growth of hyphae may lead to changes in the properties of the fermentation bed. For example, hyphal growth may result in shrinking and aggregation of particles, which, in turn, leads to shrinking of the

whole fermentation bed. When this occurs in forcefully-aerated beds, air flows preferentially around the fermentation bed, instead of through it, which reduces the efficiency of mass and heat transfer. In order to prevent the formation of aggregates in the bed, Schutsyer et al. (2003) suggested preventing the formation or aerial hyphae by mixing the fermentation bed at regular intervals in time. The problem with this strategy is that, for some fungi, the formation of aerial hyphae improves SSF production (RAHARDJO et al., 2005b).

Figure 1.3 Schematic representation of the formation of a reproductive hypha of *Rhizopus oligosporus*, the sporangiophore (adapted from Shurtleff and Aoyagi, 1979)
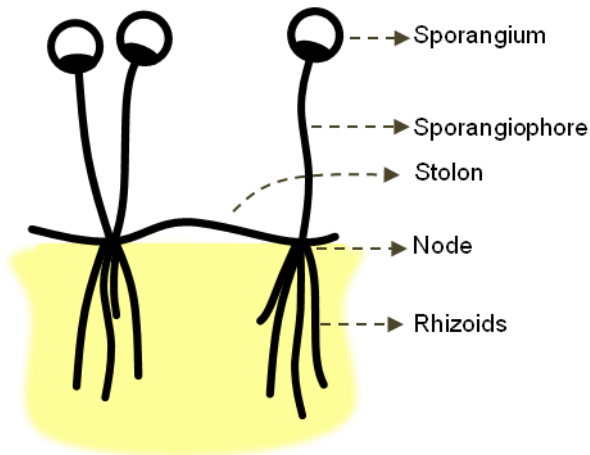
In addition, there are indications that enzymatic productivity in SSF is related to the fungal morphology, that is, to the biomass distribution profiles, how hyphae branch and the direction of growth of these branches. For example, the production of acid protease and acid carboxypeptidase in rice *koji* by *A. oryzae* is higher when the degree of penetration into the grain is lower (ITO et al., 1989). Meanwhile, mutant strains of *A. oryzae* that have a lower frequency of branching in their aerial hyphae also produce a lower amylase activity, compared with the same amount of biomass as that of the wild strain (TE BIESEBEKE et al., 2005). However, the factors that determine the distribution of penetrative hyphae inside a particle and the mode of branching in aerial hyphae have not been investigated. These two studies and the fact that hyphal growth can affect heat and mass transfer in SSF, as explained above, denote that improving SSF productivity requires a better

understanding of how hyphae grow on solid media, what determines their morphology and the contributions of each hyphal type within the mycelium. The understanding of growth and morphology of filamentous fungi on solid media can be achieved through mathematical or computational modeling, and analysis of the mycelium using confocal microscopy.

1.2 STUDYING GROWTH AND MORPHOLOGY OF FILAMENTOUS FUNGI THROUGH MATHEMATICAL MODELING

Mathematical models can be used to guide investigations by identifying the mechanisms that have the greatest influence on hyphal growth. Many models have already been developed to describe growth and morphology of the mycelium on solid media, however, there are two main problems in using these current models to study hyphal morphology in SSF. First, most models that reproduce fungal morphology do not describe biochemical phenomena, such as nutrient uptake and translocation inside the hypha. Similarly, most models that describe these biochemical phenomena limit themselves to a single hypha and do not attempt to describe the morphology of the mycelium. Second, the few models that do describe intracellular phenomena and how they affect mycelial morphology were developed exclusively for surface hyphae (BOSWELL; DAVIDSON, 2012). These models would have to be adapted to describe other hyphal types because the mechanisms that limit the extension and branching of hyphae are different for each type of hypha. For example, growth of aerial hyphae is limited to intracellular transport of carbon source nutrients (BALMANT et al., 2015), while the length of penetrative hyphae is limited by the pressure drop inside the hypha and the firmness of the medium (SUGAI-GUÉRIOS et al., 2016). Chapter 2 presents a more detailed explanation on previous mathematical models used to describe mycelial growth on solid media.

For a mathematical model to be a useful tool for elucidating how particle-scale phenomena influence the performance of SSF bioreactors, it must describe the growth of all types of hyphae, incorporating expressions describing the mechanisms that control their extension and branching. Some of the elements this model would need are:

- A description of the spatial distribution of hyphae, the positions of their branches and of their tips;

- Mass transfer equations for nutrient inside hyphae and in the solid medium;
- An equation for the rate of transport of nutrient across the membrane;
- An equation for the rate of extension of hyphae based on intracellular mechanisms;
- Rules determining when and where septa (when present) and branches are formed;
- Rules determining the direction of growth of hyphae.

A model with all these elements may be obtained by fusing and adapting previous models. In order to calibrate the model parameters of this fused model, it is necessary to have experimental data, specifically, micrographs that show how the morphology of the mycelium is formed.

1.3 STUDYING GROWTH AND MORPHOLOGY OF FILAMENTOUS FUNGI USING CONFOCAL MICROSCOPY

On solid media, the mycelium forms a three-dimensional network on, above and below the surface. In order to facilitate analysis and quantification of mycelial growth, many researchers use membranes or other means to prevent the formation of penetrative and, sometimes, aerial hyphae, so that mycelial growth is essentially bi-dimensional and includes only surface hyphae. Since most experimental data is for surface hyphae, it is no surprise that most of the mathematical models in the literature are also for these hyphae.

The best approach to visualize and quantify the growth of hyphae, including penetrative hyphae, is to make the hyphae fluorescent and observe this fluorescence using a confocal microscope (HICKEY et al., 2004). When a sample is analyzed with a confocal microscope, it is as though each image generated is a microscopically thin cut of the sample. By capturing many images of the same optical field, but at different field-depths, a 3D image of the sample can be generated using image analysis software. The settings of the confocal microscope, such as resolution, the size of the optical field and the number of field depths captured, determine the level of detail of the final image. Parameter settings that result in a higher level of detail also result in a longer time required for image capture. It is important to control the capture duration, such that there is no significant change in the position of hyphae during this capture. Another advantage of confocal microscopy is that it is non-destructive, thus, images of the same sample and the same position may be captured

at different times during the development of the mycelium, as in time-lapse.

There are two methods for making hyphae fluorescent. The first method is to add to the medium a fluorescent dye that has affinity for the hyphae. This dye is absorbed by the hyphae and, then, be capable of emitting fluorescence after excitation with an appropriate wavelength. This approach was used by Nopharatana et al. (2003a,b) to quantify growth of aerial and penetrative hyphae of *R. oligosporus* on a starch-based medium and on PDA (potato dextrose agar), using Congo Red as the dye (Figure 1.4). However, since the images were taken at 24-h intervals in their study, it is difficult to determine the moment at which each hypha started growing and how branches were formed. Nevertheless, these data have already been used to calibrate four mathematical models (NOPHARATANA et al., 1998; CORADIN et al., 2011; BALMANT et al., 2015; SUGAI-GUÉRIOS et al., 2016).

The second method is to modify the fungus genetically so that it expresses a fluorescent protein. The main advantage of this approach is that, once the strain has been modified, it can be used in numerous experiments, in different media, without the addition of any special chemical (CZYMMEK; BOURETT; HOWARD, 2004). Fluorescent proteins are particularly useful to study intracellular processes, such as regulation of gene expression, intracellular translocation processes, and different physiological states across the mycelium. Fluorescent proteins have been used, for example, to examine distribution of hydrolytic enzymes across the mycelium of surface hyphae (VINCK et al., 2005/2011). A detailed review of how fluorescence proteins and confocal microscopy have been used to study filamentous fungi was done by Czymmek et al. (2004).

Figure 1.4 Confocal micrographs of (A) aerial hyphae and (B) penetrative hyphae of *Rhizopus oligosporus* growing on PDA, at 40 h of incubation, obtained by Nopharatana et al. (2003b).
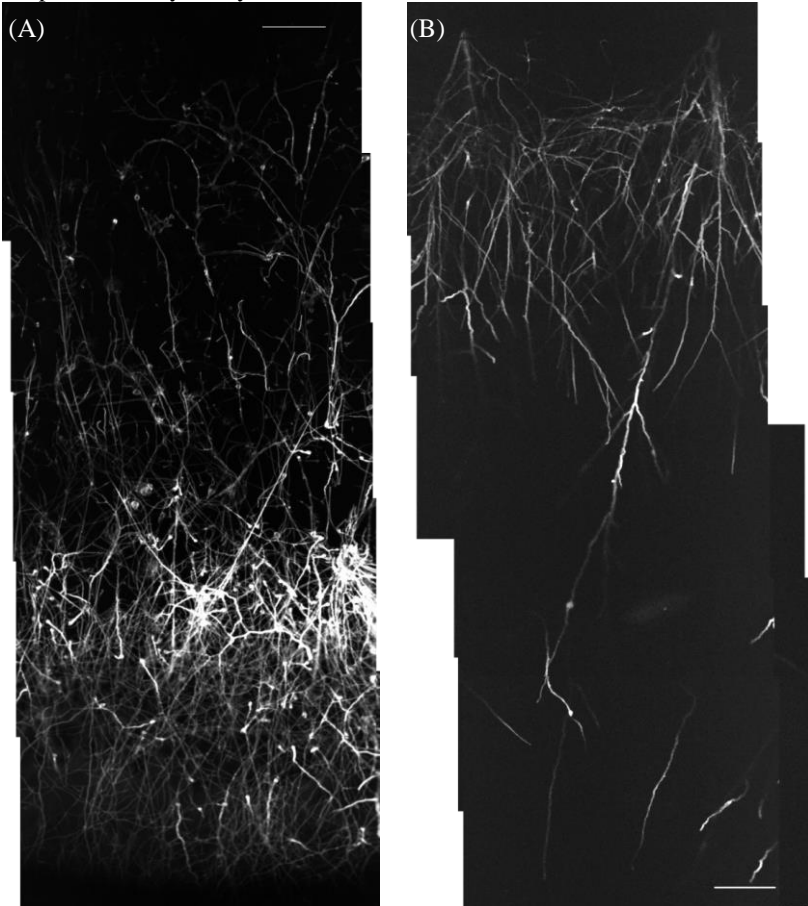
1.4 OVERVIEW OF EXPRESSION OF PECTINASES IN *Aspergillus niger*

Pectin is a structural polysaccharide that is present in the cell wall of plants. It has a complex structure, the details of which depend on its source, but it typically contains a large amount of galacturonate and also other monomers, such as glucuronate, arabinose, galactose, ramnose, xylose and fucose (GEORGIEV et al., 2012). In the case of citrus pectin, for example, galacturonate constitutes over 74% of the polymer (SIGMA, 2016). After hydrolysis of pectin, this galacturonate could be used for the synthesis of high-value products, such as 2,5-furandicarboxylic acid, which can be used to produce a polymer that has properties similar to PET (RICHARD; HILDITCH, 2009).

Due to the complex composition and structure of pectin, its hydrolysis involves a large and diverse group of enzymes (MARTENS-UZUNOVA; SCHAAP, 2009; BENOIT et al., 2012). For example, polygalacturonases are required to hydrolyze the glycosidic bonds in the region named homogalacturan, which consists of a linear chain of galacturonate. Polygalacturonases are classified as exopolygalacturonases, which act on glycosidic bonds at the extremity of a homogalacturan chain, releasing monomers, or as endopolygalacturonases, which act on the glycosidic bonds in the middle of the chain, releasing oligosaccharides (DE VRIES; VISSER, 2001). The activities of polygalacturonases are often studied using an artificial polysaccharide named polygalacturonate, which mimics the homogalacturan region.

A. niger produces all the enzymes necessary to convert pectin into monosaccharides (BENOIT et al., 2012). In addition, this fungus has more than one gene for some pectinolytic activities. For example, there are 7 genes for endopolygalacturonases and 4 genes for exopolygalacturonases in the *A. niger* genome (MARTENS-UZUNOVA; SCHAAP, 2009). In a secretome analysis using galacturonate as the carbon source (BRAAKSMA et al., 2010), the most secreted endopolygalacturonases was endopolygalacturonase B. This enzyme is coded by the gene *pgaB*, which is constitutively expressed, meaning that it is expressed regardless of the type of carbon source present in the medium (PARENICOVÁ et al., 2000). The most secreted exopolygalacturonase was exopolygalacturonase B. This enzyme is coded for by the gene *pgxB*, which is expressed only in the presence of galacturonate or galacturonate-based polysaccharides, such as pectin and polygalacturonate.

Expression of *pgxB*, as is the case for most genes in *A. niger*, is regulated by transcription factors, which are proteins that recognize specific nucleotide sequences, usually in the promoter region of a gene, and bind to these regions, either repressing or activating the expression of the gene. The presence of galacturonate in the medium induces the expression of the transcription factor *GaaR* (ALAZI et al., 2016). This transcription factor then binds to the promoter of *pgxB*, inducing its expression. On the other hand, the transcription factor *CreA*, which is expressed in the presence of glucose, inactivates transcription of *pgxB* (NIU et al., 2015). This mechanism ensures that *A. niger* expresses *pgxB* only when glucose is not available and a galacturonate-based nutrient is present. Other mechanisms may be involved, but they have not been elucidated.

The expression of most of the polygalacturonase genes in *A. niger* is induced by galacturonate, except for *pgaA*, *pgaB* and *pgaD* (MARTENS-UZUNOVA; SCHAAP, 2009). The constitutive expression of these three genes is necessary to trigger the expression of the induced polygalacturonases: in a medium that contains pectin, but not free galacturonate, initially, there is no expression of the inducible polygalacturonases. However, since *pgaA*, *pgaB* and *pgaD* are expressed and the resulting enzymes are secreted, the hydrolysis of pectin is initiated, leading to the release of galacturonate into the medium; this free galacturonate is absorbed by the fungus and induces the expression of the other polygalacturonases. The enzymes coded by *pgaA*, *pgaB* and *pgaD* are therefore called scouting enzymes, as they effectively play a role in determining which substrates are present in the medium (DELMAS et al., 2012).

The pattern of expression of scouting and non-scouting polygalacturonases in individual hyphae formed on a pectin- or polygalacturonate-containing medium may be used to classify these hyphae into scouting hyphae, namely hyphae responsible for secretion of scouting enzymes, and vegetative hyphae, namely hyphae responsible for secretion of inducible enzymes. The expression of a particular gene in a hypha can be investigated either by quantifying the amount of mRNA corresponding to this gene (LEVIN et al., 2007; BENOIT et al., 2015) or by modifying the strain so that it expresses a fusion of the studied gene with the gene of a fluorescent protein (VINCK et al., 2005/2011). In the first approach, the transcription of many genes can be analyzed at the same time, but it would require the extraction of mRNA from individual hyphae in a network of hyphae. On the other hand, with a fluorescent fusion protein, it is possible to identify differences in expression between

individual hyphae and to localize the enzyme inside the hypha, such that it is possible to determine how it is translocated through the mycelium and where it is secreted. Through this technique, usually only one or two enzymes are analyzed at the same time.

1.5 AIMS OF THE STUDY

Solid-state fermentation using filamentous fungi is an important technique for the production of enzymes, biopesticides, pigments, organic acids and other products. However, many aspects of the process are not well understood. Importantly, little is known about what determines the morphology of the mycelium, namely the spatial distribution of biomass, the branching pattern and the direction of growth, and how this morphology affects SSF productivity. An understanding of these phenomena might provide insights that can later be used to improve SSF productivity and expand its applications. In the long term, this understanding may be achieved, for example, through the combination of a three-dimensional mathematical model and microscopic visualization of hyphal growth using a fluorescent fungus. A proper mathematical model for such a purpose would be a 3D phenomenological model, describing branching, septation and decisions on the direction of growth, and incorporate equations for the limitation of growth based on nutrient availability; however, a model with all these characteristics has not been developed yet. Although parts of existing models may be incorporated into this new model, most models describe only surface or biofilm hyphae, therefore, there are many unanswered questions regarding growth of aerial and penetrative hyphae that should be elucidated before the development of this 3D phenomenological model, for example, what determines the final length of these hyphae.

The main objective of this study is to understand how the network of aerial and penetrative hyphae is formed when filamentous fungi grow on solid media and how pectinases are produced in these hyphae. In order to achieve this objective, specific objectives were proposed:

- To identify simple rules to describe the extension, branching and direction of growth of penetrative and aerial hyphae using computational models;
- To construct a fluorescent strain of *Aspergillus niger* that can be used to visualize and quantify growth on solid media;

- To use this strain to study the influence of the type of carbon source on fungal morphology;
- To study the spatial distribution of exopolygalacturonase B (*pgxB*) and endopolygalacturonase B (*pgaB*) in penetrative hyphae by fusing these genes with the gene for a fluorescent protein in order to identify if there are populations of penetrative hyphae with different roles.

1.6 STRUCTURE OF THIS THESIS

Chapter 2 presents a review on mathematical models of the growth of hyphae on solid surfaces. This review begins by presenting an overview of how filamentous fungi grow on solid particles and identifying the most important phenomena that a model for mycelial growth should include. For each of these phenomena, it then evaluates the modeling approaches that have been used previously and identifies those that would be most appropriate for incorporating into a 3D phenomenological model. This chapter was published as a chapter of the volume entitled "Filaments in Bioprocesses" of the series Advances in Biochemical Engineering/Biotechnology in 2015 by Springer International Publishing.

In chapter 3, a model, named the layer model, is proposed to describe the growth of penetrative hyphae. The purpose of the model is to explore what determines the length of penetrative hyphae and how they branch. This model was used to reproduce biomass profiles of two different fungi, *R. oligosporus* and *A. oryzae*, in artificial media (such as PDA) and in a real SSF system, being the first model to describe growth of individual hyphae in a real SSF system. This chapter was published as a research paper to be published in Biochemical Engineering Journal.

In chapter 4, the layer model is adapted to describe the growth of vegetative and reproductive aerial hyphae, with the aim of exploring what determines the direction of growth of these hyphae and when they stop extending. The model was used to describe growth of vegetative and reproductive hyphae of *Rhizopus oligosporus* on PDA. The layer model for penetrative and aerial hyphae was based on the probability distribution model developed by Balmant (2013). The changes made in developing the layer model from this probability distribution model are outlined in section 6.1. This chapter is a manuscript for a research paper.

For chapter 5, two fluorescent strains of *Aspergillus niger* were constructed. Both strains have a green fluorescent protein in their cytosol

and were used in a microscopic analysis of hyphal growth and morphology on solid media, using different types of carbon source. Each strain also expresses either *pgaB* or *pgxB* fused with the gene of a red fluorescent protein, which was used for detection of the expression of these enzymes. At the end of this chapter, there is a discussion of the implications that experimental results have for the development of a 3D phenomenological model. This chapter is a manuscript for a research paper.

Chapter 6 presents a general discussion, with an overview of the main contributions that this thesis makes to understanding how filamentous fungi grow on solid particles and how to model this growth and the resulting morphology. At the end of the chapter, a list of suggestions for future work is presented.

All references used throughout this thesis are presented at the end of the documents, including those used in the published papers.

2 MODELING THE GROWTH OF FILAMENTOUS FUNGI AT THE PARTICLE SCALE IN SOLID-STATE FERMENTATION SYSTEMS

This chapter is a reproduction of the literature review published as a chapter of the volume entitled "Filaments in Bioprocesses" (volume 149, p. 171-221; doi: 10.1007/10_2014_299) of the series Advances in Biochemical Engineering/Biotechnology in 2015 by Springer International Publishing, only the abstract, acknowledgements and the reference list were omitted. It was co-written by Wellington Balmant, Agenor Furigo Jr, Nadia Krieger and David Alexander Mitchell. Copyright © 2015 Springer International Publishing Switzerland, reprinted with permission of Springer.

2.1 INTRODUCTION

Solid-state fermentation (SSF) processes involve the growth of microorganisms on moist solid substrate particles, in situations where the spaces between the particles are filled with a continuous gas phase. Although there are some SSF processes that involve bacteria and yeasts, most SSF processes involve filamentous fungi (MITCHELL et al., 2000). For example, the filamentous fungi *Rhizopus oligosporus, Aspergillus oryzae* and *Monascus purpureus* are used to produce *tempe*, soy sauce *koji* and red rice *koji*, respectively, in SSF processes that have been practiced for many centuries in Asia. Filamentous fungi are also involved in several commercial processes of SSF that have been developed over the last few decades, and also in many potential applications that are being studied (PANDEY et al., 2000; MUSSATTO et al., 2012). Additionally, SSF processes involving filamentous fungi will be important processing steps in biorefineries (DU et al., 2008).

Mathematical models are useful tools for guiding the design, scale-up and operation of bioreactors and various models that describe heat and mass transfer within SSF bioreactors have been developed with this purpose (MITCHELL et al., 2003; MITCHELL et al., 2006). Models can also be used as tools for gaining insights into how phenomena that occur at microscopic scales control system performance. This review evaluates the state of the art in the development of such models for SSF processes that involve filamentous fungi. We address key issues that are important during the initial steps of developing any mathematical model. Firstly, it is important to know what one wants to achieve with a model, as this will determine the type of model to be developed. Secondly, with the intended

use in mind, it is necessary to express ones understanding of the functioning of the system, at an appropriate level of detail, detailing subsystems and phenomena that occur within and between these subsystems. Thirdly, before writing the equations and building the model, it is appropriate to study previously published models, as these can give insights into how the system might be represented and how specific phenomena might be described mathematically. By addressing these issues, we aim to provide a basis for the continued development of mathematical models of fungal growth at the particle scale in SSF systems.

2.2 THE APPROPRIATE SCALE FOR DESCRIBING GROWTH OF FILAMENTOUS FUNGI IN SSF PROCESSES

This review deals with models that can provide insights into how the growth of filamentous fungi at the particle scale affects SSF bioreactor performance. This section shows that a model with this purpose must describe the mycelial mode of growth, since not only can the characteristics of the mycelium influence the performance of the bioreactor, but also the manner in which the bioreactor is operated can affect the development of the fungal mycelium. It then concludes that, amongst the models that have been used to describe the growth of filamentous fungi, "mesoscale" models are the most appropriate to describe how the mycelium develops to produce a complex spatial arrangement in the heterogeneous bed of solid particles.

2.2.1 The importance of mycelial growth in SSF processes

The performance of an SSF process that involves a filamentous fungus is determined by a complex interplay between the morphological and physiological characteristics of the fungus and the factors that determine the conditions in the local environment that the fungus experiences. These factors include the design and operating variables of the bioreactor that is used, the transport phenomena that operate across the whole substrate bed and the transport phenomena that operate at the level of a single particle and the inter-particle spaces around it (Figure 2.1). Details of the design and operating variables that are available for the various SSF bioreactor types and the heat and mass transport phenomena that occur across the substrate bed in these bioreactors are discussed in depth elsewhere (MITCHELL et al., 2006).

Figure 2.1 The performance of an SSF process that involves a filamentous fungus depends on a complex interplay between the morphological and physiological characteristics of the fungus and the factors that determine the conditions of the local environment to which the fungus is subjected. Solid arrows represent the production, consumption or flow of system components. Dashed arrows represent effects of the fungus or on the fungus, with these effects being identified with underlined text.

MACROSCALE: The bioreactor

Design variables
• bioreactor type (see Figure 3.3)
• details of agitation system
• details of aeration system
• bed geometry (height & width)
• cooling system

Operating variables
• air flow rate, temperature and humidity
• frequency, intensity & duration of agitation
• addition of water to the bed

Transport phenomena at this scale lead to gradients across the bed (in one or more dimensions) with respect to:
• substrate & gas phase temperatures
• substrate moisture content & gas phase humidity
• gas phase concentrations of O_2 and CO_2

MESOSCALE: The particle and its surrounding inter-particle spaces

Operation of the bioreactor affects growth of filamentous fungi
• mixing breaks and squashes aerial hyphae
• mixing can squash particles, affecting the geometry of the solid-gas system in which the fungus is growing

The growth of filamentous fungus affects transport phenomena
• hyphae grow into the inter-particle spaces, affecting air flow
• hyphae binding particles together can cause agglomeration and affect the effectiveness of mixing
• at a larger scale, hyphae binding particles together can lead to shrinking/cracking of the whole bed, which can lead to channeling

Transport phenomena affect how manipulation of operating variables affects the local environment

Filamentous fungi
• surface hyphae
• biofilm hyphae
• aerial hyphae
• penetrative hyphae

Growth of filamentous fungi affects the particle
• attack on the particle structure, causing particle shrinkage, leading to bed shrinkage

Local conditions affect fungal growth

Local environment
pH, T, [nutrients], a_w, [O_2], [CO_2], [metabolic products]

Fungal growth affects local conditions
• consumption & production of compounds

Link between morphology of the mycelium and production of enzymes

Hydrolytic enzymes
Intra-particle phenomena
• enzyme diffusion & action
• diffusion of soluble hydrolysis products

Intra-particle phenomena affect the local environment

The particle

Before considering the interaction between fungal mycelia and SSF bioreactors, it is useful to classify the hyphae present in SSF processes into surface hyphae, biofilm hyphae, penetrative hyphae and aerial hyphae, according to the specific physical environment in which they are located (RAHARDJO et al., 2006) (Figure 2.2). Surface hyphae are located at the air-solid interface and grow horizontally on top of the surface of the solid particle; they are in intimate contact with both the air phase and the solid phase. Biofilm hyphae represent those hyphae in the part of the mycelium that is above the substrate surface but is bathed in a liquid film. The biofilm may be several hundred micrometers in depth (OOSTRA et al., 2001). Penetrative hyphae grow below the surface of the solid particle and are therefore surrounded by the moist solid matrix of the particle. Aerial hyphae are those hyphae that are located in the inter-particle spaces or at the exposed surface of the substrate bed and are surrounded on all sides by a gas phase.

This review deals with aerobic SSF processes. The various bioreactor designs that have been proposed for such processes can be classified on the basis of the strategies that are used with respect to the aeration and the agitation of the substrate bed (MITCHELL et al., 2000) (Figure 2.3). In SSF processes that involve filamentous fungi, the agitation strategy that is used will affect the spatial arrangement of the hyphae in the system. In some processes, the bed needs to remain essentially static, such as is the case in the production of fungal spores for use as biopesticides, since agitation may damage aerial reproductive structures or even prevent them from forming. If the bed is left completely static or mixed very infrequently, then hyphae can extend into the inter-particle spaces, becoming aerial hyphae. Aerial hyphae originating from several different particles can intertwine, thereby binding the particles into agglomerates. If the bed is left static for a long time and then mixed, then this mixing may tear the agglomerates apart and squash the aerial hyphae onto the particle surface, forming a biofilm. On the other hand, if the bed is mixed frequently or continuously, then aerial hyphae will simply not develop, as any hyphae that begin to extend into the air spaces will quickly be squashed onto the particle surface.

Figure 2.2 Classification of hyphae in SSF systems based on the physical environment.
This classification is similar to that of Rahardjo et al.(2006), except that it also includes surface hyphae, which grow across the surface of the substrate particle early on in the process.
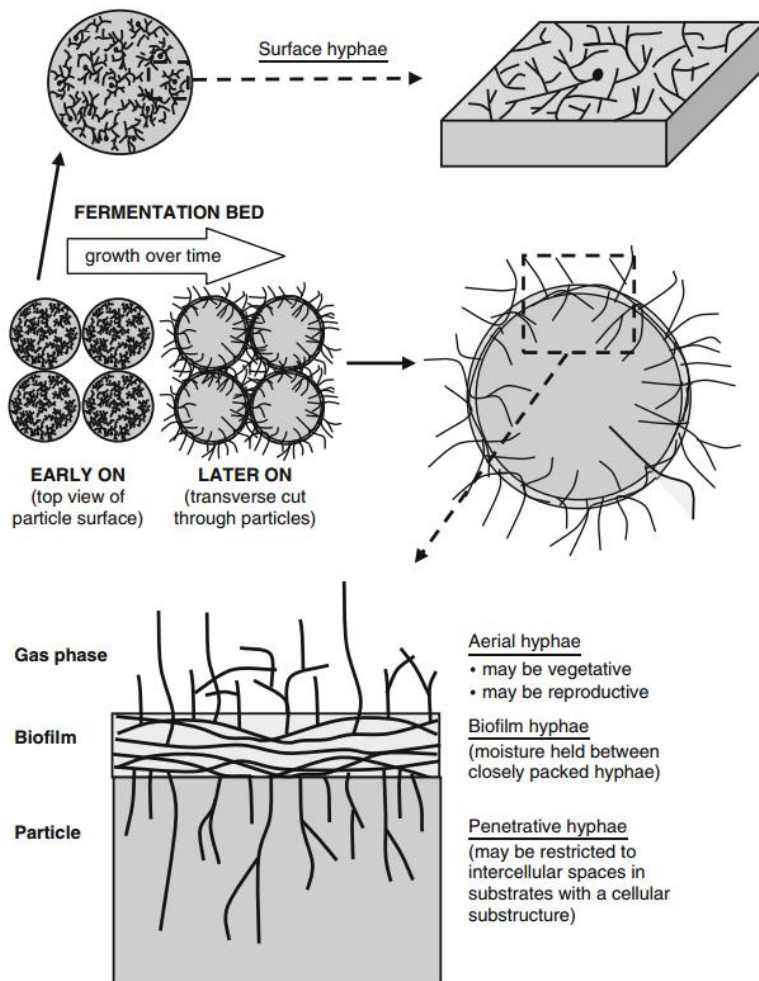
Figure 2.3 Classification of SSF bioreactors into four groups on the basis of how they are agitated and aerated (MITCHELL et al., 2000).

Agitation has significant consequences for the spatial distribution of fungal hyphae in the system, preventing the formation of aerial hyphae.
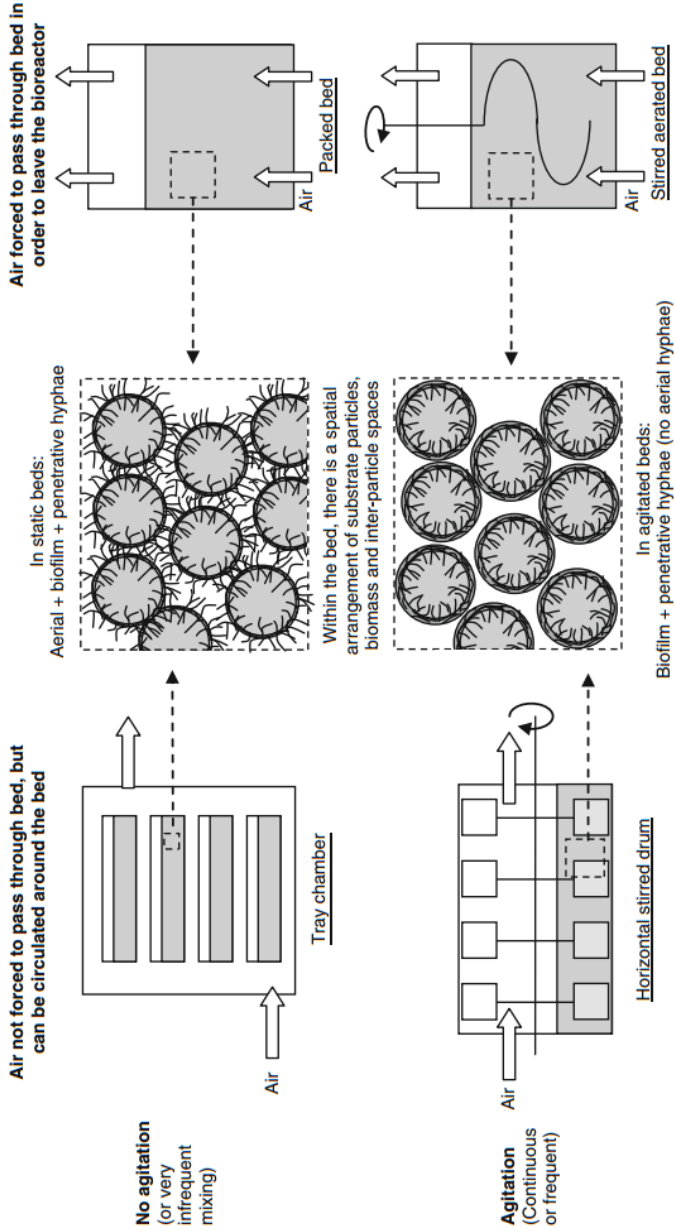
The aeration strategy that is used in the bioreactor is also important, because it will affect the delivery of O_2 to the inter-particle spaces within the substrate bed. The bed may not be forcefully aerated, but rather placed in an environment in which air is circulated around the bed. In this case, if the bed is static, then gas transport in the bed will be limited to diffusion, although some natural convection may occur if there are significant temperature gradients across the bed (SMITS et al., 1999). If the bed is agitated, as occurs for horizontal stirred drums and rotating drums, then the effectiveness with which the gas phase within the inter-particle spaces is replenished with O_2 depends on the effectiveness of the mixing. Since the mixing will squash any aerial hyphae into the biofilm on the surface of the particle, then the supply of O_2 to the fungus itself will depend on diffusion of O_2 in this biofilm.

On the other hand, a static bed may be forcefully aerated, meaning that the air is forced to flow through the inter-particle spaces of the bed in order to leave the bioreactor. In order to obtain uniform aeration over the whole bed, it is important that the air is not able to flow preferentially through regions of lower resistance. The growth of filamentous fungi can have important consequences with respect to the air flow in the bed. Firstly, the growth of aerial hyphae into the inter-particle spaces increases the resistance to air flow through the bed, affecting the efficiency of the aeration system (AURIA et al., 1995). Secondly, the tensile forces exerted by the network of aerial hyphae can contribute to contraction of the bed, causing it to crack or pull away from the bioreactor walls, leading to the phenomenon of channeling, where the air flows preferentially around the bed or through the cracks and not through the inter-particle spaces. If this occurs, then the bed can be agitated in an attempt to reseat it. However, some particles may be bound together strongly by the aerial hyphae, such that large agglomerates of particles resist being broken up. In fact, it has been suggested that the bed should be agitated early during the process to disrupt the aerial hyphae and prevent the formation of agglomerates in the first place, at least for fungi that produce abundant aerial hyphae (SCHUTYSER et al., 2003).

Although there are many studies of the relationship between the morphology and productivity of filamentous fungi in submerged culture systems (PAPAGIANNI, 2004; GRIMM et al., 2005), this topic has received much less attention in SSF systems, with only two studies. In the first study, the production of acid protease and acid carboxypeptidase in rice *koji* by *Aspergillus oryzae* was correlated with the degree of mycelial penetration into the grain: at low degrees of penetration the activities of these two enzymes were high (ITO et al., 1989). In the second study,

mutant strains of *Aspergillus oryzae* with increased branching frequency in their aerial hyphae produced significantly higher amylase and protease levels than the wild-type strain, despite producing similar overall biomass levels (TE BIESEBEKE et al., 2005).

2.2.2 Appropriate models for mycelial growth at the particle scale in SSF

It is clear from the above discussion that, for a mathematical model to be a useful tool for elucidating how particle-scale phenomena influence the performance of SSF bioreactors in processes that involve filamentous fungi, it must describe the growth of the mycelium at an appropriate scale. Current models of fungal growth in SSF can be classified as being microscale models, mesoscale models or macroscale models, based on the scale at which the fungal mycelium is described (Table 2.1). This classification is similar to that proposed by Davidson (2007) and Boswell and Davidson (2012), but applied to models for SSF.
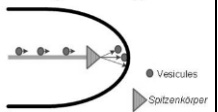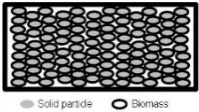
Microscale growth models are those concerned with phenomena occurring in a single hypha, and often do not describe an entire hypha. They are most commonly used to study growth and morphology of the hyphal tip and usually include a description of the functioning of the *Spitzenkörper* (GORIELY; TABOR, 2008).

Mesoscale growth models describe a network of hyphae, although, as will be discussed later (Section 2.4.1), they may or may not describe these hyphae as distinct entities. Some models focus on describing how a colony arises from a single spore or single inoculation point; such models are often referred to as single colony models. Other models describe how a mycelium develops from many points of inoculation over the substrate surface, a situation that is more common in SSF systems and which has been referred to as "overculture" (MITCHELL et al., 1989). Mesoscale models may include some of the phenomena that are described in microscale models, but at a lesser degree of detail, and they include other phenomena related to the formation of the mycelium, such as branching. When mesoscale models are used to describe growth in SSF systems, they may recognize the substrate particles, but, if so, they will only describe one or a few particles. They may describe the presence of concentration gradients for key components within these particles.

Table 2.1 Classification of mathematical models of fungal growth on solid particles according to the scale at which the system is described.

Category name	Microscale	Mesoscale	Macroscale
Scale of growth	μm	mm to cm	cm to m
Number of particles involved	None or only one	One to a few	A large number (almost uncountable)
The manner of describing the mycelium	Individual hyphae	Individual hyphae or average concentration of biomass	Average concentration of biomass
Main feature	These models focus on a specific region of the hypha (e.g. a few μm behind the tip), they do not attempt to describe a whole hypha or a mycelium	These models describe the growth of one or a few colonies interacting with each other	These models calculate concentration gradients of biomass/temperature/ O_2 across the substrate bed, but not gradients within particles
General purpose	To study intracellular phenomena that determine tip extension rate and tip morphology	To study the phenomena that determine the rate of colonization of solid particles	To study SSF bioreactor performance
What can be investigated with the models	The mechanisms involved in the *Spitzenkörper* Patterns of formation of new cell wall Tip swelling Tip extension against frictional forces Molecular motors and microtubule transport	Fungal morphology in SSF Biomass distribution inside and around a solid particle How nutrient/O_2 distribution in the extracellular environment affects development of the mycelium Shrinkage of solid particles	Overall growth and product formation in the bed Local temperature and moisture content and how they affect growth Pressure drop Shrinkage of the bed
Most important phenomena to be described by the model	Vesicle transport to the *Spitzenkörper* and from the *Spitzenkörper* to the apical cell membrane Fusion of vesicles into cell membrane and formation of new cell wall Water uptake and intracellular water transport	Transport phenomena inside the solid particle and the biofilm layer Nutrient uptake, intracellular transport and consumption Vesicle production, transport and fusion at the tip Branching and changes in growth direction	Mass and heat transfer between particles Biomass growth rate Particle shrinkage

Cont. Table 2.1

Category name	Microscale	Mesoscale	Macroscale
Examples	Tindemans et al. (2006), Sugden et al. (2007), Goriely and Tabor (2008)	Prosser and Trinci (1979), Coradin et al. (2011), Meeuwse et al. (2012)	Mitchell et al. (2003)
Illustration of the scale of growth			

Macroscale growth models describe the growth of the fungus in a bed containing a very large number of particles and are typically used to describe the growth kinetics within models of heat and mass transfer within bioreactors. These models rarely describe the gradients of components inside particles. Rather, they focus on temperature and gas concentration gradients across the fermentation bed. No attempt is made to describe individual hyphae (MITCHELL et al., 2004). Rather, empirical equations are fitted to data of biomass concentrations (often expressed as "grams of biomass per gram of total dry solids"), which will typically be obtained from measurements made on homogenized preparations obtained from samples containing hundreds or even thousands of substrate particles (VICCINI et al., 2001).

Mesoscale growth models are most appropriate for the purpose of elucidating how the mycelial mode of growth of filamentous fungi influences the performance of SSF systems. This review focuses on this type of model.

2.3 HOW THE FUNGAL MYCELIUM GROWS AND INTERACTS WITH ITS ENVIRONMENT IN SSF

In the development of any mathematical model, before writing the equations, it is essential to understand the various phenomena that occur within the system. This section provides an overview of our knowledge about how the fungal mycelium grows and interacts with its environment in SSF, at a level of detail that would be appropriate for the purposes of modeling mycelial development in SSF processes. A mesoscale model of SSF would concern itself with transport phenomena, but would not attempt to describe phenomena that occur at the cellular and molecular level in detail. Detailed descriptions of these cellular and molecular processes can be found elsewhere (STEINBERG, 2007; RIQUELME;

BARTNICKI-GARCÍA, 2008; TAHERI-TALESH et al., 2008; PEÑALVA et al., 2010; BEREPIKI et al., 2011).

In this section, it is assumed that the filamentous fungus is growing within a bed of solid particles that is initially static. Section 2.3.1 focuses on what the hyphae themselves do; Section 2.3.2 explores the intracellular and extracellular reactions and transport phenomena that are involved.

2.3.1   Development of the mycelium in an SSF system

It is not necessarily the case that all four types of hyphae identified in Section 2.2.1, namely surface, biofilm, penetrative and aerial hyphae, will be present at the same time in an SSF process. Rather, there is a developmental sequence (IKASARI; MITCHELL, 2000).

Typically the substrate will be inoculated by mixing a spore suspension in with the substrate, although mycelial fragments are sometimes used. If spores are used, initially they will be distributed over the surface of each substrate particle (Figure 2.4). The spores swell and produce a germ tube, in a process that may take several hours. This process is not completely synchronized, so different spores can germinate at different times. Also, some spores may fail to germinate. After extending a certainlength, typically 60 to 200 μm, across the surface of the substrate, this germ tube will branch to produce two daughter hyphae (TRINCI, 1974). In turn, these daughter hyphae will extend across the surface and branch, with this extension and branching process being repeated several times. The hyphal tips tend to grow into unoccupied space, in other words, away from other extending hyphae and already established hyphae. This leads to the development of microcolonies around each germinated spore, with these microcolonies being composed essentially of surface hyphae, although penetrative hyphae may also form if the O_2 level in the medium is high (RAHARDJO et al., 2006). At this stage, it may be difficult to see the fungus with the naked eye, although the texture of the surface of the substrate particle may have changed. Additionally, the biomass level may be so low that it is difficult to measure either components of the biomass (such as ergosterol or glucosamine) or the respiratory activity of the biomass.

As the microcolonies expand, the surface hyphae from different microcolonies begin to approach one another. As they do so, they may change direction to avoid one another, cross one another or stop extending (HUTCHINSON et al., 1980). Once all the available space on the

substrate surface is occupied by surface hyphae, the density of the mycelium increases with the production of penetrative and aerial hyphae.

Figure 2.4 How the presence of the various types of hyphae varies during the development of the mycelium in an SSF system that is initially left static and then agitated later in the process.
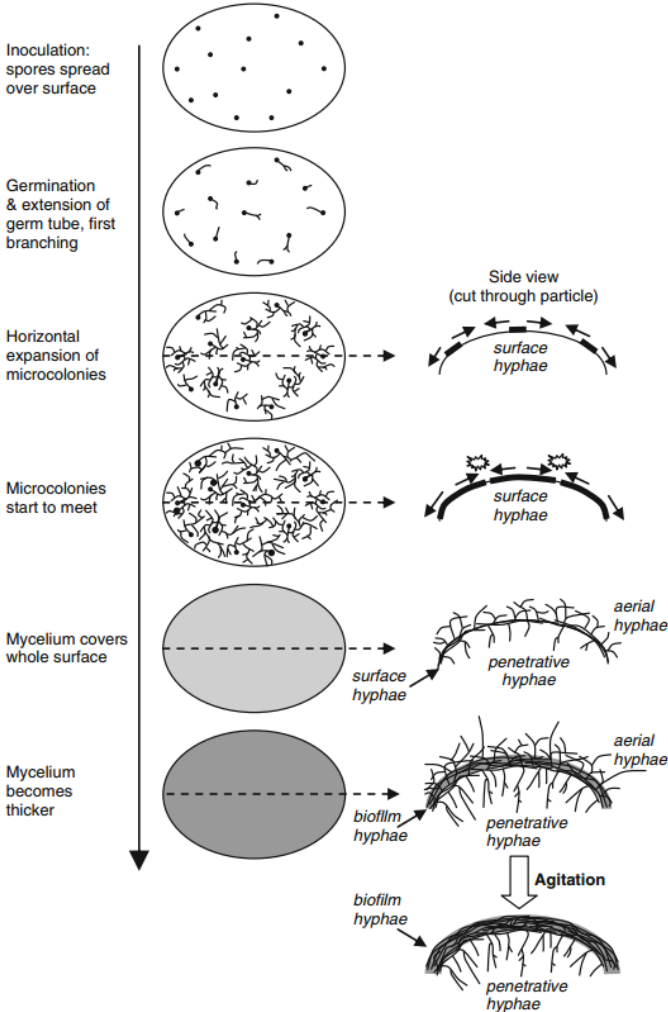
Penetrative hyphae tend to move perpendicularly away from the substrate surface if the substrate matrix is homogeneous and does not

contain significant physical barriers (NOPHARATANA et al., 2003a,b). However, many substrates derived from plants will have a cellular substructure. In this case, the penetrative hyphae will tend to follow the path of least resistance, which means that they often grow in the extracellular matrix between the cell walls within the substrate particle (JURUS; SUNDBERG, 1976). However, if the fungus has the ability to digest the cell walls within the substrate, it may penetrate into the interior of the cells, through the combined action of mechanical force and enzymatic degradation, obtaining access to the nutrients in the cell lumen (CHAHAL et al., 1983).

Aerial hyphae can be of two types, vegetative or reproductive. Vegetative aerial hyphae typically appear before reproductive aerial hyphae. Reproductive aerial hyphae are normally specialized structures, such as sporangiophores or conidiophores. There are significant differences between different fungi with respect to the degree to which vegetative and reproductive aerial hyphae are produced, and the growth patterns of these hyphae. As mentioned in Section 2.2.1, these aerial hyphae occupy part of the inter-particle space that was present in the original substrate bed.

The physical environment of a hypha, and therefore its classification, can change over the course of an SSF process. For example, if the aerial hyphae form a sufficiently dense mat above the substrate surface, a film of water may be drawn up from the substrate by capillary action into the spaces between these aerial hyphae, thereby changing the physical environment, such that these aerial hyphae and the original surface hyphae would now be classified as biofilm hyphae (RAHARDJO et al., 2006). Biofilm hyphae will also be formed if the substrate bed is mixed, since this will squash aerial hyphae, forming a mat on the substrate surface. Also, as the mycelium becomes denser, it may become difficult to distinguish particular types of hyphae. For example, if the solid material at the substrate surface is consumed during the process, then it may be very difficult to identify where the biofilm ends and the penetrative hyphae begin.

2.3.2 Phenomena occurring during growth of a filamentous fungus on a solid substrate

In this section, it is assumed that the carbon and energy source is a polymer. This is commonly the case in SSF processes, but not always. Also, in different SSF systems, polymeric carbon and energy sources that

are consumed by the microorganism may or may not contribute directly to the structural integrity of the particle. If they do, then the particle can shrink significantly during the process, causing changes in the bed structure and properties. However, this aspect will not be explored in this review. Further, it will be assumed that the bed is forcefully aerated, such that O_2 is freely available in the inter-particle spaces. However, it should be noted that, even with forced aeration, there will be a stagnant gas film attached to any surface present in the system.

2.3.2.1 Intracellular transport and other phenomena involved in hyphal extension

Hyphae grow by apical extension in a process involving the fusion of vesicles at the tip. These vesicles are produced in a sub-apical zone, which will be referred to here as the "vesicle-producing zone" and transported to the tip along microtubules within the cytoplasm (Figure 2.5) (STEINBERG, 2007; RIQUELME and BARTNICKI-GARCÍA, 2008; TAHERI-TALESH et al., 2008; PEÑALVA et al., 2010; BEREPIKI et al., 2011). In order to produce these vesicles, the cytoplasm in the vesicle-producing zone needs to receive nutrients. If the vesicle-producing zone of the hypha is not in contact with an external source of nutrients, then these nutrients must be supplied from more distal parts of the hypha.

The vesicles are surrounded by a membrane and contain enzymes involved in cell wall synthesis, both cell-wall lysing enzymes and cell-wall synthesizing enzymes. As the vesicles fuse with the plasma membrane at the tip, their membranes contribute to the extension of the plasma membrane. Cell wall precursors are probably supplied in the cytosol (RIQUELME et al., 2011). In fact, the cytosol flows from more distal parts of the hyphae to the extending tip, in a phenomenon called "cytoplasmic streaming" or "cytoplasmic flow". This cytoplasmic flow is driven by the high osmotic pressure in the tip due to the high concentrations of calcium that are maintained there (LEW, 2011). The velocity of cytoplasmic flow can be higher than the rate of extension of the tip, which is only possible if there is active efflux of water at the hyphal tip. In older regions of septate hypha, the septa may close, preventing cytoplasmic flow in these regions. In some fungi, the septum does not close completely; rather a central pore is maintained. This pore has a Woronin body beside it, which plugs the pore if the adjacent hyphal segment is damaged (MARKHAM; COLLINGE, 1987).

Figure 2.5 A simplified representation of the intracellular phenomena involved in extension of the hyphal tip.

Riquelme and Bartnicki-García (2008) report that, according to the classical model for hyphal tip growth, the tip growth machinery is within 1 to 5 μm of the "apical pole" and the vesicle-producing zone is up to 20 μm long. However, the lengths of these regions are likely to vary between different fungi.
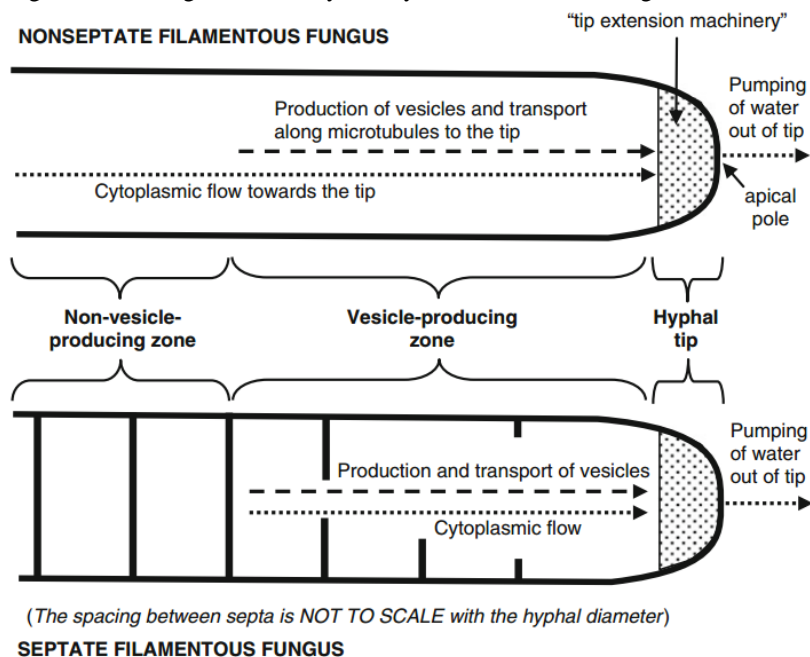
As the hypha extends, the length of the vesicle-producing zone remains essentially constant (TRINCI, 1971). In other words, the length of the fungal hypha that contributes directly to the extension of the tip remains constant. Consequently, the physiology of a particular section of a hypha at a certain location in space changes over time. The particular section is "created" when that location is first occupied by the extending tip. As the tip extends ever onwards, this section becomes part of the vesicle-producing zone, then loses its ability to produce vesicles and later undergoes an aging process in which the proportion of the cytoplasm occupied by vacuoles increases significantly (PROSSER, 1995). Later still, this section may undergo autolysis (PROSSER, 1995).

Branching of hyphae can be either apical or lateral or both, depending on the fungus and hyphal type. In apical branching, the tip itself divides. In lateral branching, a new branch appears some distance

behind the tip. Apical branching occurs when the rate of supply of vesicles to the tip is greater than the maximum rate at which vesicles can fuse at the tip (HARRIS, 2008). Lateral branches often emerge where vesicles accumulate behind septa in septate hyphae, but aseptate hyphae can also branch laterally and the role of vesicle accumulation in triggering lateral branching is not totally clear (HARRIS, 2008). It is also possible for the hyphae of some fungi to fuse by anastomosis. This can be tip-to-tip or tip-to-hypha (GLASS et al., 2004). It is not clear to what degree anastomosis occurs in SSF processes.

2.3.2.2 Extracellular phenomena involved in the growth of surface hyphae

Surface hyphae are present during the early stages of expansion of a microcolony. The germination of the spore and the initial stages of extension of the germ tube are supported by the internal reserves contained in the spores, but soon it is necessary for the extending germ tube and the new hyphae to obtain nutrients from the solid particle.

In order to utilize a polymeric carbon and energy source, the hyphae must secrete hydrolytic enzymes (Figure 2.6). Once secreted, these enzymes may remain attached to the hypha, or may be liberated into the surrounding medium. If liberated, then their diffusion in the matrix of the substrate particle will be influenced by the microscopic porosity of the matrix and by the presence of impenetrable barriers, such as intact cell walls. Once they encounter and hydrolyze polymers, then the resulting soluble hydrolysis products will diffuse through the substrate matrix. As the soluble hydrolysis products are taken up at the plasma membrane, their concentration next to the hypha decreases, leading to the formation of concentration gradients in the extracellular medium. Similar diffusion phenomena will occur for any soluble nutrients that are taken up by the hypha. In the early stages of the process, when the microcolonies are expanding across the particle surface, it is likely that the polymeric carbon and energy source will be present very close to the substrate surface, such that the distances over which the extracellular enzyme and soluble hydrolysis products need to diffuse are quite small. In fact, if hydrolysis is faster than uptake, the concentration of the soluble hydrolysis product at the surface can rise significantly (MITCHELL et al., 1991). In a forcefully aerated system, at this stage the supply of O_2 to the surface hyphae will not be limiting. CO_2 will be produced and diffuse away from the hypha into the gas phase and also, in dissolved form, into the substrate particle. Any secreted metabolites will also diffuse away from the hypha.

These secreted metabolites can be important in mediating interactions between hyphae.

Figure 2.6 Phenomena involved in the growth of surface hyphae during the initial stages of the process.
"Long triangles" represent diffusion down concentration gradients. "Dotted arrows" represent flow of water or cytoplasm. "Dashed arrows" represent transport of vesicles.
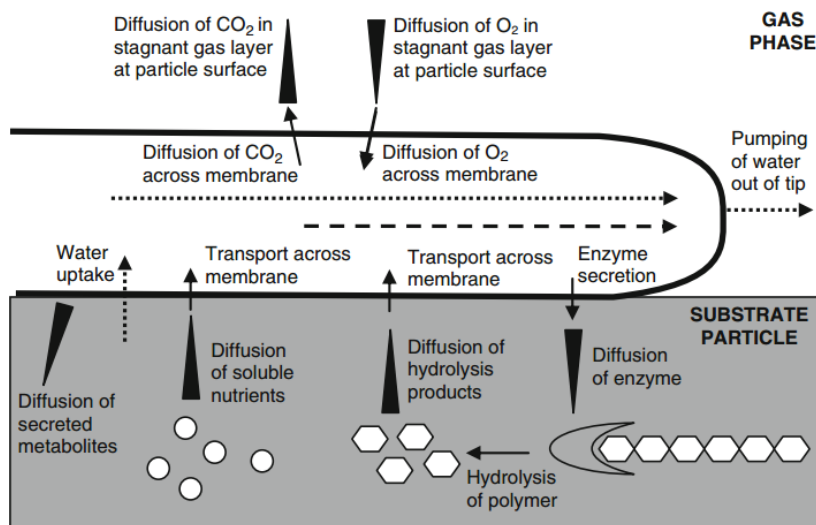
2.3.2.3   Extracellular phenomena involved in the growth of hyphae within biofilms

By the time that a biofilm has been produced in an SSF process, there are also likely to be aerial and penetrative hyphae in the system. The processes influencing the growth of aerial and penetrative hyphae are described below; here we focus specifically on what happens in the biofilm.

As the fermentation process advances, it is quite likely that the polymeric carbon and energy source will be exhausted in the region near the surface (Figure 2.7). Any enzyme that has not diffused out of this region will not contribute to the liberation of soluble hydrolysis products. Since the diffusion of enzymes in the matrix of the substrate can be quite slow, this can lead to a significant decrease in the rate of liberation of soluble hydrolysis products within the substrate particle (MITCHELL et

64

Figure 2.7 Phenomena involved in the growth of biofilm, penetrative and aerial hyphae.
"Long triangles" represent diffusion down concentration gradients. "Dotted arrows" represent flow of water or cytoplasm. "Dashed arrows" represent transport of vesicles.
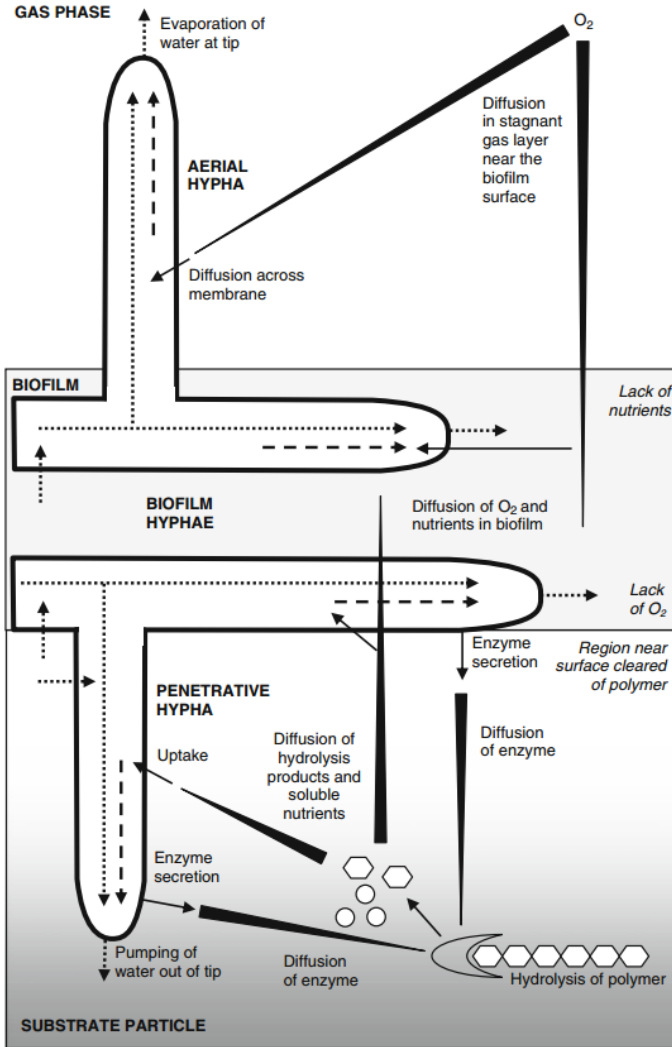
al., 1991). This, in conjunction with high uptake rates by the hyphae in the biofilm at the surface, can lead to steep concentration gradients of these soluble hydrolysis products within the particle, with very low concentrations at the interface between the biofilm and the particle. As the soluble hydrolysis products and other soluble nutrients diffuse into the biofilm, they are taken up by the hyphae. If the rate of uptake is sufficiently high and the biofilm is sufficiently thick, then these soluble hydrolysis products and nutrients can be totally consumed by the hyphae in the parts of the biofilm close to the particle-biofilm interface, with the parts of the biofilm that are further from this interface being starved of essential nutrients (RAJAGOPALAN; MODAK, 1995; MEEUWSE et al., 2012).

Additionally, even if high O_2 concentrations are maintained in the gas phase in the inter-particle spaces, the fact that O_2 transport within the biofilm is limited to diffusion means that the respiration of the hyphae in the biofilm can lead to the dissolved O_2 concentration falling to essentially zero within 100 μm depth below the interface between the biofilm and the air phase (OOSTRA et al., 2001). In other words, the parts of the biofilm closer to the surface of the substrate particle can become anaerobic.

2.3.2.4 Extracellular phenomena involved in the growth of penetrative hyphae

Penetrative hyphae are in intimate contact with the solid substrate. The matrix into which they grow will typically be moist, but with high concentrations of solids and solutes, such that much of the water will be adsorbed or complexed. These hyphae therefore need to exert turgor pressure in order to penetrate into the matrix (MONEY, 1995). There may also be physical barriers, such as the cell walls of plant materials from which the solid particles were derived. Not all fungi are capable of penetrating such barriers.

It is quite probable that the penetrative hyphae contribute to the release of enzymes into the substrate matrix (VARZAKAS, 1998) (Figure 2.7). Since penetrative hyphae are deeper within the substrate particle, when compared to biofilm hyphae, they will experience higher concentrations of soluble hydrolysis products and nutrients, but lower concentrations of O_2, at their plasma membranes. In fact, once an actively metabolizing biofilm is established at the substrate surface, the penetrative hyphae can be left in an anaerobic environment.

2.3.2.5 Transport phenomena involved in the growth of aerial hyphae

Aerial hyphae are in intimate contact with the air phase and can take up O_2 directly from the air (Figure 2.7). However, the degree to which they do this varies significantly among different fungi (RAHARDJO et al., 2002). On the other hand, the vesicle-producing region behind the extending tip of an aerial hypha must receive material from the distal part of the hypha. Since aerial hyphae can be several millimeters or even several centimeters long, depending on the fungus and the growth conditions, material for tip extension may need to be transported within the aerial hyphae over large distances. This transport probably involves cytoplasmic flow. In fact, although studies are limited, in *Aspergillus niger*, cytoplasmic flow occurs from the biofilm hyphae into the aerial hyphae, with cytoplasmic flow rates in the aerial hyphae being of the order of 10 to 15 $\mu m\ s^{-1}$ (BLEICHRODT et al., 2013).

2.4 MATHEMATICAL MODELS OF PHENOMENA INVOLVED IN THE GROWTH OF FUNGAL HYPHAE ON SOLID SURFACES

Based on the qualitative description presented in Section 2.3, a "complete" mathematical model that proposes to describe the development of fungal mycelia in SSF systems should recognize the four different types of hyphae, namely penetrative, aerial, surface and biofilm, enabling prediction not only of growth over the particle surface, but also of the biomass distribution above and below the particle surface. It should also describe the following phenomena: Physiological differentiation within the mycelium; tip extension based on the production, transport and incorporation of vesicles; nutrient and O_2 uptake and also mass transfer outside and inside the hyphae; the secretion and the hydrolytic activity of extracellular enzymes; apical and lateral branch formation, with angles similar to those found in real mycelia; and septation, in the case of septate fungi.

At present, there is no mathematical model of the growth of filamentous fungi in SSF systems that incorporates, simultaneously, all of these biomass types and growth-related phenomena. On the other hand, most of these phenomena have already been described in various fungal growth models, and the mathematical approaches used in these models could be integrated, in a modified form if necessary, into a complete model. This section describes the most appropriate mathematical approaches, from a selection of mesoscale and microscale fungal growth

models. Key features of these selected models are summarized in Table 2.2.

2.4.1 Classification of mesoscale mathematical models

It is useful to classify mesoscale models that describe the growth of filamentous fungi on the basis of which components they describe and how they treat the distribution of biomass within the spatial domain (Table 2.2). With respect to the components that are described, some models only describe the development of the fungal biomass itself, such as hyphae and tips, while other models, in addition to describing fungal biomass, recognize the contribution of other components to the growth process, such as nutrients, enzymes and vesicles. With respect to the distribution of biomass within the spatial domain, models may be classified as being either "pseudohomogeneous models" or "discrete models" (Figure 2.8). Pseudohomogeneous models, which have also been referred to as "continuum models" (DAVIDSON, 2007; BOSWELL and DAVIDSON, 2012), "reaction-diffusion models" (RAHARDJO et al., 2006) and "whole-population models" (FERRER et al., 2008), do not recognize fungal hyphae individually and therefore do not specify their exact position in space; rather they describe hyphae in terms of an average biomass concentration that may vary continuously along one or more dimensions within the spatial domain (Figure 2.8A). Conversely, discrete models, which have also been referred to as "individual-based models" (FERRER et al., 2008), specify a particular location in the spatial domain for each hyphal element and tip and distinguish this hyphal biomass from its surroundings in space; in other words, the biomass is "spatially discrete" (Figures 2.8B and 2.8C). Obviously, if the intention is to produce a model that can generate multi-dimensional images of fungal networks, similar to those that would be seen in a micrograph, this can only be achieved with discrete models and this review focuses on this type of model. However, where relevant, approaches used to describe particular phenomena in pseudohomogeneous models will be mentioned. Discrete models often treat the hyphae in a stochastic manner. For example, in the case of an extending tip that is capable of changing growth direction or branching apically, probabilities are assigned to these actions. At certain times during the simulation, a random number is generated to see whether the tip will undertake one of these actions; the action being evaluated will happen for the tip only if the random number is lower than the probability assigned to that action. This feature confers a degree of

Table 2.2 Overview of the mathematical models selected for the review.

Model	Components described[a]	Spatial treatment of biomass[b]	Type of lattice (for discrete models)[c]	Number of dimensions used to describe biomass	Treatment of temporal domain	Type of growth	Type of hyphae	Purpose of the model	Type of validation	Type of data used for validation/ calibration
Balmant (2013)	B+V	D	LB	1	Smooth	Overculture	Reproductive	For the study of intracellular phenomena in a single hypha	Calibrated	Hyphal length over time
Boswell et al. (2007)	B+N	D	LB	2	Stepwise	Single colony	Surface	For bioremediation studies	Calibrated	Rate of extension of the tip and rate of branching
Coradin et al. (2011)	B	D	LB	3	Stepwise	Overculture	Aerial and surface	For SSF studies	Quantitative	Biomass density over height above solid surface
Edelstein and Segel (1983)	B+N	P	-	1	Smooth	Single colony	Surface	For single colony studies	Qualitative	Biomass and tip densities over the radius of the colony (done in Edelstein et al. 1983)
Fuhr et al. (2011)	B+N	D	LF	3	Stepwise	Overculture	Penetrative	For wood degradation studies	Quantitative	Permeability of the wood particle
Georgiou and Shuler (1986)	B+N	P	-	1[$]	Smooth	Single colony	Reproductive and surface	For single colony studies	None	-
Hutchinson et al. (1980)	B	D	LB	2	Stepwise	Single colony	Surface	For single colony studies	Qualitative	Morphology of surface hyphae of a colony

Table 2.2(cont)

Model	Components described[a]	Spatial treatment of biomass[b]	Type of lattice (for discrete models)[c]	Number of dimensions used to describe biomass	Treatment of temporal domain	Type of growth	Type of hyphae	Purpose of the model	Type of validation	Type of data used for validation/ calibration
López-Isunza et al. (1997)	B+V+N	M	-	3	Smooth	Single colony	Germ tube	For the study of intracellular phenomena in a single hypha	Calibrated	Hyphal length over time
Meeuwse et al. (2012)	B+O+N	P	-	1	Smooth	Overculture	Biofilm	For SSF studies	Calibrated	Overall concentration of biomass, substrates and products over time
Mitchell et al. (1991)	B+N+E	P	-	0*	Smooth	Overculture	Aerial and surface	For SSF studies	Calibrated	Overall biomass concentration and glucoamylase activity over time
Prosser and Trinci (1979)	B+V	D	LF	2	Stepwise	Single colony	Surface	For single colony studies	Quantitative	Various measures of growth rates based on number of tips and total mycelial length
Rajagopalan and Modak (1995)	B+O+N+E	P	-	1$	Smooth	Overculture	Biofilm	For SSF studies	None	-

Table 2.2(cont)

Model	Components described[a]	Spatial treatment of biomass[b]	Type of lattice (for discrete models)[c]	Number of dimensions used to describe biomass	Treatment of temporal domain	Type of growth	Type of hyphae	Purpose of the model	Type of validation	Type of data used for validation/ calibration
Tunbridge and Jones (1995)	B+V	D	LF	2	Stepwise	Single colony	Surface	For single colony studies	Quantitative	The simulation results from Prosser and Trinci (1979) for number of tips and total mycelial length
Yang et al. (1992b)	B+V[#]	D	LF	3	Smooth	Pellet	Pellet	For studying pellet formation	Quantitative	Length and extension rate of the germ tube and a branch, total mycelium length and number of tips over time

[a] B = Biomass; V = Vesicles; O = O₂; N = Nutrient; E = Enzymes

[b] D = Discrete; P = Pseudohomogeneous; M = Microscale

[c] LB = Lattice bound; LF = Lattice free

Some authors use the term "precursors", representing material that is produced inside the hypha and transported to the tip. We have classified these "precursors" as being equivalent to vesicles.

* In the model of Mitchell et al. (1991), biomass is represented by an overall concentration at the solid surface, without any mention of its distribution in space, thus, biomass is described without any dimension.

$ In the model of Georgiou and Shuler (1986), the biomass concentration varies along the radius of a circularly symmetrical colony. In the model of Rajagopalan and Modak (1995), the dimension described by the model is the radius though a spherical particle covered with a biofilm; the biofilm thickness increases during the simulation.

variability on the results of the simulation, such that two simulations that start with the same initial conditions give different final mycelial morphologies.

Figure 2.8 Typical results that can be obtained with mesoscale models.
(A) Plots of the concentrations of biomass and tips as a function of distance from the solid surface, generated by a pseudohomogeneous model. (B) Images generated by a discrete 2D lattice-based model at different times of growth. (C) Images generated by a discrete 2D lattice-free model at different times of growth. The images used to illustrate the discrete models correspond to the marked area of the graph for the pseudohomogeneous model.
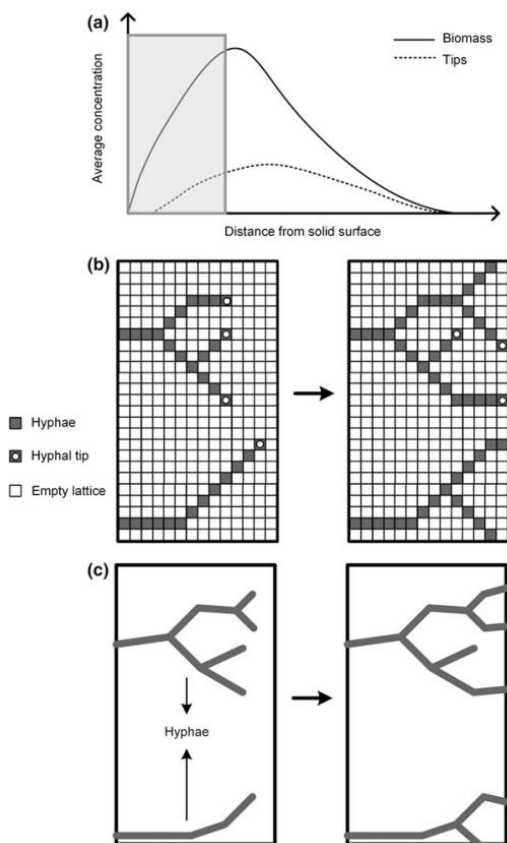
Discrete models can be further classified according to two criteria. Firstly, they can be classified as "smooth" or "stepwise", based on how

time is treated in the model: time progresses continuously in a smooth model but in discrete steps in a stepwise model, with these time steps normally being of the same size, although this is not essential. Secondly, they can be classified as being "lattice-based" or "lattice-free", on the basis of whether the hyphae are restricted to specific geometries or are free to grow in any position and direction in space (HOPKINS and BOSWELL, 2012). These two classifications are discussed in the following subsections.

2.4.1.1 Smooth and stepwise models

In a smooth model, state variables change continuously with time. The rates of change in these state variables, such as hyphal length or vesicle concentration, are typically expressed in the form of continuous differential equations. Conversely, in a stepwise model, state variables change abruptly with each time step, with the changes being expressed in the form of algebraic equations. In the specific case of hyphal extension, in smooth models, the hyphal length increases in a continuous manner over time. In stepwise models, new "units" of biomass are incremented in each time step. These "units" are often of a defined length, but it is also possible to add units of varying lengths.

There are three important considerations with respect to this classification. Firstly, these model types are often referred to in the general mathematical modeling literature as "continuous change and discrete change models" or "continuous time and discrete time models". In the context of the current review, where we have used the word "discrete" in relation to the spatial domain, we prefer to use a different pair of words with relation to the temporal domain. Secondly, the distinction between smooth and stepwise models is based on the formulation of the model equations, not on the mathematical methods used to solve them. This consideration is important, since the set of differential equations that is written in a smooth model is usually too complex to be solved analytically and is therefore solved using numerical methods. These methods may involve discretization of the temporal domain; however, the use of discretization as a mathematical tool to obtain an estimate of the solution of a smooth function does not make the function itself stepwise. Thirdly, even though the use of a very small time step may allow a stepwise model to make predictions that resemble smooth functions, the equations, as formulated, are not smooth.

2.4.1.2   Lattice-based and lattice-free models

In lattice-based models (Figure 2.8B), hyphae are only allowed to occupy positions within a previously defined lattice, which may consist of a network of segments or of a grid of "cells" (the latter being the case of cellular automata models, where the "cells" do not necessarily represent cells in the biological sense). The status of each segment or "cell" can change during the course of the simulation. For example, in a cellular automata model of fungal growth, when the simulation is initiated, a "cell" in a given location may have the status of "active tip". As the hyphal tip extends away from this location, the status of the "cell" (which now represents a part of the hypha behind the tip) changes to "active hypha" and a previously "empty" neighbor "cell" receives the status "active tip" (Figure 2.8B). Since the hyphae are constrained to be within these "cells", the images generated are restricted by the geometry of the lattice, which might not allow the model to represent the true geometry of a fungal mycelium. On the other hand, since the position of each hypha is registered, it is a simple matter to detect when a hyphal tip tries to occupy a "cell" that is already occupied by an existing hypha and thereby describe avoidance reactions or anastomosis.

In lattice-free models (Figure 2.8C), hyphae are described as line segments that can have any position and orientation within the spatial domain. Hyphal extension is represented by adding a new line segment at the tip of a previous segment, while branching is represented by adding two line segments at the tip (apical branching) or a new line segment at some position along an already existing segment (lateral branching). The added segments may have variable lengths and directions. In this manner, it is possible to generate images in which there are varying angles between hyphae and branches. The main disadvantages of lattice-free models are, firstly, that they do not describe the volume or area occupied by the hypha and, secondly, it is computationally much more difficult, compared to lattice-based models, to check whether an extending hypha will try to occupy a space that is already occupied by an existing hypha.

The degree to which these two model types generate images that resemble a real mycelium depends on the size of the lattice for a lattice-based model and the rules that are used, for a lattice-free model. For example, a lattice-based model that uses lattice divisions of the same scale as the diameter of the hypha and allows various angles of growth and branching may result in a more realistic image than a lattice-free model with branching angles being restricted always to 90°.

2.4.2 The representation of the physical system

2.4.2.1 The representation of the hyphae

For a mesoscale model to be useful for describing the morphology of a fungal mycelium in SSF, the manner of representing hyphae must comply with three requirements. Firstly, it must be possible to reproduce the morphology of the mycelium in a three dimensional environment with branching distances and angles that are similar to those seen under the microscope. Secondly, it must be possible to combine the physical representation with the mathematical equations that determine the rates of growth and other internal processes. Thirdly, it must be possible to represent different physiological states, not only in different regions of the hyphae at the same time, but also in the same hyphal segment, but at different times during the simulation. Table 2.3 lists various manners in which the hyphae have been physically represented in the selected models.

The representation used by Coradin at al. (2011) provides the basis for a model that can comply with all three requirements (Table 2.3). These authors used a stochastic and discrete lattice-based model to describe the distribution, in three dimensions, of vegetative and reproductive aerial hyphae within the space above a solid surface. This space was divided into cubes, with each cube having the same cross-sectional area as a hypha. A cube could be empty or occupied by a hyphal segment, a hyphal tip or a spore. Active hyphae extended through the addition of new cubes at their tips. The hyphae grew upwards, downwards, horizontally or diagonally. Vegetative hyphae could branch apically, with the daughter hyphae choosing directions of growth stochastically, amongst the available empty spaces around the branching tip. The number of cubes added per iteration was chosen so that the average distance between branches was of the same order as that reported by Trinci (1974). After a certain period of growth, all vegetative hyphae stopped growing and some active tips differentiated into reproductive hyphae. The reproductive hyphae also branched, but, contrary to vegetative hyphae, they only grew upwards.

The main advantage of the model of Coradin et al. (2011) is that the small lattice size allows a realistic representation of hyphal morphology and biomass distribution in space, while facilitating the localization of hyphae. Further, although the model does not contain

Table 2.3 Approaches used in previous models to represent hyphae and their environment.

Model	Type of lattice	Size of hyphal lattice	How extension occurs	Type of environment
Ideal approach	Any geometry with volume (i.e. 3D)	At the scale of the hyphal diameter	Based on the rate of vesicle fusion at the tip	Gas phase, biofilm layer and solid particle
Coradin et al. (2011)	Cubic	10 µm	-	Gas phase (as empty cubes)
Balmant (2013)	Cubic	10 µm	Uses mass balance equations for intracellular maltose and vesicles, with the extension rate being proportional to the rate of fusion of vesicles at the tip	Gas phase (as empty cubes)
Boswell et al. (2007)	Triangular for biomass and hexagonal for environment	100 µm	Extension depends on the probability of the hypha extending to an adjacent part of the lattice; this probability is proportional to the intracellular nutrient concentration	Solid particle, without penetration of hyphae
Tunbridge and Jones (1995)	Lattice free	-	The size of the mycelium is calculated first, without defining its distribution in space, with the extension rate being proportional to the rate of fusion of vesicles at the tip	No interactions with or descriptions of the surroundings
Fuhr et al. (2011)	Segments positioned randomly for biomass and rectangular parallelepiped for environment	50 µm	Extension depends on probabilities of the hypha extending to another pit, which is related to the nutrient concentration at the pit	Solid particle with penetration of hyphae

expressions for mass balances on intracellular components, it was designed for later incorporation of these expressions. This was done by Balmant (2013), who treated the series of cubes that represented a hypha in the model of Coradin et al. (2011) as a series of well-mixed tanks, with transport of intracellular material between adjacent tanks. Balance equations were written for two components, maltose and vesicles, over

each tank. In this well-mixed tank approach, these balance equations have the form of ordinary differential equations, unlike the partial differential equations that arise when balance equations are written over a hypha as a single continuous entity. The tanks forming the hypha were divided into three types: a "tip-tank" at the end of the hypha, vesicle-producing tanks and non-vesicle-producing tanks. A different set of equations was used for each type of tank, representing the physiological differences between them (more details on the equations used are provided in Section 2.4.3.1). Growth occurred through the addition of new tanks at the tip, with this addition depending on the rate of fusion of vesicles to the membrane within the tip-tank.

Although Balmant (2013) only modeled the extension of a single aerial hypha, with maltose being supplied at the base of the hypha, the well-mixed tank approach has the flexibility to be extended to describe phenomena involved in the development of a hyphal network in an SSF system, such as branching, nutrient absorption across the sides of the hypha (i.e. across the plasma membrane) and enzymatic hydrolysis of polymeric carbon and energy sources within the solid matrix, as will be discussed in later subsections. For convenience, from this point on, this approach will be referred to as the "Coradin-Balmant approach".

A model that can produce a realistic mycelial morphology, while describing internal processes, is that of Tunbridge and Jones (1995) (Table 2.3). It is a discrete, lattice-free model describing the growth of surface hyphae from a single spore. It incorporates the earlier model of Prosser and Trinci (1979), in which the hyphae are divided into sections. Vesicles are transported between adjacent sections, with the extension rate being proportional to the rate at which vesicles fuse at the tip (more details on the internal processes are provided in section 2.4.3.1). Since Prosser and Trinci (1979) did not aim to reproduce the morphology of the mycelium, they used 90° angles between branches and did not include changes in the direction of growth of extending hyphae. Tunbridge and Jones (1995) added random changes in growth directions and different angles between branches, by dividing the simulation into two parts. The first part uses the model of Prosser and Trinci (1979) to determine the final size of the mycelium, namely the position of each branch and the overall number of tips. In the second part, hyphal segments and branches are drawn in two-dimensional space, with random variations in growth direction and branch angles.

There would be two main problems with any attempt to adapt the Tunbridge and Jones (1995) model for the modeling of SSF systems. Firstly, it is lattice-free, therefore, the hyphae have no volume.

Consequently, if this approach were to be extended to describe growth in a three-dimensional environment, it would be difficult to track the position of each hypha and thereby avoid two hyphae occupying the same position in space. Secondly, since growth is calculated before the spatial distribution of the mycelium is determined, it would not be possible to include inactivation of hyphae due to high local biomass concentrations or to include the effects of the variation in the concentrations of nutrients in the local surroundings.

Another approach is that of Boswell et al. (2007) (Table 2.3). In this discrete model of the colonization of soil particles by a fungus, both the mycelium and the medium are represented by two-dimensional lattices. The medium is divided into a hexagonal lattice, with homogeneous concentration of nutrient within each hexagon. This is overlaid with a triangular lattice of 100-µm line segments that connect the centers of adjacent hexagons. Hyphae grow along these line segments, such that angles between adjacent hyphal segments are restricted to either 120° or 180°. The advantage of this model is that it already considers the interactions with the extracellular environment, while this still needs to be incorporated into the Coradin-Balmant approach. Also, the superposition of hyphae is prevented, since only a single hypha is allowed to enter each hexagon of the substrate lattice. On the other hand, the 100-µm long segments would not be appropriate for SSF systems, since a hyphal segment of this length could contain significant gradients of internal compounds and experience significant gradients of external compounds. Further, the two-dimensional triangular lattice only allows representation of surface hyphae and, even then, it does not even allow a proper representation of observed morphologies of these hyphae.

2.4.2.2   The representation of the surroundings

In SSF, a hypha can be in contact with one or more of three phases: the gas phase, the liquid of the biofilm layer and the matrix of the solid particle. The processes occurring in these phases should be described by mass balance equations that include mass transfer and the consumption and release of key compounds, such as O_2, soluble nutrients and enzymes.

In discrete models, the extracellular environment is also divided into a regular lattice. In the Coradin-Balmant approach, it would be divided into well-mixed tanks of the same size and shape as the ones used for the hyphae. This would facilitate the representation of the hyphae extending into their surroundings: as the hyphal tip extends into a tank, the status of that tank would change from "surrounding phase" to "hyphal

tip". Further, appropriate mass balances for enzymes, their hydrolysis products and other nutrients would be written over those tanks that represent the matrix of the substrate particle.

The two-dimensional hexagonal lattice that is used to represent the substrate in the model of Boswell et al. (2007) would not be appropriate for describing SSF systems: It would not be possible to describe how part of the volume within the solid particle is occupied by penetrative hyphae, nor to represent properly the concentration gradients that occur with depth below the particle surface.

Various models for growth of fungi over solid surfaces have treated the solid matrix as a homogeneous environment, without any physical barriers to diffusion, such as is the case when an artificial medium composed of a nutrient solution and a solidifying agent (e.g. agar or κ-carrageenan) is used (BOSWELL et al., 2007; MITCHELL et al., 1991). However, in SSF, the substrate particle is often composed of plant tissues, with cellular divisions, and the cell wall structure must be degraded in order for the hyphae to reach the nutrients contained within. The only model that describes penetrative growth of fungal hyphae in a plant tissue was developed by Fuhr et al. (2011). It is a three-dimensional discrete lattice-based and stochastic model for the growth of penetrative hyphae of a white-rot fungus in wood. The wood cells are represented by rectangular parallelepipeds (Table 2.3), the walls of which contain randomly distributed pits. These pits are locations of the cell wall that are easily degraded by the fungus, allowing hyphae to invade adjacent cells. In the model, hyphae extend from one pit to another, forming straight lines connecting the pits. All nutrients necessary for growth are considered to be concentrated at these pits. This model represents cell wall penetration well but presents some limitations, for example, it represents hyphae as segments without volume and it does not describe the occupation of the cell lumen by the hyphae nor does it describe the consumption of the nutrients inside the lumen.

The division of the extracellular space into cubes, as was done in the model of Coradin et al. (2011), allows for the representation of cellular substructures in particles. Agglomerations of cubes could be designated as substrate particles, with particular divisions between cubes representing cell walls. These particular divisions would be barriers to the diffusion of components and it would be made difficult for the hyphal tip to cross them.

2.4.3 Intracellular phenomena supporting growth at the tip

The production of new fungal biomass requires the supply of several different nutrients. However, for simplicity, it is common to assume that the carbon source is limiting and that all other nutrients are in excess; this section will focus on models that make this assumption. However, it should be noted that the models of Georgiou and Shuler (1986) and Meeuwse et al. (2012) describe the metabolism of both a carbon source and a nitrogen source, which enabled them to relate key events to the absence of nitrogen, such as the formation of reproductive structures or the production of intracellular carbohydrate reserves. The supply of molecular oxygen (O_2) can also be limiting; this aspect is discussed in Section 2.4.6.

2.4.3.1 Appropriate mass balance equations for nutrients and vesicles

Given the key roles of vesicles in tip extension and in initiation of branching (Section 2.3.2.1), a morphological model should describe their production, translocation and consumption within the hyphae. This should be done in a simplified manner, but the model should have at least three features. Firstly, vesicle production should be described as being limited to a specific region of the hypha (the vesicle-producing zone) and as depending on the concentration of a limiting nutrient. Secondly, translocation of vesicles to the tip along the cytoskeleton should be at a rate different from cytoplasmic flow. Thirdly, the tip extension rate should be proportional to the rate of vesicle consumption at the tip. Also, since the extension rate of a new hyphal branch increases exponentially with time until it reaches a maximum value and then remains constant, even if the vesicle concentration increases behind the tip membrane (PROSSER; TRINCI, 1979), the rate of vesicle consumption at the tip should be described using saturation kinetics. Saturation kinetics would also be appropriate to describe vesicle production. Finally, a single type of vesicle should be sufficient for mesoscale models, instead of trying to describe subpopulations of different types of vesicles. Among the mesoscale models for fungal growth, the only model to incorporate all of these characteristics is that of Balmant (2013) and, as a result, it is the only one to have predicted the vesicle concentration peak at the tip that occurs experimentally: of all the vesicles in the 50 μm nearest to the tip, about 60% are present in the first 10 μm behind the tip, decreasing to 17% in the region between 10 and 20 μm behind the tip and to less than 11%

in each of the remaining 10-µm segments (COLLINGE; TRINCI, 1974; GOODAY, 1971).

The model of Balmant (2013) describes the extension of a single unbranched aerial hypha, using a series of well-mixed tanks (Figure 2.9). Mass balance equations for maltose and vesicles were written over each of the three different types of tanks. In non-vesicle-producing tanks and vesicle-producing tanks, maltose is transferred between adjacent tanks by convective flow of the cytoplasm and diffusion, while vesicles are actively transported along the cytoskeleton towards the tip. Maltose is consumed for maintenance and, in the vesicle-producing tanks, also for vesicle production. The mass balance for maltose in the vesicle-producing tanks is given by:

$$\frac{d\,S_i|_j}{dt} = \overbrace{\frac{v}{\Delta z}(S_i|_{j-1} - S_i|_j)}^{\text{convection}} + \overbrace{\frac{D_S}{\Delta z^2}(S_i|_{j-1} - 2\,S_i|_j + S_i|_{j+1})}^{\text{diffusion}} - \overbrace{m\rho_X}^{\text{maintenance}} - \overbrace{\frac{1}{Y_\phi}\frac{k_p\,S_i|_j}{K_P + S_i|_j}}^{\substack{\text{vesicle}\\\text{production}}}$$

$$(2.1)$$

where $S_i|_j$ is the concentration of maltose in tank j, t is the cultivation time, v is the velocity of flow of the cytoplasm, Δz is the length of a tank, D_S is the diffusivity of maltose inside the hypha, m is the maintenance coefficient, ρ_X is the mass of dry cell material per unit of volume occupied by the hypha, Y_ϕ is the yield coefficient for production of vesicles from maltose, k_p is the maximum rate of vesicle production and K_P is the saturation constant for vesicle production.

The balance for vesicles in the vesicle-producing tanks is given by:

$$\frac{d\phi|_j}{dt} = \underbrace{\frac{\psi}{\Delta z}(\phi|_{j-1} - \phi|_j)}_{\substack{\text{active}\\\text{transport}}} + \underbrace{\frac{k_p\,S_i|_j}{K_P + S_i|_j}}_{\substack{\text{vesicle}\\\text{production}}}$$

$$(2.2)$$

where $\phi|_j$ is concentration of vesicles in tank j and ψ is the velocity of active transport of vesicles.

Figure 2.9 Illustration of the mass balances over vesicle-producing tank j in the model of Balmant (2013).
(A) Balance for maltose; and (B) Balance for vesicles.
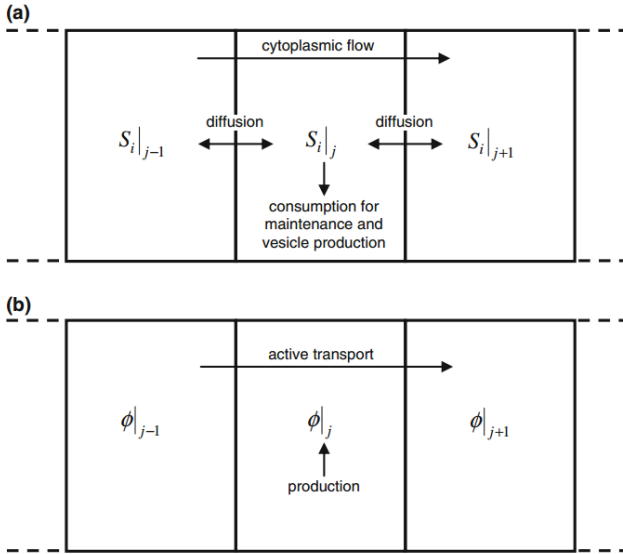
As a new tank is formed at the tip, the vesicle-producing tank that is furthest from the tip is converted into a non-vesicle-producing tank. The balances on the non-vesicle-producing tanks are similar to equations (2.1) and (2.2), but without the terms related to vesicle production.

Vesicle consumption occurs only in the tip-tank, increasing the length (L) of this tank at a rate that is proportional to the rate of vesicle consumption. Thus, the velocity of extension of the tip-tank is given by:

$$\frac{dL}{dt} = Y_L \frac{k_c \left.\phi\right|_n}{K_C + \left.\phi\right|_n}$$

(2.3)

where Y_L is the extension of hyphal length per mass of vesicles consumed, k_c is the maximum rate of vesicle consumption and K_C is the saturation constant for vesicle consumption. When the length of the tip-tank reaches double that of a normal tank (i.e. when $L = 2\Delta z$), it divides. The two new normal-sized tanks (i.e. each with $L = \Delta z$) each have concentrations of maltose and vesicles equal to the values for the double-sized tip-tank immediately before division. This approach to tip extension results in a

continuous increase in hyphal length. This contrasts with various stepwise models, in which a new segment of hypha of a fixed size is added per growth step, thus resulting in instantaneous production of new segments.

The tip-tank only consumes vesicles, it does not produce them. Thus, the balances on maltose and vesicles in this tank are, respectively:

$$
\frac{d\,S_i|_n}{dt} = \underbrace{-\left(\frac{S_i|_n}{L}\right)\frac{dL}{dt}}_{\substack{\text{tank}\\\text{extension}}} + \underbrace{\frac{v}{L}S_i|_{n-1}}_{\text{convection}} + \underbrace{\frac{D_S}{L\left(\dfrac{L+\Delta z}{2}\right)}(S_i|_{n-1}-S_i|_n)}_{\text{diffusion}} - \overbrace{m\rho_X}^{\text{maintenance}}
\tag{2.4}
$$

$$
\frac{d\,\phi|_n}{dt} = \underbrace{-\left(\frac{\phi|_n}{L}\right)\frac{dL}{dt}}_{\substack{\text{tank}\\\text{extension}}} + \underbrace{\frac{\psi}{L}\phi|_{n-1}}_{\substack{\text{active}\\\text{transport}}} - \underbrace{\left(\frac{1}{AL}\right)\frac{k_c\,\phi|_n}{K_C+\phi|_n}}_{\text{consumption}}
\tag{2.5}
$$

where A is the cross-sectional area of the hypha. The first term on the right-hand side of each equation describes the dilution that occurs due to the increase in the tank volume caused by tip extension.

Two other models that describe vesicles are those of Prosser and Trinci (1979) and López-Isunza et al. (1997). In the model of growth of surface hyphae of Prosser and Trinci (1979), processes involving nutrients are not described. The vesicle production rate is constant and vesicle production occurs throughout the entire mycelium, instead of being limited to the vesicle-producing zone. The rate of tip extension is proportional to the rate of vesicle fusion at the tip, which is described by saturation kinetics. The model of López-Isunza et al. (1997) describes the extension of a single germ tube, across the substrate surface, before the formation of the first branch. Two types of vesicles are described: Macrovesicles are produced throughout the germ tube, while microvesicles are produced at the tip from macrovesicles; production rates for both vesicles follow Michaelis-Menten-type kinetics. Partial differential equations describe the diffusion of nutrients and macrovesicles in both the axial and radial dimensions of the tube. Tip extension depends on the rate of vesicle fusion at the tip, which is directly proportional to both the concentration of microvesicles and the length of

the germ tube and follows saturation kinetics with respect to the concentration of macrovesicles. However, this model would not be appropriate for SSF, since the description of both radial and axial diffusion would be unnecessarily complex for the modeling of a whole mycelium. Another major drawback of this model is that it is not predictive, as the final length of the germ tube is used, at the start of the simulation, to calculate key parameters, namely the Damköhler numbers for vesicle production and cell wall synthesis at the tip.

2.4.3.2   Nutrient absorption across the membrane

The absorption of soluble nutrients across the plasma membrane of the hypha is often included in mathematical models for fungal growth. Since the transport of polar molecules across this membrane is mediated by carriers, it exhibits saturation kinetics and should be described by an expression similar to the following:

$$r_a = \frac{k_{max}S_e}{K_t + S_e}TA_L$$

(2.6)

where r_a is the rate of transport, S_e is the concentration of nutrient in the extracellular medium, T is the transporter concentration per area of the plasma membrane, A_L is the area of contact of the plasma membrane with the extracellular medium, k_{max} is the maximum specific transport rate and K_t is the saturation constant. The term T could be removed from the equation if the transporters were assumed to be evenly distributed across the area of contact along the hypha, as done by Edelstein and Segel (1983), who also considered that the area of contact was proportional to the biomass concentration. Transport could be included in the model of Balmant (2013) by adding an expression similar to equation (2.6) to the balance equations for intracellular maltose for those tanks in contact with extracellular nutrients (i.e. to equations (2.1) and (2.4)).

Some kinetic expressions that have been used in models to date do not allow for saturation, for example, that of Boswell et al. (2007), in which the uptake rate is first-order in the external substrate concentration (Table 2.4). On the other hand, López-Isunza et al. (1997) described, individually, the extracellular uptake by the transport protein, the diffusion of the transporter-substrate complex across the membrane and the release of substrate into the cytosol. However, this added complexity

does not bring any tangible advantages over equation (2.6) for mesoscale models.

Table 2.4 Approaches used by previous models in the description of intracellular substrates.

Model	Consumption of substrate	Intracellular transport	Absorption rate
Ideal approach	For vesicle production and cellular maintenance	Axial diffusion and cytoplasmic transport towards the tip	A function of the concentration of extracellular substrate through saturation kinetics and proportional to the absorption area (see Eq. (2.6))
Balmant (2013)	For vesicle production and cellular maintenance	Axial diffusion and cytoplasmic transport towards the tip	No absorption, rather supply of maltose from a source tank representing vegetative mycelium in the biofilm, from which the single unbranched aerial hypha that was modeled extended
Boswell et al. (2007)	For biomass production, cellular maintenance and absorption and active transport costs	Axial diffusion and active transport towards the highest concentration of tips	$r_a = c_1 S_i S_e X$
Edelstein and Segel (1983)	For biomass production and cellular maintenance	Axial diffusion and cytoplasmic transport towards the highest concentration of tips	$r_a = c_2 \dfrac{k_{max} S_e}{K_t + S_e} X$
López-Isunza et al. (1997)	For microvesicle and macrovesicle production	Axial and radial diffusion and axial convection towards the tip	Rate for nutrient uptake by the transporter: $\dfrac{k_{max} S_e T}{K_t + S_e}$ Rate for diffusion of the transporter-substrate complex in the membrane: $\propto \dfrac{\partial^2 \theta}{\partial \eta^2}$ Rate for intracellular release: $c_3 \theta$
Meeuwse et al. (2012)	Glucose: for biomass production, cellular maintenance and product formation. Alanine: for biomass production	Diffusion*	Free diffusion*

* In the model of Meeuwse et al. (2012), the biofilm layer is described as a homogeneous layer, without distinguishing the biomass and the liquid film individually.

2.4.3.3 Consumption of intracellular substrate for cellular maintenance

During the development of the mycelium, intracellular substrate is required to produce energy for other processes besides the production of vesicles, such as for active transport of nutrients across the membrane, transportation of vesicles along the cytoskeleton and enzyme production. It is not necessary for a model to describe the rates of intracellular substrate consumption for all of these processes individually; they can be combined in a single maintenance term. This maintenance term is usually expressed as the product of the biomass concentration and a constant maintenance coefficient, as in the models of Balmant (2013) and Meeuwse et al. (2012).

On the other hand, Boswell et al. (2007) explicitly described the substrate consumption associated with active transport across the membrane (Table 2.4). In their model, the substrate absorption rate (r_a) was expressed as:

$$r_a = c_1 S_i S_e X$$

(2.7)

where c_1 is a proportionality constant, S_i is the concentration of intracellular substrate, S_e is the concentration of extracellular substrate and X is the concentration of biomass participating in the absorption process. This expression is included in the balance equations for both the intracellular and the extracellular substrate, but with different values for the proportionality constant (c_1), such that more nutrient is removed from the external medium than it is added to the intracellular space. The difference between the rates therefore represents the amount of substrate needed to provide the energy for the active transport across the membrane. This approach requires an additional parameter to be determined, related to the energy cost of nutrient transport across the plasma membrane, and, at the moment, it is unclear if these energy costs are so high that they should be accounted for separately from the maintenance coefficient. For simplicity, it seems better to subsume all the processes for nutrient consumption that are not associated directly with growth within a general maintenance coefficient with a constant value.

2.4.3.4 Considerations about cytoplasmic flow and transport of vesicles

Once inside the hypha, nutrients diffuse and are transported towards the tip by the cytoplasmic flow, while vesicles are transported

actively along the cytoskeleton, at a rate that is different from the rate of cytoplasmic flow. Although intracellular diffusion of nutrients is commonly described in models, cytoplasmic flow has only been included in the models of López-Isunza et al. (1997) and Balmant (2013). Further, only the latter model allowed for different rates of cytoplasmic flow and vesicle transport (Table 2.4).

The models of López-Isunza et al. (1997) and Balmant (2013) describe a single nonseptate hypha and, hence, do not allow for changes in the cytoplasmic flow or the rate of vesicle transport when septa or branches are formed. In fact, adequate data about how these phenomena affect intracellular transport are not available, although some considerations can be made. For example, unplugged septa, such as those in *Aspergillus*, would not prevent cytoplasmic flow, but might reduce the flow rate. Additionally, the formation of new branches would increase the total cross-sectional area of flow after a branch, thus, if the flow rate in the mother hypha were to remain constant, the flow rate in each daughter branch would decrease. On the other hand, branching increases the number of tips, which is where the driving force of the cytoplasmic flow is generated (LEW, 2011); thus, the flow rate per tip might remain constant, with an increase in the flow rate in the mother hypha. At the very least, the cytoplasmic flow needs to be high enough to supply cytoplasm to the growing tips: the cytoplasmic flow in a given hyphal segment should be equal to or higher than the sum of the extension rates of the tips that are connected to it (HEATON et al., 2010).

For vesicles, the rate of transport depends on the cytoskeleton and on motor proteins, hence, it is influenced by the formation or interruption of these structures. Therefore, the rate of transport of vesicles may not be affected by an unplugged septum if its formation does not interrupt the cytoskeleton. On the other hand, it will be influenced by the formation of apical branches, which divides the vesicle flow between the two daughter hyphae.

Once an adequate understanding of these phenomena is obtained, descriptions can easily be incorporated into discrete models. One possible approach has already been implemented by Prosser and Trinci (1979) for vesicle transport: During the formation of an unplugged septum, the flow rate of vesicles decreased, linearly, to 10% of the flow rate that was present before septation began. For lateral branches, 90% of the vesicles continued in the direction of the main hypha, while 10% entered the lateral branch. On the other hand, the consequences of branching for cytoplasmic flow were not described in their model.

2.4.3.5   Septation

In septate hyphae, it is important to model septation because it influences intracellular transport of vesicles and nutrients and may be related to the formation of lateral branches. The only two models to have described septation have related it to the duplication of nuclei in the apical compartment. The first model, of Prosser and Trinci (1979), was applied to the growth of surface hyphae of *Aspergillus nidulans* and *Geotrichum candidum*. In this model, the apical compartment initially has four nuclei. This compartment extends, in very small steps; when the volume to nuclei ratio within it reaches a critical value, the number of nuclei starts to increase exponentially. When there are eight nuclei, a septum is formed in the middle of the apical compartment, dividing the nuclei equally on the two sides of the septum. The second model, of Yang et al. (1992b), describes the formation of pellets of *Streptomyces tendae* and *Geotrichum candidum* in submerged fermentation. This model also starts with four nuclei in the apical compartment. New nuclei are formed constantly, at a rate that is inversely proportional to the number of nuclei. Septation also occurs when the number of nuclei in the apical compartment reaches eight, dividing this compartment in half.

At the moment, there is no advantage to be gained in modeling the kinetics of formation of nuclei in mesoscale models of fungal growth in SSF. Septation could be modeled deterministically, by triggering septum formation at the moment the apical compartment reaches a certain length. This would lead to uniform spacing between septa. Alternatively, a stochastic expression could be used, leading to variable distances between septa. In both cases, the formation of the septa could be instantaneous or it could last for a certain period of time, in the manner of Prosser and Trinci (1979). In the model of Balmant (2013), particular interfaces between adjacent tanks could be designated as being septa, with appropriate changes in the diffusivities between the two tanks. Since both the distance behind the tip at which septum formation occurs and the time taken for the septum to form vary from fungus to fungus, any model will need to be calibrated with the use of microscopic observations of the particular fungus being modeled.

2.4.3.6   Formation of branches

Branching can be triggered in a model using either a deterministic or a mechanistic approach (Table 2.5). The deterministic approach would be used in a model that does not describe vesicles. It is based on the

Table 2.5 Approaches used by previous models in the description of branching and changes in growth direction.

Model	Type of branches	Formation of branches	Angles between branches	Changes in growth direction of unbranched hypha
Ideal approach	Describing the type of branching in the fungus being modeled	Based on vesicle concentration	Angles following a normal distribution	Angles following a normal distribution
Coradin et al. (2011)	Apical	In every iteration, at the active tips	Angles depend on the chosen direction of growth, which is determined through probabilities based on the distance from the particle surface	None
Hutchinson et al. (1980)	Lateral	In every iteration, with the distance between the active tip and the start of the new branch following a gamma function	Angles following a normal distribution centered at 56° and with a standard deviation of 17°	None
Prosser and Trinci (1979)	Apical and lateral	Occurs when concentration of vesicles at the tip or behind a septum surpasses a critical value	90° angles with mother hypha	None
Tunbridge and Jones (1995)	Same as Prosser and Trinci (1979)	Same as Prosser and Trinci (1979)	Angles following a normal distribution centered at 65° and with a standard deviation of 15°	20% probability of changes of direction occurring, with the new angle following a normal distribution centered at 10° and with a standard deviation of 3°
Yang et al. (1992a,b)	Lateral	Occurs a certain time after septation, with the time lapse being described by a normal distribution	Angles following a normal distribution centered at 0° and with a standard deviation of 29.1°	Angles following a normal distribution centered at 0° and with a standard deviation of 10.1°

principle that the ratio of the total hyphal length to the number of tips within the mycelium, a parameter called the hyphal growth unit (HGU), remains almost constant during development of the mycelium (TRINCI, 1974): whenever the HGU were to surpass a chosen value, then branching would occur, either at the tip or at a randomly-selected position within the sub-apical zone. In the mechanistic approach, branching occurs when there is accumulation of vesicles behind a septum (lateral branching) or at a tip (apical branching) (TRINCI, 1974). This could be done either by establishing a critical concentration of vesicles above which branching would occur or by expressing the probability of branching as being proportional to the concentration of vesicles.

The mechanistic approach could be incorporated into the model of Balmant (2013), since vesicles are already described to determine the extension rate. However, before incorporating branching, it is important to verify which type of branching occurs for each type of hypha for the fungus being modeled. For example, *Rhizopus oligosporus* grown on agar seems to form both apical and lateral branches in penetrative hyphae, but only apical branches in aerial hyphae (NOPHARATANA et al., 2003a,b). The choice of direction of growth of the new branch is discussed in Section 2.4.5.

2.4.3.7   Physiological differentiation within the mycelium

Many mathematical models for fungal growth on solid particles consider only the growth of surface hyphae. However, as explained in Section 2.3.1, growth of microcolonies over the substrate surface is only important in the initial stages of an SSF process. During much of the process, biofilm, aerial and penetrative hyphae are present simultaneously, with each hyphal type interacting with its environment in a different way. Another important characteristic of a mycelium is physiological differentiation: active hyphae can become inactive (i.e. losing the ability to extend), vegetative hyphae can give rise to reproductive hyphae, and a particular region of the hypha that is originally producing vesicles can stop producing them as the tip and the accompanying vesicle-producing zone extend away from it. A mesoscale model of SSF should be able to describe these changes.

The importance of describing differentiation of vegetative hyphae into reproductive hyphae was demonstrated by Coradin et al. (2011). These authors simulated density profiles for aerial hyphae of *Rhizopus oligosporus*, as a function of height above the surface of a solid substrate, and compared them with experimental results of Nopharatana et al.

(2003b). Nopharatana et al. (2003b) obtained an "early profile", before sporangiophores appeared, and a "later profile", after sporangiophores appeared. In the work of Coradin et al. (2011), a model including only vegetative hyphae could only describe the early profile; it was only possible to describe the later profile by incorporating reproductive hyphae, with different extension and branching rules than those of the vegetative hyphae, into the model. This would explain why the pseudohomogeneous model of Nopharatana et al. (1998), which considered only vegetative hyphae, gave biomass profiles that were similar to the early profile of Nopharatana et al. (2003b), but not to the later profile.

The simplest approach to describing different physiological states within a single hypha is that used by Balmant (2013). The model recognizes three separate regions with different physiologies: first, a non-vesicle-producing zone, which only consumes substrate for cellular maintenance and therefore does not contribute to tip extension; second, a vesicle-producing zone, where substrate is consumed for maintenance and vesicle production; and, third, a tip, in which vesicles are incorporated, driving hyphal extension. This approach could be further adapted to describe other types of physiological differentiation, for example, the production of hydrolytic enzymes being limited to the tip-tank. In addition, it is possible to have different maintenance coefficients for each type of tank, reflecting their different physiologies.

The trigger used for each differentiation process varies. Inactivation of a hyphal tip should occur when there is either no available internal substrate or no empty space to extend to. For example, in the model of Boswell et al. (2007), inactivation of a hyphal segment occurs when the concentration of intracellular substrate is less than the value that is required for cellular maintenance. On the other hand, in the model of Coradin et al. (2011), who did not include substrate-related phenomena, inactivation of a tip occurs when it tries to extend, for the second time, into a cube in the lattice that is already occupied by biomass.

A simple way to describe differentiation of vegetative hyphae into reproductive hyphae is to use the age of the mycelium as the trigger, as done by Coradin et al. (2011). However, the formation of reproductive structures can also be triggered by growth conditions, such as a low nutrient concentration or a low water activity in the surroundings. A combination of triggers was used by Georgiou and Shuler (1986) in their pseudohomogeneous model for growth of surface and aerial hyphae in a single colony: reproductive hyphae were only formed from vegetative hyphae that were older than 24 h (representing the time required to

accumulate the intracellular carbohydrates used to support the growth of reproductive structures) and only when the concentration of nitrogen was lower than a critical value.

2.4.4   Phenomena occurring within the matrix of the substrate particle

The most important phenomena that occur within the matrix of the solid particle and which, therefore, should be included in a mesoscale model for fungal growth in SSF, are: enzyme secretion near the hyphal tip, enzyme diffusion in the matrix of the solid particle, hydrolysis of polymeric carbon and energy sources into soluble hydrolysis products and diffusion of these soluble hydrolysis products, soluble nutrients and O_2 in the matrix of the solid particle.

Mitchell et al. (1991) incorporated several of these phenomena into a pseudohomogeneous model for fungal growth on the surface of a solid medium. Experimentally, formation of penetrative biomass was prevented by a membrane placed directly on the surface of the solid, while nutrients and enzymes could diffuse across the membrane (MITCHELL et al., 1989).

In the model, processes involving the components within the solid particle (i.e. starch, glucose and glucoamylase) are described with mass balance equations, forming a system of partial differential equations. The mass balance equation for glucose (S_e) includes diffusion in the medium and formation through the hydrolysis of starch by glucoamylase, following Michaelis-Menten kinetics:

$$\frac{\partial S_e}{\partial t} = \underbrace{D_S^e \frac{\partial^2 S_e}{\partial z^2}}_{\text{diffusion}} + \underbrace{Y_E \frac{k_{cat} E S_p}{K_m + S_p}}_{\text{formation}}$$

(2.8)

where z is the depth in the substrate matrix, D_S^e is the effective diffusivity of glucose in the matrix of the particle, Y_E is the yield of glucose from starch, k_{cat} is the catalytic constant of glucoamylase, S_p is the concentration of starch and K_m is the saturation constant.

Starch is considered to be immobile, thus, its mass balance equation describes only its hydrolysis by glucoamylase:

$$\frac{\partial S_p}{\partial t} = -\frac{k_{cat} E S_p}{K_m + S_p}$$

(2.9)

The mass balance equation for glucoamylase within the matrix of the particle includes only diffusion:

$$\frac{\partial E}{\partial t} = -D_E \frac{\partial^2 E}{\partial z^2}$$

(2.10)

where D_E is the effective diffusivity of the glucoamylase in the solid particle and E is the glucoamylase concentration.

Secretion of glucoamylase occurs only at the surface of the solid medium, so that the secretion rate is used as a boundary condition:

$$J_E\big|_{z=0} = D_E \frac{\partial E}{\partial z}\bigg|_{z=0} = r_E H(t_E - t)$$

(2.11)

where $J_E\big|_{z=0}$ is the flux of glucoamylase across the surface of the particle, r_E is the rate of secretion of glucoamylase (which has a constant value while glucoamylase is being secreted), $H(t_E-t)$ is a Heaviside function, which is equal to 1 when $t<t_E$ and 0 when $t>t_E$, therefore t_E is the time when the secretion of glucoamylase ceases. Equation (2.11) is a simple empirical description of the experimentally observed secretion profiles: In real SSF systems, enzyme production depends on complex induction and repression mechanisms that are, as yet, not sufficiently understood for incorporation into mesoscale mathematical models.

This model was able to describe a key experimental observation, namely the clearing of starch from the region near the surface of the substrate particle due to the action of the glucoamylase. Once this happened, only the glucoamylase that managed to diffuse past the cleared zone could contribute to the release of glucose from the starch within the substrate matrix. As a result, the rate of supply of glucose to the biomass at the surface limited the growth rate for most of the cultivation (MITCHELL et al., 1991).

This approach to modeling the processes that occur within the matrix of the substrate particle could be incorporated into a discrete model, such as that of Balmant (2013). The extracellular matrix would be divided into well-mixed tanks, of the same size as the tanks used to

describe the hypha. Mass balance equations similar to equations (2.8) to (2.11) would be written for the extracellular components, except that all equations would be ordinary differential equations in time, since there is no spatial coordinate. It would be necessary to limit enzyme secretion to the tanks representing the hyphal tips, as this is the site at which it occurs (WÖSTEN et al., 1991). Of course, it would also be necessary to describe the growth of penetrative hyphae, as enzyme secretion from these hyphae reduces the distance over which the enzyme must diffuse in order to reach the polymeric carbon and energy source (VARZAKAS, 1998; RAHARDJO et al., 2006).

2.4.5   Choice of hyphal growth direction

A mathematical model that proposes to reproduce the morphology of the fungal mycelium in SSF in a realistic manner must allow for changes in the direction of growth of an extending unbranched hypha and also for realistic angles between branches, similar to those observed in micrographs. The direction of growth of hyphae results from a combination of many factors, such as the substrate composition, the fungal species under study, the type of hypha and tropisms.

In a model, the direction of hyphal extension could be chosen stochastically or deterministically. The stochastic approach was used by Hutchinson et al. (1980) and Yang et al. (1992a,b), who showed, experimentally, that the angles formed between daughter and mother hyphae followed a normal distribution (Table 2.5). They then developed lattice-free models in which the angles between branches followed a normal distribution with a mean of 56° and a standard deviation of 17°, for surface hyphae of *Mucor hiemali* (HUTCHINSON et al., 1980), and with a mean of 90° (i.e. perpendicular to the direction of the parent hypha) and a standard deviation of 29.1°, for pellet growth of *Streptomyces tendae* in submerged liquid fermentation (YANG et al., 1992a).

For an extending unbranched hypha within a pellet, Yang et al. (1992a) observed that, although the hypha does deviate, the overall growth direction changes little. In their model, an extending hypha intermittently changed its growth direction according to a normal distribution centered at 0°, with a standard deviation of 10.1°. Hutchinson et al. (1980) did not incorporate changes in growth direction of an extending unbranched hypha in their model.

The advantages of this stochastic approach are its simplicity and its ability to generate patterns that appear similar to real mycelia. The

drawback is that these angles must be measured experimentally for each type of hypha. Also, for this approach to be used in a lattice-based model, the measured angles need to be distributed amongst the limited number of angles that are available in the particular lattice used.

The deterministic approach to controlling branch angles and growth directions of hyphae is based on tropisms. It requires identification of the factors that influence growth direction and the explicit incorporation of these factors in the model. Such factors might include the concentrations of nutrients or inhibitory compounds in the surroundings, but it is difficult to identify all the influences, especially since most studies on tropism are for surface hyphae. As a result, our current knowledge is insufficient for incorporating the deterministic approach into mesoscale SSF models.

2.4.6 Availability of O_2 and respirative or fermentative metabolism

As the mycelium develops on the particle surface, producing an ever thicker biofilm, a stage will be reached when the supply of O_2 into the interior of the biofilm is lower than the rate of consumption of O_2 by the biomass (Section 2.3.2.3). The lack of O_2 will affect growth of hyphae in the anaerobic regions of the biofilm and of penetrative hyphae within the substrate particle. O_2 diffusion in the extracellular environment and consumption for hyphal growth and maintenance must therefore be incorporated into a mesoscale mathematical model of SSF. As O_2 diffuses freely across the plasma membrane, it is not necessary to include special expressions (i.e. expressions for carrier-mediated transport similar to equation (2.6)) to describe O_2 transport into the hypha; however, a mass balance of O_2 within the hypha should be included. Intracellular phenomena that rely on O_2 can be expressed as functions of the local intracellular O_2 concentration.

The main question is which biological phenomena should be expressed as depending on the concentration of O_2 and how this dependence should be expressed mathematically. The two phenomena that are the most affected by the O_2 concentration are the growth rate and the type of metabolism, which can be "respirative" or "fermentative". The only model to relate the growth rate to O_2 concentration in SSF was that of Rajagopalan and Modak (1995), a pseudohomogeneous model that describes the growth of a fungal biofilm around a spherical particle, without hyphal penetration into the particle. The rate of biomass growth

(r_X) was expressed as depending on the concentrations of glucose and O_2 in the biofilm layer, according to a double-Monod expression:

$$r_X = \frac{\mu_{max} S^f}{K_s + S^f} \frac{C_{o_2}^f}{K_{O_2} + C_{o_2}^f} X$$

(2.12)

where μ_{max} is the maximum specific growth rate constant, S^f is the concentration of glucose in the biofilm, K_s is the saturation constant for glucose, $C_{o_2}^f$ is the O_2 concentration in the biofilm and K_{O_2} is the saturation constant for O_2. In a model that describes hyphal tip extension as depending on the production and consumption of vesicles, the influence of O_2 concentration could be incorporated into the expression for vesicle production. In the model of Balmant (2013), this could be done by using the expression of Rajagopalan and Modak (1995) within the term for vesicle production in the mass balance of maltose (i.e. within equation (2.1)). With this modification, the mass balance of maltose would be:

$$\frac{d S_i|_j}{dt} = \overbrace{\frac{v}{\Delta z}(S_i|_{j-1} - S_i|_j)}^{\text{convection}} + \overbrace{\frac{D_S}{\Delta z^2}(S_i|_{j-1} - 2 S_i|_j + S_i|_{j+1})}^{\text{diffusion}}$$

$$\underbrace{-m\rho_X}_{\text{maintenance}} - \frac{1}{Y_\phi} \underbrace{\frac{k_p S_i|_j}{K_P + S_i|_j} \frac{C_{O_2}|_j}{K_{O_2} + C_{O_2}|_j}}_{\substack{\text{consumption} \\ \text{for growth}}}$$

(2.13)

where $C_{o_2}|_j$ is the O_2 concentration in tank j.

As some fungi can switch to fermentative metabolism in regions of the mycelium where O_2 is limiting, the local intracellular O_2 concentration could be used in the model as a trigger for a metabolic shift between respirative and fermentative metabolism. In other words, fermentative metabolism would occur at O_2 concentrations lower than a critical value. In fermentative metabolism, the mass balance equations for nutrient or vesicles would have the same form as in respirative metabolism, but the parameters related to rates and yields would have different values. However, we currently know little about fermentative metabolism in filamentous fungi and this is probably the reason that

fermentative metabolism has never been included in a mesoscale model for SSF. In the few models that do include a balance for O_2, such as those of Rajagopalan and Modak (1995) and Meeuwse et al. (2012), whenever the O_2 concentration reaches zero, biomass growth and any other biological reactions stop completely.

A balance equation for O_2 will include consumption terms. Typically there will be two consumption terms, one related to the production of biomass or vesicles and the other related to maintenance metabolism. Rajagopalan and Modak (1995) considered that O_2 was used only for biomass growth, so that the mass balance for O_2 in the biofilm was:

$$\frac{\partial C_{o_2}^f}{\partial t} = \underbrace{\frac{D_{o_2}^f}{r} \frac{\partial}{\partial r}\left(r^2 \frac{\partial C_{o_2}^f}{\partial r} \right)}_{\text{diffusion}} - \underbrace{\frac{1}{Y_{X/O_2}} \frac{\mu_{\max} S^f}{K_s + S^f} \frac{C_{o_2}^f}{K_{O_2} + C_{o_2}^f} X}_{\text{consumption for growth}} \qquad (2.14)$$

where $D_{o_2}^f$ is the effective diffusivity of O_2 in the biofilm layer, r is the radial position in the biofilm and Y_{X/O_2} is the yield of biomass based on O_2 consumption.

A different approach was adopted by Meeuwse et al. (2012). Their pseudohomogeneous model describes the growth of a fungal biofilm over the surface of a substrate particle, without hyphal penetration. In this model, the rate of O_2 consumption (r_{O_2}) is calculated based on the rates of biomass growth, nutrient consumption and metabolite production:

$$r_{O_2} = 1.1675 r_X + 1.4325 r_{LI} + r_{IP} + 1.5 r_{EP} + 3.75 r_N + r_S \qquad (2.15)$$

where r_{LI} is the rate of production of lipids, r_{IP} is the rate of production of storage carbohydrates, r_{EP} is the rate of production of extracellular products, r_N is the rate of consumption of alanine and r_S is the rate of consumption of glucose. However, other than a cessation of O_2-consuming processes in the absence of O_2, the rates of growth and production of metabolites were not influenced by the O_2 concentration itself.

There are at least three important questions, the answers to which might influence future model development. Firstly, does the growth rate

really depend on the O_2 concentration? Above a certain O_2 concentration, growth is fully respirative, and it may not be useful to express the growth rate as a function of O_2 concentration if K_{O_2} is very low (RAHARDJO et al., 2005a). Of course, if fermentative metabolism does occur in the absence of O_2, then it is still necessary to describe the effect of the type of metabolism on the growth rate. Secondly, how would the shift to anaerobic conditions change the kinetic and yield parameters used for calculating the maintenance coefficient and vesicle production rate? It would be important to determine these parameters for both respirative and fermentative metabolism, before incorporating fermentative metabolism in the model. Thirdly, do hyphae that are in aerobic regions supply O_2 or metabolites derived from respirative metabolism to the penetrative hyphae? This possibility was raised by Nopharatana et al. (2003a), who suggested that hyphae penetrating into deep regions of the substrate particle might receive ATP or other precursors from hyphae closer to the surface. Later, te Biesebeke et al. (2006) showed that the genomes of *Aspergillus* species contain several genes that code for domains of hemoglobin and that the superexpression of one of these domains in *Aspergillus oryzae* resulted in a higher growth rate and greater enzyme production compared to the parent strain. If there is such a transport system for intracellular O_2 or precursors of biosynthesis, then a segment of hypha surrounded by an anaerobic environment might not turn to fermentative metabolism if it receives these precursors. This would affect how the fermentative metabolism is triggered.

2.5   CONCLUDING REMARKS

Many SSF processes involve filamentous fungi and a mathematical model of what happens at the particle scale could be an important tool for understanding not only how the mycelial mode of growth of these fungi affects bioreactor performance but also how bioreactor operation affects the development of the mycelium. However, there is currently no model that describes, at an appropriate level of detail, all of the relevant mass transfer and biological processes that occur in the spatially heterogeneous bed of solid substrate particles. Notwithstanding, we have shown that many of the individual phenomena that would be included in such a model have been adequately represented in models that have already been developed to describe fungal growth in various systems. Further, we have argued that the Coradin-Balmant approach to representing the system, which involves treating the hyphae as series of well-mixed tanks, has

several advantages. First, it allows a realistic representation of the network of hyphae in the mycelium. Second, it can readily be extended, through the incorporation of new expressions, to describe phenomena that one may desire to include in the model. Third, it involves only ordinary differential equations, expressed in terms of time; in other words the spatial coordinate does not appear in the balance equations and, consequently, there is no need to solve partial differential equations. Fourth, as a consequence of the division of hyphae into tanks, it becomes a simple matter to represent different physiologies along a single hypha. In conclusion, it is our opinion that the current knowledge that is available in the literature can underpin the development of a suitable mesoscale model for describing the growth of filamentous fungi in SSF.

3 COLONIZATION OF SOLID PARTICLES BY *Rhizopus oligosporus* AND *Aspergillus oryzae* IN SOLID-STATE FERMENTATION INVOLVES TWO TYPES OF PENETRATIVE HYPHAE: A MODEL-BASED STUDY ON HOW THESE HYPHAE GROW

3.1 INTRODUCTION

The performance of a solid-state fermentation (SSF) process with a filamentous fungus is influenced by the extent of growth of the network of hyphae formed above and inside the solid particles of the bed. At the mesoscale, the inter-particle spaces are filled up by hyphae and the substrate particles soften and shrink as a result of hydrolysis by enzymes secreted by the fungus. These mesoscale processes have consequences for the macroscale: in forcefully-aerated beds, they cause the pressure drop to rise and, eventually, the shrinking of the substrate bed and subsequent formation of preferential flow channels; these phenomena reduce the effectiveness of heat removal from the bed. It is therefore essential to understand these mesoscale processes (SUGAI-GUÉRIOS et al., 2015).

For the study of mesoscale processes, the hyphal network is divided into four types of hyphae: surface, biofilm, penetrative and aerial (SUGAI-GUÉRIOS et al., 2015; RAHARDJO et al., 2006). These different types of hyphae are formed at different stages of the colonization of the substrate particle and are subjected to different growth conditions, with different hyphae suffering from either limited O_2 availability or limited nutrient availability, or both. Although all these hyphal types have important roles in SSF processes, few experimental studies have focused on penetrative hyphae. Further, there has been no attempt to model the growth of penetrative hyphae in SSF; modeling work has focused on the other types of hyphae (SUGAI-GUÉRIOS et al., 2015).

Penetrative hyphae grow into the intercellular spaces of the solid substrate, pushing cells of the substrate apart, and, if the extracellular enzymes necessary for digestion of cell wall polymers are produced, they

are also able to grow into the lumen of the cell, gaining access to the nutrients within (CHAHAL et al., 1983). At the mesoscale, the growth of penetrative hyphae provides physical support, anchoring the mycelium to the solid particle, and improves the rate of hydrolysis of extracellular nutrients by decreasing the distance between the sites where enzymes are secreted and where the polymeric nutrients are located (MITCHELL et al., 1989; VARZAKAS, 1998). In addition, the spatial distribution of biomass inside the particle correlates with the production of some enzymes. For example, the production of acid protease and acid carboxypeptidase in rice *koji* by *Aspergillus oryzae* is related to the degree of hyphal penetration into the grain, with higher production occurring at lower degrees of penetration (ITO et al., 1989). However, the factors that determine the degree of penetration have not been investigated.

Another aspect that needs to be investigated is the formation of two types of penetrative hyphae by some fungi, which can be easily observed in the micrographs of *Rhizopus oligosporus* growing on PDA (potato dextrose agar) (NOPHARATANA, 1999; NOPHARATANA et al., 2003). Micrographs obtained at 16 h and 40 h of cultivation show two populations of penetrative hyphae: short penetrative hyphae and long penetrative hyphae. Most of the biomass inside the PDA consists of short penetrative hyphae, which have many branches but only grow as deep as 2.0 mm in 40 h; meanwhile, long penetrative hyphae have few and short branches but penetrate up to 4.5 mm into the medium in 40 h. Both types of penetrative hyphae extend from nodes that are connected by stolons, forming rhizoids, and provide anchorage for the reproductive aerial hyphae (SHURTLEFF; AOYAGI, 1979). However, it is unclear as to why two different types of penetrative hyphae are formed.

The purpose of this work was to develop a discrete model, which we call a layer model, to describe the growth of penetrative hyphae in solid media. The rules used in the layer model are based on a visual analysis of micrographs of penetrative hyphae of *R. oligosporus* in PDA obtained by Nopharatana et al. (2003b). The model was used to describe the density profiles with depth for penetrative hyphae of *R. oligosporus* in PDA and in an artificial medium with κ-carrageenan, obtained by Nopharatana et al. (NOPHARATANA et al., 2003a), and for penetrative hyphae of *A. oryzae* in particles of a real solid substrate, namely rice grains, obtained by Ito et al. (1989). The layer model was further used to raise hypotheses regarding the factors that influence the distribution of penetrative hyphae as a function of depth from the solid surface. A discrete approach was chosen because it can be extended later to describe

the growth of penetrative hyphae in a three-dimensional space, similar to the model that Coradin et al. (2011) developed for aerial hyphae.

3.2 MODEL DEVELOPMENT

3.2.1 Data for growth of penetrative hyphae in PDA

The layer model was developed to describe the growth of penetrative hyphae of *Rhizopus oligosporus* in PDA, based on the micrographs obtained by Nopharatana et al. (2003b) for 16 and 40 h of incubation. It recognized the existence of the two types of penetrative hyphae visible in these micrographs, long and short penetrative hyphae, with different growth rules being used for each type of hypha.

Nopharatana et al. (2003b) used their micrographs to generate biomass concentration profiles as a function of depth inside the medium, for both incubation times. At depths greater than 1.2 mm, which represents the region occupied only by the long penetrative hyphae, there was no significant difference in the profiles at the two times, 16 and 40 h. This indicates that the long penetrative hyphae had grown to their maximum length before the first micrographs were obtained, at 16 h, and, consequently, it is not possible to determine when these hyphae stopped growing. Therefore, this data set is not helpful for the adjustment of parameters of a model for long penetrative hyphae. The biomass concentration profiles of Nopharatana et al. (2003b) can, on the other hand, be used to calibrate a model for the growth of short penetrative hyphae, which grew significantly between 16 h and 40 h. Therefore, the layer model of penetrative hyphae was developed for both types of penetrative hyphae but calibrated only for short penetrative hyphae.

There are only two other sources of quantitative data for penetrative biomass in the literature: one is for *R. oligosporus* growing in a starch-containing medium with κ-carrageenan as the gelling agent (NOPHARATANA et al., 2003a), but it presents the same problem for long penetrative hyphae, with the first micrograph being taken after they stopped extending; the other is for *Aspergillus oryzae* growing on rice *koji* (ITO et al., 1989), but it only contains data for the short penetrative hyphae.

The experimental profiles of concentration of penetrative hyphae with depth from Nopharatana et al. (2003b) correspond to short and long penetrative hyphae together. In order to use this data to calibrate the model for short penetrative hyphae, it was necessary to obtain their

concentration profile. Since long penetrative hyphae have only few short branches, their concentration was assumed to be constant at 0.28 g L^{-1} over the entire depth. This value was obtained as the average, in both the 16-h and 40-h micrographs, between the depths of 1.6 and 3.1 mm, where there are only long penetrative hyphae. This value was subtracted from the measurements at all depths obtained by Nopharatana et al. (2003b) to give the concentration profile of short penetrative hyphae.

3.2.2   Overview of the layer model for penetrative hyphae

The space below the medium surface is divided by horizontal planes into a stack of discrete layers, each 140 µm thick (Figure 3.1). Branching can only occur at the divisions between layers and, therefore, this layer thickness imposes a minimum distance between branches of 140 µm (TRINCI, 1974). The area analyzed in the simulation is 1 mm², such that the volume of each layer is 0.14 mm³. Hyphae are represented by segments that are 140 µm long and have a cross-sectional area of 100 µm^2, which is approximately the cross-sectional area of hyphae of *R. oligosporus* (NOPHARATANA, 1999). These segments may be attached to other segments at both ends, or they may be free at one end. A free end may represent either the original site of hyphal penetration into the solid or a tip. Tips can be inactive (incapable of adding new segments) or active (capable of adding new segments).

The simulation occurs in iterations. During each iteration, an active hyphal tip produces a new segment, which is always oriented vertically downwards (Figure 3.1), with the active tip being relocated to the free end of the new segment. At the end of each iteration, each tip is always located exactly on one of the planes that mark the boundaries between the layers (Figure 3.1). The exact horizontal position of the segment within the layer is not defined, only the layer to which the segment belongs. Before the end of each iteration, new branches may be formed and tips may inactivate. The rules governing these phenomena differ for short and long penetrative hyphae and are described in the next sections.

During the simulation, for the decisions ruled by probabilities, random numbers were generated using the random_number and random_seed functions of FORTRAN, which generates random numbers (x) uniformly distributed over the range $0 \leq x < 1$.

Figure 3.1 Schematic drawing of the procedure used in the layer model for the addition of new segments of short penetrative hyphae inside the medium.
The expanded view of the first three layers below the medium surface shows the segments added in the first three iterations), the numbers indicate the iteration in which each segment was formed. The arrows inside the segments indicate the direction of growth and the symbol '×' indicates the position of the tip in the segment; a white '×' represents an active tip while a black '×' represents an inactive tip. New segments are formed at the surface in every iteration and hyphae only extend downwards. The drawing is not to scale and is for illustrative purposes; it does not represent a specific simulation result.
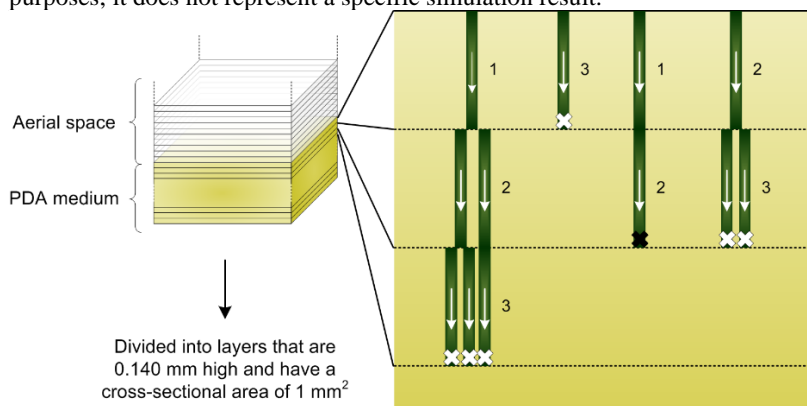
3.2.3   Layer model for growth of short penetrative hyphae

The model for short penetrative hyphae initiates with a defined number of hyphal tips (N_0), located immediately under the solid surface, from which penetrative hyphae extend in the first iteration, occupying the first layer (Figure 3.2A). In all the following iterations, new tips are added immediately below the surface, at a rate defined by N_h (tips per hour). The hourly formation of new tips at the surface could represent the continuous formation of penetrative hyphae from existing nodes or the establishment of new nodes, through the extension of stolons to new regions.

During the iteration in which they are formed, new tips only extend. For older tips, at the beginning of each iteration, each active hyphal tip is tested to determine how many hyphae will extend from that tip (0, 1 or 2). This is done by generating two random numbers and comparing them to the probability of extension (P_E), which is given by:

$$P_E = P_{E,\max}\left(1 - \frac{d}{d_{\lim}}\right)^k$$

(3.1)

Figure 3.2 Flowsheet of the layer model for penetrative hyphae.
(A) The submodel for the growth of short penetrative hyphae. In each iteration, new tips are formed at the surface and under the surface through apical branching. The parameter values used in this submodel are given in Table 3.1. (B) The submodel for the growth of long penetrative hyphae. In this submodel, new tips are formed only through subapical branching. The simulation ends at 40 h for short penetrative hyphae and at tf for long penetrative hyphae.
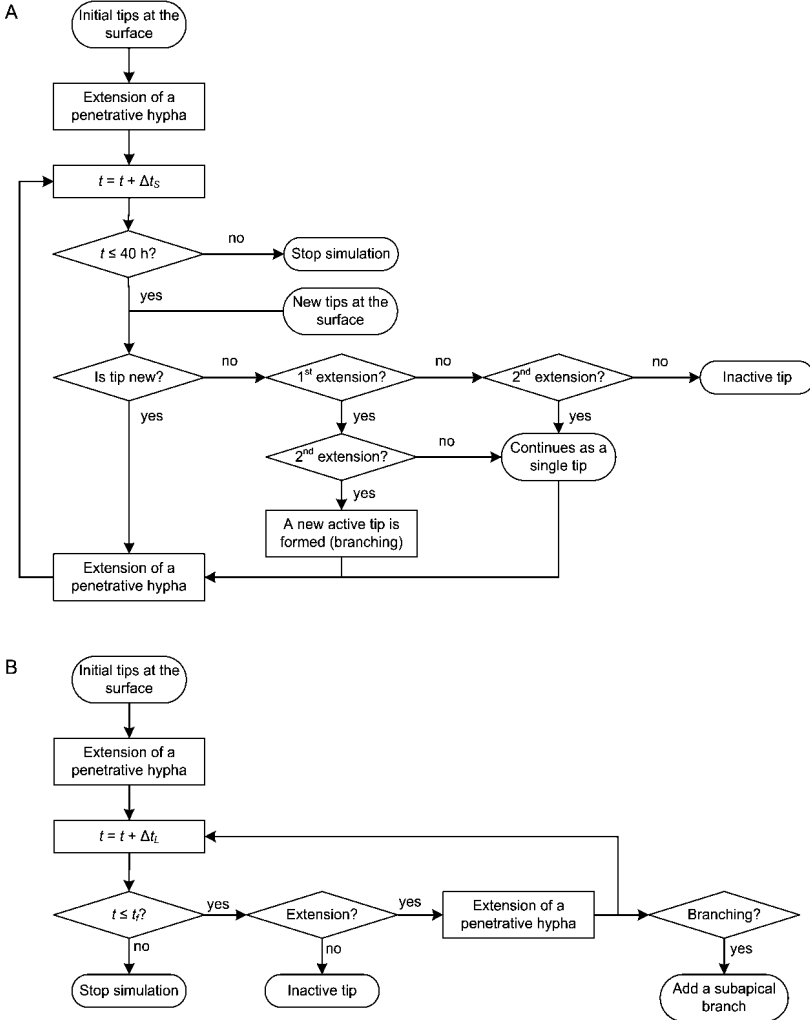
In this equation, $P_{E,\max}$ is the maximum probability of penetrative hyphae extending, d is the current depth of the hyphal tip, $d_{\lim}$ is the limiting depth for growth of short penetrative hyphae and k is a measure of how the probability of extension varies with depth. If both random numbers are less than P_E, then the active tip branches, such that two segments extend from it (Figure 3.2A). If only one of the random numbers is less than P_E, then the hypha remains as a single hypha and extends. If neither random number is less than P_E, then the tip is inactivated. This procedure to determine if a tip will branch was chosen based on the micrographs of Nopharatana et al. (2003b), in which short penetrative hyphae present few branches, which seem to be apical, and the distance between branches is not regular. The simulation ends at 40 h of cultivation.

3.2.4 Layer model for growth of long penetrative hyphae

A layer model for long penetrative hyphae was developed, however, none of the parameters of the layer model for long penetrative hyphae were determined, due to lack of appropriate experimental data, that is, of changes in biomass concentration with time. The rules used in the model for long penetrative hyphae and the values of its parameters remain to be validated with appropriate data.

The model for long penetrative hyphae also initiates with a number of hyphal tips immediately below the surface, from which hyphae extend in the first iteration, however, there is no addition of new tips in the following iterations (Figure 3.2B). At the end of each iteration, for each tip of a long penetrative hypha, one random number is generated and compared to the value of P_E given by equation (3.1). In this case, a different (higher) value is used for $d_{\lim}$, because long penetrative hyphae reach greater depths and there is almost no inactivation at smaller depths. If the random number is less than P_E, then a new segment is added at the hyphal tip; if not, then the tip inactivates.

In the model for long penetrative hyphae, branches are subapical, that is, they extend from the end of a segment that is not a tip. In order to determine when these branches occur, for each long penetrative hypha, one random number is generated and compared to the value of P_B, which is a constant with a low value. If the random number is less than P_B, then a new segment with a fixed length is added to a junction between two existing segments. Then, the depth of the horizontal plane at which the

new segment is added (d_n) is determined using a new random number (n_R):

$$d_n = trunc\left(n_R \times n_L\right) + 1$$

<div align="right">(3.2)</div>

where n_L is the length of the hypha that will receive the branch, expressed in "number of layers", and *trunc* means that the number resulting from the multiplication within the parentheses is truncated to give a whole number. These rules were based on the micrographs of Nopharatana et al. (2003a,b), in which long penetrative hyphae have short lateral branches distributed at a variety of distances from the tip.

3.2.5   Quantification of biomass in each layer

Each time that a new segment is formed during an iteration, the corresponding amount of biomass is added to the appropriate layer, increasing the dry biomass concentration of the layer by 0.01 g L^{-1} for each 140-µm segment. This value is based on the dry weight of biomass per volume for *R. oligosporus* (NOPHARATANA et al., 1998). For example, the segment distribution of penetrative hyphae illustrated in Figure 3.1 would correspond to 0.04 g L^{-1} in the first layer below the surface, 0.05 g L^{-1} in the second layer, 0.03 g L^{-1} in the third layer and no biomass in the fourth layer. Note that since the model represents the system as a stack of layers, the biomass concentration for each layer is plotted over the whole depth of the layer and, therefore, the plots have a stepwise appearance.

Due to the fact that the model is stochastic, each simulation results in a slightly different concentration profile. Each profile presented in this work corresponds to the average of three simulations. The experimental biomass concentrations obtained by Nopharatana et al. (2003b) were taken at 100-µm intervals; for comparison with the layer model, a weighted average was used to adjust their data to intervals of 140 µm. Model parameters were adjusted to fit the experimental data, by trial and error, minimizing the average of the squares of the absolute errors (E^2):

$$E^2 = \frac{\sum\limits_{i=1}^{n_p}\left(X_{exp,i} - X_{pred,i}\right)^2}{n_p}$$

<div align="right">(3.3)</div>

where $X_{\exp,i}$ (g L^{-1}) is the experimental value for layer i, $X_{\text{pred},i}$ (g L^{-1}) is the average value predicted by the layer model for layer i and n_p is the number of experimental data points.

3.3 RESULTS

3.3.1 Calibration of the layer model for short penetrative hyphae

Parameters N_0, N_h, $P_{E,\max}$, $d_{\lim}$, k and Δt_S were adjusted to give good fits of the layer model to the data of Nopharatana et al. (2003b) for both 16 h and 40 h of cultivation, with a single set of values (Figure 3.3). The values of the adjusted parameters are listed in Table 3.1. The adjusted value of Δt_S of 1.6 h gives a corresponding extension rate of 870 µm h^{-1}, which is of the same order of magnitude as rates that have been measured for hyphae of similar fungi, such as *Rhizopus stolonifer* (TRINCI, 1971).

Figure 3.3 Comparison between experimental data of biomass concentration of short penetrative hyphae in PDA obtained by Nopharatana et al. (2003b) and the profiles for short penetrative hyphae obtained with the layer model at 16 h and 40 h.
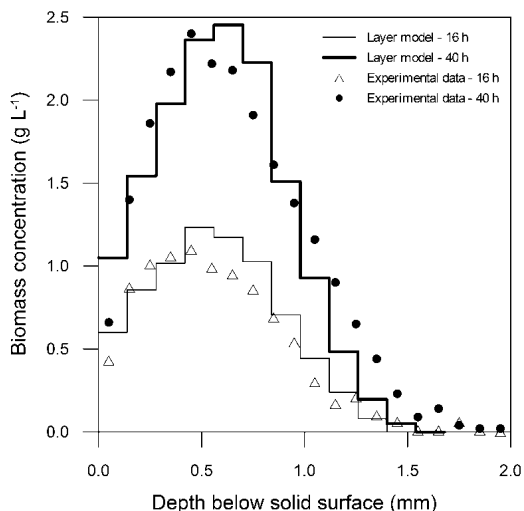
Table 3.1 Model parameters of the layer model for short penetrative hyphae

Fungus	*Rhizopus oligosporus*	*Rhizopus oligosporus*	*Aspergillus oryzae*
Medium	PDA	starch medium	rice grains
$P_{E,max}$	0.80	0.35	0.47
d_{lim} (mm)	1.8	1.2	0.4
k (-)	1	1	1
N_0 (tips)	33	1600	1
N_h (tips h^{-1})	2	40	55
Δt_S (h)	1.6	1.6	1.0
E^2 (g^2 L^{-2})	0.012 (for 16 h) and 0.039 (for 40 h)	1.9 (for 24 h) and 1.5 (for 48 h)	0.15 (for 26, 30, 34 and 38 h)

3.3.2 Sensitivity analysis of the layer model

Five of the model parameters, N_0, N_h, $P_{E,max}$, d_{lim} and k, were varied in order to determine how they affect the biomass distribution at 40 h. All parameters influenced the biomass concentration profile with depth, with the parameters related to limitation of growth, $P_{E,max}$, d_{lim} and k, having most influence. $P_{E,max}$ is related to the firmness of the solid and indicates the probability of a tip penetrating into the solid when the tip is located at the solid surface ($d = 0$). This parameter depends on the fungal species and on the properties of the solid. Increasing $P_{E,max}$ from 0.60 to 1.00 completely changed the biomass profile, altering the depth at which the peak biomass concentration occurred, the biomass concentration at the peak and the maximum depth reached by the hyphae (Figure 3.4A). The fact that the adjusted value for this parameter was high (0.80) indicates that the penetration of *Rhizopus oligosporus* into PDA is a reasonably easy process and, therefore, most of the tips that attempt to penetrate the solid succeed.

Figure 3.4 Sensitivity of the predicted profiles for short penetrative hyphae at 40 h to the parameters $P_{E,\max}$, N_h and k.

(A) Effect of the maximum probability of penetrative hyphae extending, $P_{E,\max}$; (B) Effect of k, the exponent of Eq. (3.1); (C) Effect of number of new tips per hour, N_h. In each case, the thicker continuous line corresponds to the parameter value that was adjusted to the experimental data.
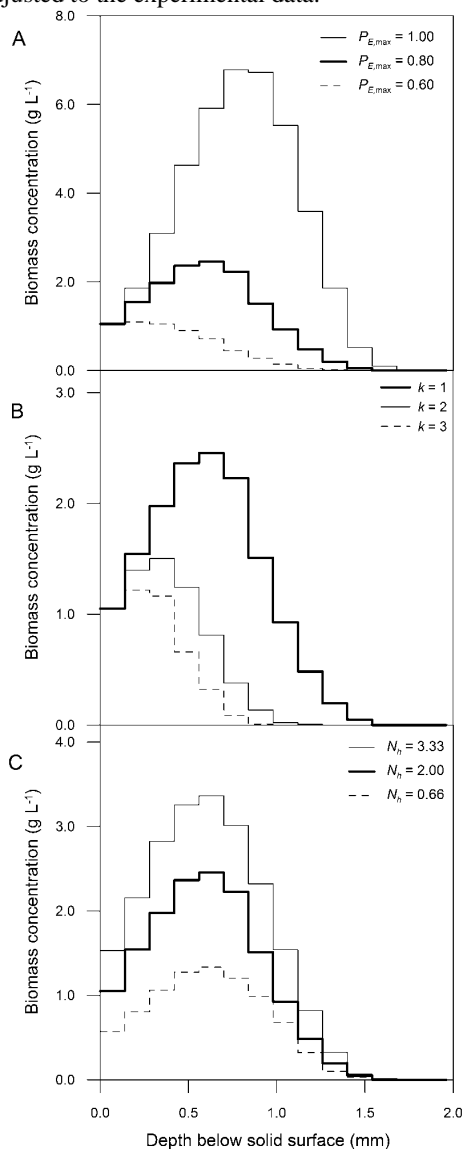
When the parameters d_{lim} and k of equation (3.1) were varied, the biomass profiles were similar in shape, but they reached different maximum depths, with the peaks also being located at different depths. Parameter d_{lim} represents the maximum depth that a hypha can reach in a solid that offers negligible resistance to penetration. When d_{lim} was varied from 1.0 mm to 2.6 mm, the maximum depth reached by the hyphae during the simulation was always 70% of the value of d_{lim}, and the position of the peak was at a half of the maximum depth reached. Parameter k describes how the degree of limitation of growth varies as a function of depth: with $k = 1$, the probability of extension decreases linearly with depth; with $k = 2$, this probability decreases quadratically; and with $k = 3$, this probability decreases cubically. As a consequence, the higher the value of this parameter, the lower will be the probability of extension at any given depth, thus total biomass and maximum depth reached will be lower (Figure 3.4B).

The penetration of new tips into the solid at the surface (reflected in the values of N_0 and N_h) is affected by the firmness of the medium and by the concentration of surface hyphae (which is not represented in the layer model). Parameters N_0 and N_h influence total biomass, however, they have less effect on the shape of the biomass profile itself, with the maximum depth and the position of the peak being the same when N_0 was varied from 20 to 40 tips and N_h was varied from 0.66 to 3.33 tips per hour (Figure 3.4C). This occurs because, in the model, the extension of penetrative hyphae is limited by depth and not by local biomass concentration, thus, an increase in hyphal tips does not affect when and where hyphae stop extending.

3.3.3 Application of the layer model to short penetrative hyphae growing in a different medium

In order to test the ability of the layer model to describe penetrative growth in other media, some model parameters were adjusted to fit the model to the profiles reported by Nopharatana et al. (2003a) for the growth of *R. oligosporus* in a starch-containing medium with κ-carrageenan as the gelling agent. Profiles of biomass concentration as a function of depth were obtained from micrographs taken at 24 h and 48 h. These micrographs show the formation of short and long penetrative hyphae, although rhizoids, if present, are not discernable. As in PDA, there was no significant growth of long penetrative hyphae from 24 h to 48 h. In order to divide the experimental profiles of biomass into short and long penetrative hyphae, a linear function was used to describe the

concentration of long penetrative hyphae as a function of depth. This function was adjusted to the biomass concentrations at depths below 1.1 mm at both 24 h and 48 h, since this region contains only long penetrative hyphae. Therefore, the concentration of long penetrative hyphae (X_{LP}) was estimated as:

$$X_{LP} = 2.0633 - 8.4232d$$

(3.4)

The experimental biomass concentrations obtained by Nopharatana et al. (2003a) were taken at 100-µm intervals; for each interval, X_{LP} was calculated using the middle depth of the interval (i.e. d = 50 µm, 150 µm, 250 µm, etc) and this was subtracted from the experimental data to give the estimated profiles for the concentrations of the short penetrative hyphae. Then, for comparison with the layer model, a weighted average was used to adjust this data to intervals of 140 µm.

The layer model for short penetrative hyphae presented a good fit to the experimental data with new values for four parameters, N_0, N_h, $P_{E,max}$ and d_{lim} (Figure 3.5, Table 3.1). The changes in these parameters reflect differences in the composition and firmness of the starch medium, which caused biomass profiles that had three main differences from those obtained in PDA: (i) The highest biomass concentrations occurred at the solid surface in the starch medium, whereas in PDA they occurred 0.45 mm below the surface; (ii) Hyphae penetrated to smaller depths in the starch medium, reaching a maximum depth of 2.55 mm, compared to 4.35 mm in PDA; (iii) Penetrative biomass reached higher local concentrations in the starch medium, with a maximum local concentration of 34.4 g L^{-1} at the solid surface at 48 h, whereas the maximum local concentration in PDA was 2.68 g L^{-1}, 0.45 mm below the solid surface at 40 h.

The firmness of the starch medium, which contains 5% κ-carrageenan and 5% starch, is higher than that of PDA, the only gelling component of which is 1.5% agar. As a consequence, its resistance to penetration by fungal hyphae is higher. This could explain why the penetrative biomass tends to be more concentrated near the surface of the starch medium than it is in PDA. In the model, the higher firmness of the medium translates into a reduction of both $P_{E,max}$, from 0.80 for PDA to 0.35 for the starch medium, and d_{lim}, from 1.8 mm for PDA to 1.2 mm for the starch medium (Table 3.1). With the reduction of $P_{E,max}$, the number of branches in the short penetrative hyphae also decreases, reflecting what is seen in the micrographs.

Figure 3.5 Comparison of the predictions of the layer model with experimental data obtained by Nopharatana et al. (2003a) at 24 and 48 h for the concentration of short penetrative hyphae on a starch-based medium.
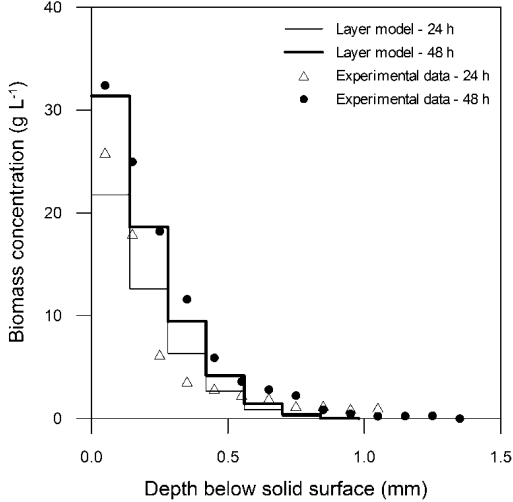
The presence of higher biomass concentrations in the starch medium down to a depth of 0.8 mm is probably due to two reasons. First, the carbon source is more concentrated, 5% starch, compared to 2% glucose in PDA. Second, growth on the starch medium requires the production of hydrolytic enzymes, which are secreted only at the tips of the hyphae (WÖSTEN et al., 1991), hence there are more hyphal tips in the starch medium. In the model, this translates into a higher penetration of tips at the surface: the simulation for the starch medium initiates with 1600 hyphal tips (N_0) and 40 new tips are formed per hour (N_h, Table 3.1). The duration of the iterations was not changed when applying the model to the starch medium, so that the extension rate of hyphae was the same for both media.

The higher firmness of the starch medium may have also caused the zigzag growth of the penetrative hyphae, which is visible in the micrographs of Nopharatana et al. (2003a).

3.3.4 Application of the layer model for short penetrative hyphae to a real SSF system

The layer model for short penetrative hyphae was also applied to describe the profiles of penetrative biomass of *Aspergillus oryzae* in SSF

of rice grains that were reported by Ito et al. (1989). They determined the biomass concentration profile as follows: at different incubation times, the fermentation was interrupted and the rice grains were polished, resulting in a pool of grains with different diameters; the glucosamine content in each polished grain was measured to determine "accumulated biomass concentration as a function of accumulated *koji* weight" and this value was converted into biomass concentration as a function of depth (ITO et al., 1989). In the resulting profiles, the biomass concentration was highest at the solid surface, decreasing exponentially with depth. For each profile of biomass concentration measured, the authors fitted an exponential curve, reporting the fitted curve without providing the measured data.

A micrograph of a section of a *koji* particle shows an area of dense biomass close to the surface and a few long penetrative hyphae (ITO et al., 1989; MATSUNAGA et al., 2002). Although Ito et al. (1989) themselves did not explicitly suggest that these were two different types of penetrative hyphae, they probably represent short and long penetrative hyphae. What Ito et al. (1989) did say was that the biomass concentrations below approximately 200 µm were difficult to measure with accuracy and did not fit into the same exponential curve as the data for short penetrative hyphae. They then subtracted the biomass concentration below 200 µm from the biomass concentrations measured at all depths. We interpret this to mean that the data reported by Ito et al. (1989) correspond only to short penetrative hyphae.

The data set used to adjust the parameters of the layer model corresponds to biomass profiles taken every 4 h between 22 h and 38 h. The biomass concentrations at 22 h are very low, indicating that the lag phase ended around the time this measurement was taken; zero time in the model simulations therefore corresponds to 22 h in the results of Ito et al. (1989). Also, the concentrations at 22 h at the corresponding depths were subtracted from the biomass data at the other times reported by Ito et al. (1989). Although a few short hyphae had already penetrated the particle at 22 h, the simulation starts with only the tips at the surface and no biomass inside the solid. This consideration has negligible effect on the predicted results at 16 h of simulation (corresponding to 38 h in the experiment of Ito et al. (1989)).

The rules of the layer model were not changed for this simulation, only the parameters and the system dimensions. The cross-sectional area of the hyphal segments is set at 9 µm², based on the diameter of 3.3 µm reported for hyphae of *Aspergillus oryzae* (MÜLLER et al., 2002). The height of each layer is 21 µm, maintaining the same proportionality

between layer height and hyphal diameter as that used for *R. oligosporus*. The area of each layer is 0.09 mm²; since this represents less than 1% of the estimated surface area of a *koji* grain (based on the author's micrographs), the use of Cartesian coordinates instead of polar coordinates is acceptable. The addition of a new hyphal segment increases the dry biomass concentration of the layer by 0.01 g L^{-1}.

The model parameters, N_0, N_h, $P_{E,max}$ and d_{lim}, and the duration of the iterations were adjusted to fit the growth profiles at each incubation time (26, 30, 34 and 38 h), using a single set of values (Table 3.1). The simulation initiates with 1 hyphal tip (N_0) and 55 new tips are formed per hour (N_h). In the case of *A. oryzae*, which does not form nodes at the surface, these new tips may be formed from surface hyphae. Each tip has a maximum probability of extension ($P_{E,max}$) of 0.47 and a limiting depth of penetration (d_{lim}) of 0.4 mm, these low values being a consequence of the presence of a cellular structure within the grain. Each iteration corresponds to 1 h of cultivation, resulting in an extension rate of 21 µm h^{-1}. With these parameters, the simulation results in profiles for short penetrative hyphae (i.e. down to 0.2 mm depth) that are similar to those of Ito et al. (1989) (Figure 3.6).

Figure 3.6 Comparison of the predictions of the layer model with experimental data obtained by Ito et al. (1989) for the concentration of short penetrative hyphae of *Aspergillus oryzae* in rice koji for increasing incubation times, of 26, 30, 34 and 38 h, which correspond to simulation times of 4, 8, 12 and 16 h, respectively. The concentration of long penetrative hyphae was not included in the original data reported by Ito et al. (1989).
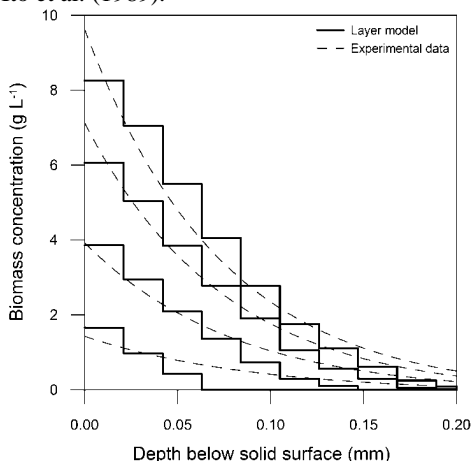
3.4   DISCUSSION

3.4.1   First model to describe biomass concentration profiles of penetrative hyphae

The proposed layer model is the first model to describe concentration profiles of penetrative hyphae with depth inside solid substrates. It does this using simple rules for the extension and inactivation of these hyphae. It was able to describe penetrative growth in particles with and without a cellular substructure, namely rice grains and gels, for two fungi that grow with different morphologies, namely *Rhizopus oligosporus*, which is asseptate and forms rhizoids, and *Aspergillus oryzae*, which is septate.

For all modeled systems, the rules and structure of the model were the same, only the values of the model parameters were changed, reflecting differences due to the medium composition and fungal type. Each system modeled had a different profile of biomass concentration, including a profile with a peak of concentration within the solid (Figure 3.3) and another profile with an exponential decrease in biomass density (Figure 3.6), nevertheless, the model was flexible enough to describe these different growth profiles.

The only previous mathematical model to describe penetrative hyphae was developed for the study of degradation of wood by the white-rot fungus *Physisporinus vitreus* (FUHR et al., 2011). This model uses a three-dimensional discrete lattice, in which the wood cells are represented by rectangular prisms and hyphae are treated as segments extending as straight lines between the walls of the wood cells. Due to the use of segments without volume or mass to represent hyphae, this model is not appropriate to generate profiles of biomass concentration with depth to be compared to the findings of Ito et al. (1989). In addition, the hyphal length increases continuously as long as the hyphae are able to bore holes in the cell walls, thus, this model does not include a mechanism to stop growth in solids without cellular substructure.

Furthermore, all previous mesoscale models for SSF (according to the classification proposed by Sugai-Guérios et al. (2015)), including those for biofilm, surface and aerial hyphae, describe fungal growth on artificial media and not on particles in real SSF systems. With its description of the data of Ito et al. (1989) for the growth of penetrative hyphae in the rice grains of *koji*, the layer model is the first mesoscale model applied to growth of hyphae in a real SSF system.

A 3D model for the growth of penetrative hyphae, based on the simple rules developed in the current work, could be fused with the 3D model developed by Coradin et al. (2011) for aerial hyphae. The resulting discrete 3D model could be used to explore the roles of aerial and penetrative hyphae in important mesoscale phenomena in SSF systems, such as particle shrinkage and the binding together of substrate particles. Such a 3D model could be further developed, resulting in a "full mesoscale morphological model", as proposed by Sugai-Guérios et al. (2015). These developments would include the incorporation of mathematical expressions describing intracellular processes, such as nutrient uptake, the production and translocation of vesicles and the incorporation of vesicles at the hyphal tip (BALMANT et al., 2015). Different regions of the mycelium would be treated as having different physiological states: based on the results of the current work, differences would be recognized not only for aerial and penetrative hyphae, but also for short and long penetrative hyphae (SUGAI-GUÉRIOS et al., 2015).

3.4.2   One of the factors limiting the length of penetrative hyphae may be the firmness of the particle

In all conditions simulated with the layer model for short penetrative hyphae, there is a maximum length that hyphae can reach and the overall amount of biomass within the substrate increases mainly due to the penetration of new tips at the surface. In the model, there are two main factors that limit the continued extension of penetrative hyphae: $P_{E,\max}$ and the expression within parentheses in equation (3.1). The current subsection explores the possible mechanisms associated with $P_{E,max}$ while the next subsection explores the possible mechanisms associated with the expression within parentheses.

We suggest that $P_{E,\max}$, which is the parameter with the most influence on the shape of the biomass profile, is related to the firmness of the solid. Therefore, different values of $P_{E,\max}$ should be used when the same fungus is grown on media with different firmness, for example, for *R. oligosporus* grown on PDA and on the starch medium (NOPHARATANA et al., 2003a,b). In other words, we suggest that the firmness of the medium determines the shape of the profile of biomass concentration with depth.

The same logic would be applied if we were to model the results of Varzakas (1998), which show differences in the growth of *R. oligosporus* on defatted soy flour particles and on soybean tempeh. Soy

flour particles and soybean tempeh both have a cellular substructure, however, the cells in the soy flour particles are disassociated and, thus, there is more space between the cells for penetrative hyphae to grow. Therefore, soy flour particles are less resistant to hyphal penetration than soybeans and, consequently, longer penetrative hyphae are formed in soy flour than in soybean tempeh (VARZAKAS, 1998). If these data were modeled with the layer model, then $P_{E,\max}$ would be higher for soy flour.

3.4.3 Another factor limiting the length of penetrative hyphae may be the pressure drop inside the hypha

The expression between parentheses in equation (3.1) is a function of depth involving two parameters, $d_{\lim}$ and k. The adjusted value of $k = 1$ means that the probability of extension decreases linearly with depth, reaching zero at $d_{\lim}$. This raises the question as to what phenomenon might be responsible for a linear decrease in the probability of extension with depth. Here we discuss three elements that might affect the growth of penetrative hyphae: (i) O_2 concentration inside the medium; (ii) nutrient availability; and (iii) the turgor pressure within the hypha.

Low O_2 concentrations below the surface could potentially limit the extension of penetrative hyphae. The concentration of O_2 inside the particle depends on the rate of consumption by penetrative hyphae (for growth and for maintenance) and on the rate of diffusion from the gas phase at the surface and inside the solid phase. Since the diffusivity of O_2 in solid particles is low, the rate of consumption is often higher than the rate of diffusion, thus, the concentration of O_2 is the highest at the solid surface and decreases with depth, such that the variation of the O_2 concentration with depth is roughly proportional to the concentration of biomass in each given depth, with the concentration of O_2 being almost constant with depth in a region without biomass (SUDO et al., 1995; OOSTRA et al., 2001). As the concentration of penetrative biomass increases, the concentration of O_2 in deeper regions of the solid may decrease to zero (OOSTRA et al., 2001). In previous mesoscale models, it has been assumed that when the concentration of O_2 is zero, hyphae stop extending (RAJAGOPALAN; MODAK, 1995; MEEUWSE et al., 2012), however, this may not be the case. One possibility is that hyphae shift to fermentative metabolism (SUDO et al., 1995; ALEXOPOULOS et al., 1996) and another possibility is that hyphae transport O_2 to the tips of penetrative hyphae using hemoglobin-like proteins (TE BIESEBEKE et al., 2006/2010). It remains unclear if penetrative hyphae are able to

grow in hypoxia and, if so, how they do it (SUGAI-GUÉRIOS et al., 2015), therefore, there is insufficient evidence to affirm that the lack of O_2 inside the solid limits the length of penetrative hyphae.

The second hypothesis considered was that nutrient availability determined the probability of extension. In the case of growth on PDA, where nutrient hydrolysis is not required, the profile of dextrose concentration as a function of depth would start as uniform (i.e. no gradient), and gradually change into a gradient starting at almost zero concentration close to the surface until maximum concentrations deep within the medium, in the regions unoccupied by the mycelium (RAJAGOPALAN; MODAK, 1995; MEEUWSE et al., 2012; MITCHELL et al., 1990). Therefore, deeper within the medium there are more nutrients, thus, the lack of nutrients for supporting tip extension would not be a cause for hyphae to stop penetrating into the medium.

The third hypothesis considered was that turgor pressure within the hypha might affect the depth of penetration. The mechanical penetration of the solid structure of a particle by a hypha requires turgor pressure at the hyphal tip, with this turgor pressure being maintained by ion transporters at the cost of ATP (MONEY, 2008; LEW, 2011). Lew (2011) suggested that there is a linear pressure gradient within the hypha and that the velocity and the direction of intracellular cytoplasmic flow depend on this pressure gradient. Therefore, since *R. oligosporus* is an aseptate fungus and assuming that intracellular flow in penetrative hypha is directed towards the tip (as has been shown to be the case in most surface hyphae) (LEW, 2011), the penetrative hypha would have the highest pressure at the base of the hypha (located at the surface), decreasing linearly towards the tip. This means that, as a penetrative hypha extends, the overall pressure drop from the base of the hypha to the tip increases, decreasing the turgor pressure at the tip. Eventually, the pressure at the tip might fall to such low values that the hypha can no longer penetrate the solid structure and hyphal extension stops. Therefore, it may be that the maximum length of a hypha is related to its internal pressure drop. In order to calculate the internal pressure drop, we need to make two assumptions. First, we assume that the pressure gradient ($\Delta P/L$) inside a hypha is not affected by the length of the hypha. Second, we consider that extension of the tip stops when the turgor pressure at the tip reaches a limiting pressure (P_{min}), which would result in a maximum hyphal length of d_{lim}. Then the internal pressure gradient may be written as:

$$\frac{\Delta P}{L} = \frac{P_{base} - P_{tip}}{d} = \frac{P_{base} - P_{\min}}{d_{\lim}}$$

(3.5)

Substituting equation (3.5) into equation (3.1) gives:

$$P_E = P_{E,\max} \left(\frac{P_{tip} - P_{\min}}{P_{base} - P_{\min}} \right)$$

(3.6)

This equation suggests that the probability of extension is proportional to the difference between the pressure at the tip and the minimum turgor pressure for penetration of the solid.

3.4.4 Long penetrative hyphae scout for nutrients while short penetrative hyphae are responsible for fixation into the particle and improving nutrient hydrolysis

In addition to being visible in the micrographs of Nopharatana et al. (2003a,b) and Ito et al. (1989), short and long penetrative hyphae have also been observed in soybeans inoculated with *Rhizopus oligosporus* for tempeh production (JURUS; SUNDBERG, 1976) and in rice inoculated with *A. oryzae* (MATSUNAGA et al., 2002). Although these two types of penetrative hyphae were reported as long ago as the 1970s (JURUS; SUNDBERG, 1976), their roles have not been investigated.

The only previous hypothesis to explain the differences between long and short penetrative hyphae was raised by Nopharatana et al. (2003a), who suggested that these hyphae have different physiologies: short hyphae grow close to the surface where there is enough O_2 concentration for aerobic growth, meanwhile, long hyphae suffer from O_2 limitation almost since the beginning and have fermentative metabolism or receive biosynthetic precursors and ATP from their base. However, analysis of their data indicates that most of the extension of long penetrative hyphae occurs in the first hours of cultivation, when O_2 concentration inside the medium should not be limiting (SUDO et al., 1995; OOSTRA et al., 2001; RAHARDJO et al., 2002).

Our hypothesis is that each hyphal type has a different role and grows during a different stage of the development of the mycelium. We suggest that, at least in the case of *Rhizopus oligosporus*, long penetrative hyphae are formed during the transition between the lag and the exponential phases, when there is still a significant amount of O_2 throughout the medium, and their role is to explore the composition of the

medium and to search for new colonization sites. This is done by secreting a pool of hydrolytic enzymes, so-called scouting enzymes, similar to what is done by surface hyphae in the outer region of a colony according to the suggestion of Delmas et al. (2012). These scouting enzymes initiate extracellular hydrolysis of the substrate, generating oligo- or monosaccharides, which are then converted to inducing sugars; these inducing sugars are detected by the other hyphal types (short penetrative hyphae, biofilm and surface hyphae) and trigger them to secrete hydrolytic enzymes that are appropriate for the particular polymers present in the medium (DELMAS et al., 2012; AMORE et al., 2013). Long penetrative hyphae would also search for new colonization sites within the solid particle, therefore, they would also be present even in media with readily available nutrients, such as glucose. It is important to note that long penetrative hyphae are not driven by chemotropism, since they are present in the micrographs obtained in the early stages of the cultivation, when there should not be significant concentration gradients. Due to these characteristics, we suggest that long penetrative hyphae be called *scouting penetrative hyphae*.

Short penetrative hyphae, on the other hand, grow during most of the development of the colony and would have two roles. Their first role would be to anchor the colony to the substrate particle, preventing the removal of the entire colony from the solid particle due to wind, animals or, in SSF, agitation of the fermentation bed. The second role of the short penetrative hyphae would be, as suggested by Mitchell et al. (1989), to decrease the distance between the site of enzyme secretion and the polymeric substrate, with their tips secreting a significant amount of enzymes, all specific for the medium composition. We suggest that short penetrative hyphae be called *vegetative penetrative hyphae*, in analogy to aerial vegetative hyphae. These proposed roles agree with the suggestion made for surface hyphae by Moore et al. (2005), namely that densely branched hyphae are more likely to act in nutrient absorption while sparsely branched hyphae are more likely to explore the resources of the medium.

Since secretion of hydrolytic enzymes occurs at the tips and is higher when the number of tips increases (WÖSTEN et al., 1991; TE BIESEBEKE et al., 2005; BARRY and WILLIAMS, 2011), it could be that the starch medium with *R. oligosporus* has more tips of vegetative penetrative hyphae as a strategy to increase enzyme production. Meanwhile, in PDA, vegetative penetrative hyphae are only required for anchorage, so they are fewer and longer. This hypothesis could be verified by investigating the regulation of genes known to control the formation

of tips, for example, the (KEX2-like) proprotein convertase-encoding gene (*pclA*) and phospholipid transfer protein gene (*pg/pi-tp*) in *Aspergillus* strains (TE BIESEBEKE et al., 2005), in order to confirm if they are expressed differently in media with monomeric or polymeric nutrients.

A better understanding of the differences between scouting and vegetative penetrative hyphae requires microscopic image analysis of their growth and transcriptome analysis of each hyphal type. Image analysis can be used to determine exactly when each hyphal type starts and stops growing and if different hyphal types have different cellular structures, for example, different hyphal diameters or, in the case of *A. oryzae*, different distances between septa or patterns of closure of septa. For example, larger diameters or the absence of septa may cause the pressure drop in scouting penetrative hyphae to be lower and, if the hyphal final length is, in fact, related to the pressure drop along the hypha, then this may be the reason why these hyphae are longer. Furthermore, the transcriptome analysis may be used to determine genes that result in morphological differences between scouting and vegetative penetrative hyphae and whether these hyphae do indeed produce different hydrolytic enzymes. This kind of analysis has been done for adjacent surface hyphae (DE BEKKER et al., 2011), but not for penetrative hyphae.

3.5 CONCLUSION

The layer model proposed in this work is a discrete model that describes the extension of short and long penetrative hyphae using simple rules that can be translated to factors that could limit the length of penetrative hyphae, namely, the firmness of the particle and the pressure drop inside the hypha. The model was able to describe three distinct profiles of biomass concentration with depth, including a profile obtained in a real SSF system, namely the growth of *Aspergillus oryzae* on rice *koji*; hence, this is the first model to describe the growth of individual hyphae in a real SSF system.

Also for the first time, specific roles have been suggested for the short and long penetrative hyphae that are formed by *Rhizopus oligosporus* and *Aspergillus oryzae* growing in solid particles. We suggest that long penetrative hyphae, also named scouting penetrative hyphae, are formed early in the development of the mycelium and they search for new colonization sites across the particle and explore the composition of the particle by producing a pool of hydrolytic enzymes that generate the metabolic signals necessary for the induction of the

appropriate enzymes in the short penetrative hyphae. These short penetrative hyphae, also named vegetative penetrative hyphae, are responsible for anchoring the colony to the solid particle and for improving substrate hydrolysis by secreting large quantities of hydrolytic enzymes into the particle.

4   STERIC IMPEDIMENT LIMITS VEGETATIVE GROWTH OF AERIAL HYPHAE OF *Rhizopus oligosporus* IN SOLID-STATE FERMENTATION: A MODEL-BASED STUDY ON HOW THESE HYPHAE GROW

The work presented in this chapter was developed in collaboration with Wellington Balmant and under the orientation of Nadia Krieger from Federal University of Paraná. A manuscript with the results contained in this chapter is under preparation for submission.

4.1 INTRODUCTION

In a solid-state fermentation (SSF) process, filamentous fungi grow on the surfaces of the solid particles of the bed, as well as inside the particle and above the particle surface, forming surface, penetrative and aerial hyphae, respectively. In the particular cases that a liquid film is formed on the particle surface, the hyphae that grow within this film are called biofilm hyphae. Aerial hyphae may be classified as vegetative and reproductive hyphae, and are mainly involved in spore production and O_2 absorption (RAHARDJO et al., 2002). For example, for *Aspergillus oryzae* growing on an artificial medium with wheat flour, aerial hyphae are responsible for up to 75% of the O_2 uptake (RAHARDJO et al., 2002).

The growth of aerial hyphae has important consequences for SSF processes: they fill up the inter-particle spaces, causing the pressure drop to rise in forcefully-aerated beds. This decreases the efficiency of heat and mass transfer to the process air. Further, in some cases, aerial hyphae bind the particles into agglomerates that are difficult break, so that heat transfer becomes limited to conduction and mass transfer becomes limited to diffusion.

Despite the importance of aerial hyphae, there are only two mathematical models for the growth of this type of hypha at the mesoscale. The model of Nopharatana et al. (1998) is a pseudohomogenous model and uses partial differential equations to describe the concentrations of tips, biomass and intracellular glucose as a function of height above the surface. Tip growth occurs through the movement of the tips, described as a diffusion-like process, as tips move freely in any direction based on the gradient of tip concentration. On the other hand, the model of Coradin et al. (2011) is a 3-dimensional discrete lattice-based model, in which the space above the surface is divided into 10 μm long cubes. The status of each cube is initially "empty", but it changes with the extension of hyphae to "hyphal tip" or "fungal biomass".

Hyphae can grow horizontally, vertically or diagonally, upwards or downwards, and they form apical branches in every iteration of the model. The direction of growth of a hyphal tip is chosen using a random number and probabilities attributed to each direction.

The simulation results from both models were compared to the experimental profile of concentration of aerial biomass as a function of height, measured for *Rhizopus oligosporus* growing on potato dextrose agar (PDA) at 16 h and at 40 h of incubation (NOPHARATANA et al., 2003b). However, neither of these models reproduces the experimental profiles well. The model of Nopharatana et al. (1998) results in a profile similar to the experimental data only for 16 h, which is before vegetative hyphae stop extending and reproductive hyphae begin to grow. On the other hand, the model of Coradin et al. (2011) predicts a high peak of biomass concentration immediately on the surface of the medium (approximately 42 g L^{-1} at 40 h), a smaller peak of concentration at 0.2 mm above the surface (approximately 31 g L^{-1} at 40 h) and a very small peak at 2.2 mm above the surface (approximately 8 g L^{-1} at 40 h); in the experimental profile, the highest biomass concentration was at the surface (approximately 35 g L^{-1} at 40 h) and it only decreased with height, without any other peaks in concentration.

The purpose of this paper is to understand better what influences the distribution of aerial hyphae as a function of height. This was achieved in three steps, using the data for growth of aerial hyphae of *Rhizopus oligosporus* on PDA (NOPHARATANA et al., 2003b). The first step was analysis of the experimental data in order to obtain estimates for separate populations of vegetative aerial hyphae and reproductive aerial hyphae. The second step was the development of a discrete model with rules that are simpler than those of Coradin et al. (2011). The structure of the model was the same as the recently developed layer model for penetrative hyphae (SUGAI-GUÉRIOS et al., 2016), however, given that penetrative and aerial hyphae have different morphologies, a different set of rules was necessary to describe growth and branching of aerial hyphae. The final step was a sensitivity analysis, which was conducted to evaluate the influence of each parameter of the model in the biomass distribution above the surface.

4.2 MODEL DEVELOPMENT

The micrographs of aerial hyphae of *Rhizopus oligosporus* on PDA at 16 h and 40 h of incubation (NOPHARATANA et al., 2003b) were used to develop the rules of the layer model, and the corresponding

biomass concentration profiles as a function of height above the medium surface were used to calibrate the model parameters. Sporangiophores are visible in the micrograph obtained at 40 h, but not in the micrograph obtained at 16 h, which indicates that reproductive hyphae were formed between 16 h and 40 h (NOPHARATANA, 1999; NOPHARATANA et al., 2003b). Consequently, the biomass concentration profile obtained at 40 h corresponds to the biomass of both vegetative and reproductive aerial hyphae. The separation of this profile into vegetative and reproductive hyphae was done as follows: first, it was observed that the profile for 16 h, which contains only vegetative hyphae, fits into a half-normal distribution curve; second, two half-normal distribution curves were fitted to the profile for 40 h, with each curve representing one of the types of aerial hypha.

4.2.1   Curve fitting of the half-normal distribution

Half-normal distributions were fitted to the data of Nopharatana et al. (2003b) for concentration of the aerial hyphae (X, g L^{-1}) as a function of height (h, mm) above the medium surface. For both vegetative and reproductive biomass, the maximum value of the biomass concentration was assumed to occur at the medium surface. For vegetative hyphae, this assumption was based on the concentration profile of Nopharatana et al. (2003b) for 16 h, in which the biomass concentration is highest at the medium surface. For reproductive hyphae, this assumption was based on the mode of growth of reproductive hyphae of *Rhizopus oligosporus* on PDA: these hyphae grow from the nodes directly above the rhizoids, with these nodes being situated immediately above the particle surface, and branches are rare for this type of hypha (SHURTLEFF; AOYAGI, 1979). For the data for 16 h of incubation, a single half-normal distribution curve was fitted:

$$X = \frac{X_{V0}\sqrt{2}}{\sigma_V \sqrt{\pi}} \exp\left(-\frac{h^2}{2\sigma_V^2}\right) \tag{4.1}$$

where X_{V0} (g mm L^{-1}) is the area under the curve of the entire half-normal distribution for the plot of biomass concentration of vegetative hyphae as a function height and σ_V (mm) is the standard deviation for the concentration of vegetative hyphae, namely the height above the surface under which 68.27% of the vegetative hyphae are to be found. For the fitting at 16 h, σ_V was calculated directly from the experimental data of

Nopharatana et al. (2003b). In this manner, X_{V0} was the only parameter that was adjusted in the fitting procedure.

For the data obtained at 40 h, the sum of two half-normal distributions was fitted:

$$X = \frac{X_{V0}\sqrt{2}}{\sigma_V \sqrt{\pi}} \exp\left(-\frac{h^2}{2\sigma_V{}^2}\right) + \frac{X_{R0}\sqrt{2}}{\sigma_R \sqrt{\pi}} \exp\left(-\frac{h^2}{2\sigma_R{}^2}\right) \qquad (4.2)$$

where X_{R0} (g mm L^{-1}) is the area under the entire half-normal distribution curve for reproductive hyphae and σ_R (mm) is the standard deviation for reproductive hyphae, namely the height above the surface under which 68.27% of the reproductive hyphae are to be found. The values of X_{V0} and σ_V are higher for 40 h than for 16 h because vegetative hyphae continued to grow after 16 h. For the fitting at 40 h, all four parameters (X_{V0}, σ_V, X_{R0}, and σ_R) were adjusted for the curve to fit the experimental data.

Fitting of the distribution curves was done using the Solver tool of Microsoft Excel®, minimizing the average of the squares of the absolute errors (E^2):

$$E^2 = \frac{\sum\limits_{i=1}^{n_p}\left(X_{\exp,i} - X_{\mathrm{pred,i}}\right)^2}{n_p} \qquad (4.3)$$

where $X_{\exp,i}$ (g L^{-1}) is the ith experimental data point, $X_{\mathrm{pred,i}}$ (g L^{-1}) is the corresponding value predicted by the fitted curve and n_p is the number of experimental data points.

4.2.2   Overview of the layer model for aerial hyphae

The layer model for aerial hyphae uses the same structure as that of the layer model for penetrative hyphae (SUGAI-GUÉRIOS et al., 2016), namely the space above the medium surface is divided by horizontal planes into a stack of discrete layers, and hyphae are represented by 140-μm long segments (Figure 4.1). The representation of hyphal extension is also the same in both models, with new hyphal segments being added in each iteration to the end of an existing segment that represents an active tip. The exact horizontal position of the segment within the layer is not defined, only the layer to which the segment belongs and the position of the tip, which, for vegetative hyphae, is

always located immediately above one of the planes that mark the boundaries between the layers, and, for reproductive hyphae, is always located immediately immediately below the planes (Figure 4.1). Before the end of each iteration, tips may inactivate or, in the case of vegetative hyphae, new branches are formed.

Figure 4.1 Schematic drawing of the procedure used in the layer model for the addition of new segments of vegetative aerial hyphae in the aerial space.
The expanded view of the first three layers above the medium surface shows the segments added in the first four iterations, the numbers indicate the iteration in which each segment was formed. The arrows inside the segments indicate the direction of growth and the symbol '×' indicates the position of the tip in the segment; a white '×' represents an active tip while a black '×' represents an inactive tip. In the first iteration, a single hypha is formed from a germinated spore (represented by a circle) and grows horizontally on the surface. In the following iterations, if the active tip is at the surface, hyphae can grow horizontally or vertically upwards, otherwise hyphae may grow horizontally, upwards or downwards. The drawing is not to scale and is for illustrative purposes; it does not represent a specific simulation result.
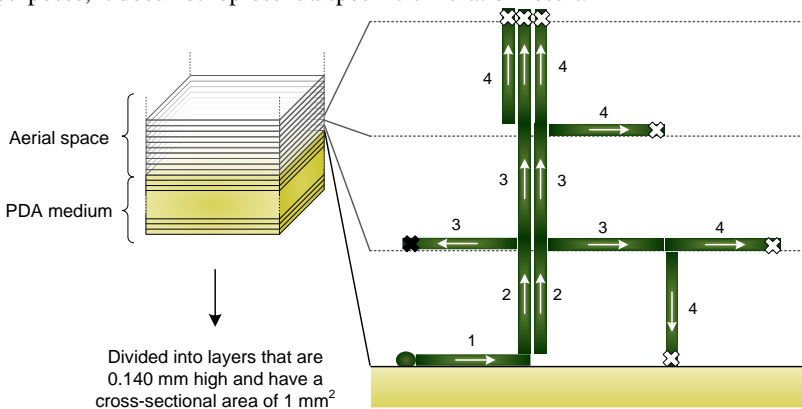
The model differs from that of Sugai-Guérios et al. (2016) with respect to the rules governing branching and inactivation of aerial hyphae and with respect to the direction of growth of vegetative hyphae. Vegetative aerial hyphae can be oriented horizontally, vertically upwards or vertically downwards (Figure 4.1), whereas in Sugai-Guérios et al. (2016) penetrative hyphae can only grow downwards. In addition, vegetative aerial hyphae branch in every iteration, while in Sugai-Guérios et al. (2016) vegetative penetrative hyphae could extend without branching. As a result, vegetative aerial hyphae have more branches than

do penetrative hyphae and the distance between branches is always the same, 140 µm.

The simulation for aerial hyphae is divided into two phases. In the first phase, only vegetative hyphae grow and the remaining active tips of these hyphae inactivate at the end of this phase (t_D, time of differentiation). In the second phase, only reproductive hyphae grow and this phase lasts from the time of differentiation until the simulation ends at 40 h. The duration of each iteration, which is different for each phase of the simulation, and the time of differentiation were adjusted to the experimental data. The rules of the model also differ for vegetative and reproductive aerial hyphae and are described in the following subsections.

During the simulation, for the decisions ruled by probabilities, random numbers were generated using the random_number and random_seed functions of FORTRAN, which generates random numbers (x) uniformly distributed over the range $0 \leq x < 1$.

4.2.3   Layer model for growth of vegetative aerial hyphae

The simulation begins with 400 spores distributed on the medium surface, corresponding to the inoculum concentration used by Nopharatana et al. (2003b). Each spore has a probability of germinating at the beginning of the first iteration, P_G (Figure 4.2A). Each spore that germinates forms one hyphal segment that extends horizontally on the surface. The active tips of these new segments may become inactive before the end of the iteration, as described below. If a tip does not inactivate, then it branches, thereby generating an extra active tip.

During the second iteration, the segments that form from the active tips can be orientated either horizontally or upwards (active tips on the solid surface cannot extend downwards). The probability of an active tip choosing to extend upwards is 50%. If it chooses to do so, then, at the end of the iteration, the active tip is located immediately above the horizontal plane that separates the first and the second layer (Figure 4.1).

This process of extending and either inactivating or branching repeats itself during the growth of vegetative hyphae. Any active tip that is located above the surface rather than on it (i.e. located in layer 2 or higher, rather than in layer 1) can choose to add a segment that is oriented upwards or downwards or horizontally, with each orientation having an equal chance of being chosen. The direction taken by each active tip is evaluated independently, such that the two active tips formed by a branching event may or may not choose to move in the same direction.

Figure 4.2 Flowsheet of the layer model for aerial hyphae.
(A) The submodel for the growth of vegetative aerial hyphae, which extend until the time of differentiation (t_D). (B) The submodel for the growth of reproductive aerial hyphae, which begin to extend at the time of differentiation. The simulation ends at 40 h. The parameter values used are given in Table 4.1.
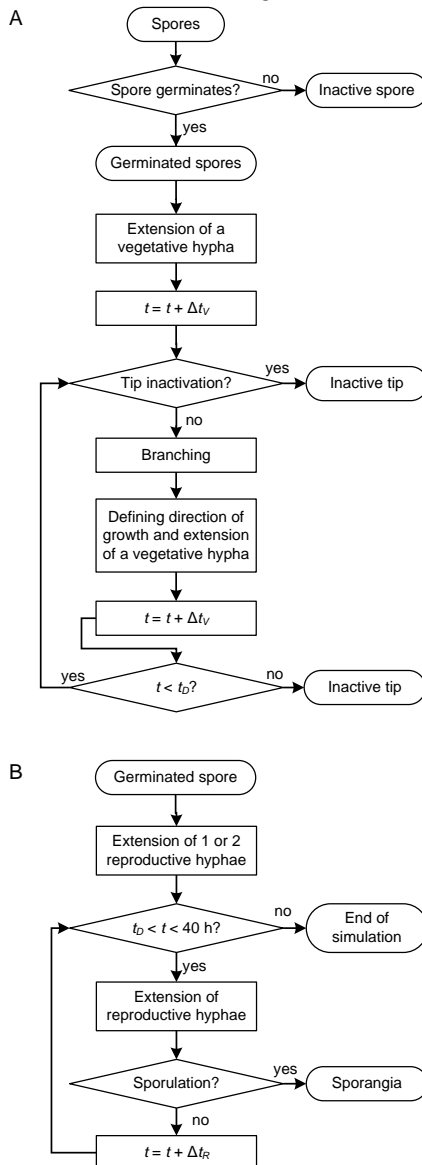
For horizontal movements, the segment is always formed immediately above the horizontal plane that separates two layers (Figure 4.1).

The test for inactivation is carried out for each active tip before the end of each iteration. This test is based on the consideration that, as biomass concentration in a layer increases, it is more likely that an extending tip will encounter other hyphae. In this case, the tip may either deviate and continue extending or stop extending, thus, inactivating (HUTCHINSON et al., 1980). The probability that any active tip, located in layer j, will inactivate (P_I) is proportional to the concentration of hyphal biomass in layer j (X_j):

$$P_I = \left(\frac{X_j}{X_{max}} \right)^{m_e} \tag{4.4}$$

where X_{max} is the maximum possible biomass concentration in a layer, considering steric impediment (LAUKEVICS et al., 1985), which means that there is always some unoccupied space between hyphae because hyphae rarely grow attached to each other. The exponent m_e is related to the fact that a hypha may undergo multiple encounters before inactivating, representing how sensitive a tip is to the biomass concentration around it: for example, for a determined pair of values of X_j and X_{max}, a low value of m_e induces a higher probability of inactivation than a high value of m_e.

4.2.4 Layer model for growth of reproductive aerial hyphae

For *Rhizopus oligosporus*, reproductive hyphae extend from the nodes at the surface that support the rhizoids (SHURTLEFF; AOYAGI, 1979). These nodes correspond to either the positions of the germinated spores or new nodes that were formed during vegetative growth through the extension of stolons. One or two reproductive hyphae are formed per node, therefore, the number of reproductive hyphae formed can be higher than the number of germinated spores. In the layer model, at the time of differentiation (t_D), all vegetative aerial tips are inactivated and active reproductive tips are formed on the surface. The number of reproductive tips formed is proportional to the number of germinated spores: each germinated spore forms at least one reproductive tip and a certain percentage of them (N_{rep}) forms two tips.

Reproductive hyphae extend only upwards and do not branch. Before the end of each iteration, the active tip may stop extending in order

to start the process of formation of the sporangia, represented in the model as tip inactivation. The probability that any active tip will inactivate ($P_{I,RH}$) is given by:

$$P_{I,RH} = \left(\frac{h}{h_{\lim,RH}} \right)^{n_e} \tag{4.5}$$

where $h_{\lim,RH}$ is the highest height reached by reproductive hyphae and n_e is a measure of how the probability of inactivation varies with height.

4.2.5   Quantification of biomass in each layer

The same approach used in the layer model for penetrative hyphae is used for aerial hypha. Each time that a new segment is formed during an iteration, the corresponding amount of biomass (0.01 g L^{-1}) is added to the appropriate layer. For example, the segment distribution of aerial hyphae illustrated in Figure 4.1 would correspond to 0.04 g L^{-1} in the first layer above the surface, 0.05 g L^{-1} in the second layer, 0.04 g L^{-1} in the third layer and no biomass in the fourth layer. Note that since the model represents the system as a stack of layers, the biomass concentration for each layer is plotted over the whole depth of the layer and, therefore, the plots have a stepwise appearance.

Due to the fact that the model is stochastic, each simulation results in a slightly different concentration profile. Each profile presented in this work corresponds to the average of three simulations. The experimental biomass concentrations obtained by Nopharatana et al. (2003b) were taken at 100-µm intervals; for comparison with the layer model, a weighted average was used to adjust their data to intervals of 140 µm. Model parameters were adjusted to fit the experimental data, by trial and error, minimizing the error calculated by equation (4.3).

4.3   RESULTS

4.3.1   Fitting of the half-normal distribution curves to the biomass concentration profiles

A single half-normal distribution curve (equation (4.1)) was fitted to the data of Nopharatana et al. (2003b) for the concentration of vegetative aerial hyphae at 16 h of incubation. The value of σ_V, obtained directly from the data, was 0.2676 mm. The curve fitting gave a value of

11.66 g mm L^{-1} for X_{0V}, with a fitting error (equation (4.3)) of 0.61 g^2 L^{-2}. The fitted curve describes the experimental data very well, with only a slight deviation at the medium surface (Figure 4.3A).

Figure 4.3 Comparison between experimental data of biomass concentration of aerial hyphae (vegetative and reproductive hyphae combined) in PDA obtained by Nopharatana et al. (2003b) and the profiles obtained with the half-normal distribution curves at (A) 16 h and at (B) 40 h.
The half-normal distribution curves consider vegetative and reproductive hyphae as different subpopulations.
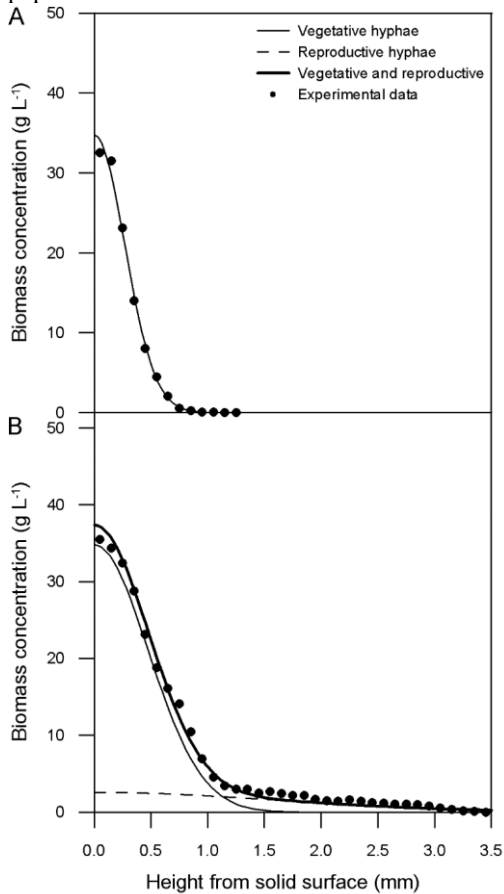
The sum of two half-normal distribution curves (equation (4.2)) was fitted to the data of Nopharatana et al. (2003b) for the concentration

of aerial hyphae at 40 h, which includes both vegetative hyphae and reproductive hyphae. The best fit was obtained with X_{0V} = 20.66 g mm L^{-1} and σ_V = 0.4742 mm for vegetative hyphae and X_{0R} = 5.20 g mm L^{-1} and σ_R = 1.6077 mm for reproductive hyphae, with a fitting error of 0.57 g^2 L^{-2}. The fitted curve for total biomass describes the experimental data very well, again with only a slight deviation at the medium surface (Figure 4.3B). According to the fitted profiles for the different types of biomass, the vegetative biomass falls to negligible values (approximately 0.1 g L^{-1}) by a height of about 1.6 mm while the reproductive biomass extends to heights as high as 3.5 mm, the same maximum height observed in the micrograph of 40 h obtained by Nopharatana et al. (2003b). The resulting half-normal distribution curves were used in the next step, in order to adjust the parameters of the layer model.

4.3.2   Calibration of the layer model for aerial hyphae

Parameters t_D, Δt_{VH}, Δt_{RH}, P_G, X_{max}, m_e, N_{rep}, $h_{lim,RH}$ and n_e were adjusted to give good fits of the layer model to the half-normal distribution curves, calculated at intervals of 140 μm for both 16 h and 40 h of cultivation, with a single set of values for these parameters. The distribution curves were used instead of the experimental profiles, because they consider vegetative and reproductive hyphae individually. The values of the adjusted parameters are listed in Table 4.1. The adjusted duration of each iteration during the growth of vegetative aerial hyphae was 2.29 h (Δt_V), which corresponds to an extension rate of 61 μm h^{-1}, and for each iteration during the growth of reproductive aerial hyphae, it was 0.772 h (Δt_R), which corresponds to an extension rate of 181 μm h^{-1}. In the fitting process, X_{max} was adjusted at a value of biomass concentration that corresponds to 40% of the volume of the layer being occupied by hyphae, which is similar to the value of 34% determined by Auria et al. (1995) in SSF with *Aspergillus niger*. The value of $h_{lim,RH}$ was taken from the micrographs of Nopharatana et al. (2003b). The exponent n_e was adjusted to 3, thus the tips of reproductive hyphae are unlikely to inactivate close to the surface and more likely to inactivate close to the limiting height $h_{lim,RH}$.

After the calibration was done, the predictions of the layer model were compared with the experimental data of Nopharatana et al. (2003b). The agreement was good for both 16 h and 40 h of incubation (Figure 4.4). The errors obtained for vegetative and reproductive hyphae combined were 2.9 g^2 L^{-2} for 16 h and 3.4 g^2 L^{-2} for 40 h.

Table 4.1 Model parameters of the layer model for vegetative and reproductive aerial hyphae

Symbol	Value	Description
General parameters		
$Area$	1 mm²	Area of study
A	100 μm²	Cross sectional area of the hypha
h_{layer}	140 μm	Height of each layer
ρ_X	100 g L^{-1}	Density of the hyphal biomass
I	400 spores mm^{-2}	Inoculation rate
t_D	20.57 h	Time at which differentiation of aerial hyphae occurs
Parameters for vegetative aerial hyphae		
P_G	50%	Probability of germination for each spore
P_I	Eq. (4.4)	Probability of inactivation of tips of vegetative hyphae
X_{max}	40 g L^{-1}	Maximum biomass concentration for each layer
m_e	1	Exponent of Eq. (4.4)
Δt_{VH}	2.29 h	Duration of each iteration for the phase during which vegetative hyphae grow
Parameters for reproductive aerial hyphae		
N_{rep}	20%	Percentage of germinated spores that form two reproductive hyphae
$P_{I,RH}$	Eq. (4.5)	Probability of inactivation of tips of reproductive hyphae
$h_{lim,RH}$	3.5 mm	Limiting height for growth of reproductive hyphae
n_e	3	Exponent of Eq. (4.5)
Δt_{RH}	0.772 h	Duration of each iteration for the phase during which reproductive hyphae grow

Figure 4.4 Comparison between experimental data of biomass concentration of aerial hyphae in PDA obtained by Nopharatana et al. (2003b) and the profiles for aerial hyphae (vegetative and reproductive hyphae combined) obtained with the layer model at 16 h and at 40 h.
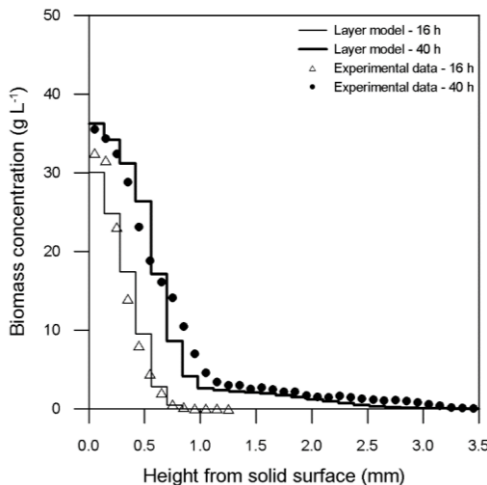
4.3.3 Sensitivity analysis of the layer model

Parameters P_G, X_{max} and m_e were varied in order to determine how they affect the predictions of the layer model with respect to the biomass profiles of vegetative hyphae with height above the surface and total biomass formed until the moment of differentiation (t_D). The parameters with the greatest influence on the simulation results were X_{max} and m_e. X_{max} does not affect the maximum height achieved, but the biomass concentration in each layer increases as X_{max} increases, especially close to the surface (Figure 4.5A). Consequently, the total biomass of vegetative hyphae obtained with $X_{max} = 55$ g L^{-1} is 27% higher than that with $X_{max} = 40$ g L^{-1} and 92% higher than that with $X_{max} = 25$ g L^{-1}. The biomass concentration did not reach the limiting biomass concentration (X_{max}) before differentiation occurred, in any of the simulations with $m_e = 1$.

The exponent m_e measures how the probability of inactivation of vegetative tips varies as a function of biomass concentration in a layer and indirectly indicates how likely it is for a vegetative aerial hypha to stop extending when it encounters other hyphae. In the fitted model, extension stops with few encounters ($m_e = 1$), but for the sensitivity analysis we tested $m_e = 2$ and $m_e = 3$, which would mean more encounters before inactivation. Only the simulation undertaken with $m_e = 1$ results in a profile similar to a half-normal distribution at the time of differentiation. The result with $m_e = 2$ was close to the result with $m_e = 3$ (Figure 4.5B), with at least three layers with biomass concentration equal to or higher than X_{max} (40 g L^{-1}). Biomass concentration higher than X_{max} is possible because the inactivation test considers the biomass concentration in the layer within which the tip is positioned before extension and not the biomass concentration in the layer to which the tip is extending. In other words, a tip may extend to a "crowded" layer if it is coming from a "non-crowded" layer (which would usually be a downward movement). However, once in a "crowded" layer, the tip will inactivate. The fact that the best result was obtained with $m_e = 1$ suggests that a *Rhizopus oligosporus* hypha is likely to stop growing when it encounters another hypha or an obstacle.

It is important to note that m_e is not exactly equal to the number of encounters, since the actual position of a segment within a layer is not considered in the layer model. Consequently, the effect of m_e on the profile predicted by the model is very different from that of the corresponding parameter in the model of Coradin et al. (2011), in which

Figure 4.5 Sensitivity of the predicted profiles for vegetative aerial hyphae at 40 h to the parameters X_{max} and m_e.

(A) Effect of the maximum biomass concentration for each layer, X_{max}; (B) Effect of m_e, the exponent of Eq. (4.4). In each case, the thicker continuous line corresponds to the parameter value that was adjusted to the experimental data.
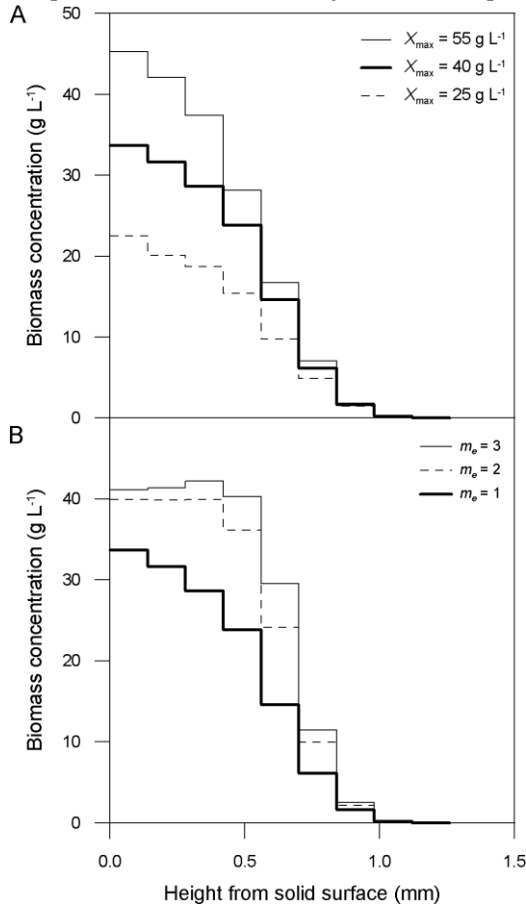
each hypha is tracked individually. In their case, the number of encounters before inactivation that gave the best fit was two and this parameter had a significant effect on both the maximum biomass concentration and the shape of the profile near the surface: with only one encounter allowed, the biomass profile was almost flat, with a peak in concentration of almost 10 g L^{-1}; with three allowed encounters, the biomass profile was similar

to that for two allowed encounters, but with a higher biomass concentration close to the surface, above 50 g L^{-1}.

The germination rate (P_G) had little influence on the density profile of vegetative hyphae, even when varied from 30% to 70%. This suggests that the growth of vegetative biomass is not strongly limited by the germination rate itself, since branching can compensate for low germination rates. The same result was found in the sensitivity analysis with the model of Coradin et al. (2011). On the other hand, germination probability directly affects the number of reproductive hyphae, which, in the layer model, is proportional to the number of germinated spores, but it does not affect the maximum height of reproductive hyphae.

Parameters N_{rep}, $h_{lim,RH}$ and n_e were also varied to see their effects on the biomass profiles of reproductive hyphae with height at 40 h of incubation. As expected, varying N_{rep} from 1 to 1.4 tips per germinated spore had an effect similar to that of the variation in P_G, affecting the number of tips, but not the maximum height reached.

The parameters of equation (4.5), $h_{lim,RH}$ and n_e, influence the height that the reproductive hyphae reach before sporulation, but not the number of sporangia that are formed. With $n_e = 2$, 50% of the reproductive hyphae stop growing at heights greater than 1.47 mm, while with $n_e = 4$, 50% of the reproductive hyphae stop growing at heights greater than 2.45 mm. Similarly, 50% of the sporulation occurred at heights higher than 1.61 mm when h_{lim} was set at 2.5 mm and at heights higher than 2.45 mm when h_{lim} was set at 4.5 mm.

4.4 DISCUSSION

4.4.1 Steric impediment and random walk rule the growth of vegetative aerial hyphae

Although the layer model uses simple rules to govern the movement of hyphal tips, it generated profiles for the aerial biomass that were quite close to the experimental profiles of Nopharatana et al. (2003b). Basically, tips of vegetative hyphae move freely in a random walk, that is, with all available directions having the same probability of being chosen, until the hyphal tips are inactivated, which occurs when there is not enough available space for them to extend into.

Random walks are commonly used to describe chemical and biological phenomena, including hyphal growth (CODLING et al., 2008; INDERMITTE et al., 1994). The classic example of a random walk is the

unidimensional diffusion of particles in fluids: all particles are initially placed in the middle of the system; each particle has a 50% probability of moving to the right and 50% to the left; after some time, most particles will have moved the same amount of times to the right and to the left and will be in their starting position, but some particles will have moved more to the right and other particles more to the left. With a high number of particles, their distribution in space will generate a normal distribution curve, which also occurred for the distribution biomass of vegetative hyphae at 16 h measured by Nopharatana et al. (2003b). In the model of Nopharatana et al. (1998), the movements of the tips were described as obeying a diffusion-like process, which indirectly means that the tips moved in a random-walk fashion. Consequently, the simulation profile of Nopharatana et al. (1998) in the first hours was similar to a half-normal distribution curve. This result, combined with the good agreement between the layer model and the experimental data, indicates that tips of vegetative aerial hyphae, at least in the case of *R. oligosporus*, move in random walk through the air phase.

The model of Coradin et al. (2011) had rules that prevented it from fitting the experimental data well, namely the rules for choosing the direction of growth for vegetative hyphae and the rules for growth of reproductive hyphae (these rules are addressed in subsection 4.4.2). In their model, when choosing the direction of extension, a vegetative hypha may grow horizontally, vertically or diagonally in any direction, with the probability assigned to each direction depending on the height of the tip. For example, tips immediately above the surface have 95% probability of extending upwards and 5% of extending horizontally; as tips reach higher heights, the probabilities of extending upwards and of extending horizontally decrease slowly while the probability of extending downwards increases, reaching 20% at a height of 1 mm. Therefore, in their model, the probably of a tip returning back to the surface is very low and it decreases as the tip approaches the surface; this is probably what causes a peak in concentration 0.2 mm from the surface instead of a peak at the surface. In addition, there is no known mechanism by which the height at which the hyphal tip finds itself would affect its choice of direction.

As for the probability of inactivation, the layer model considers that there is a maximum hyphal concentration in aerial space. The concept of a maximum concentration of aerial hyphae, as explained by Laukevics et al. (1985), is related to the maximal packing that can be achieved with hyphae. They evaluated different ways to pack cylindrical hyphae, without branches, and, even with the highest packing possible, which is

achieved with parallel cylinders touching one another side-by-side, hyphae can occupy only 76.5% of the space available. If the space between neighbor hyphae is equivalent to the diameter of a hypha, for example, the space occupied by hyphae is reduced to 19.6%. They also analyzed reported data from the literature and concluded that the maximum packing that can be achieved in SSF is 15%. During growth of *Aspergillus niger* on a synthetic resin imbibed with a nutrient solution, Auria et al. (1995) estimated that hyphae occupied 34% of the interparticle volume.

The value of maximum biomass concentration per layer adjusted in the model is equivalent to 40% of the volume being occupied by hyphae, which is higher than these reported values. This difference is due to the fact that these values from the literature are averages for the entire air space of the fermentation bed, which may include spaces that have not reached the maximum biomass concentration, whereas the value in the model is the absolute maximum for any localized region of the bed. For example, at 16 h of incubation, in the experiment of Nopharatana et al. (2003b), hyphae occupied 33% of the air space immediately above the surface (heights from 0 to 0.1 mm), but, considering the whole height of the biomass layer (heights from 0 to 1.2 mm), hyphae occupied in average 10% of the air space.

Steric impediment is described indirectly in the layer model, being based on the average biomass concentration in space, since a proper description of this phenomenon requires tracking of the exact positions of all hyphae present and of the extending tips. This tracking was achieved in the model of Coradin et al. (2011), in which extension of vegetative aerial hyphae was also limited by steric impediment. In their model, a hypha is not allowed to extend in the cubes adjacent to existing hyphae, including the parental hypha and the other daughter hypha from a branching process. In addition, a hypha stops extending when it encounters an existing hypha, which is considered a prohibited movement; if a hypha makes two prohibited movements, it will inactivate. Such an approach does not require the maximum biomass concentration as a parameter, rather, a maximum density appears as a consequence of the rules for inactivation of the tips.

Similarly to the layer model of the present work, Nopharatana et al. (1998) also described steric impediment through a maximum biomass concentration: when this concentration was reached at a certain height, the tips at that height could not extend or branch and tips from other heights could not move into that position. This was the only limitation for growth of aerial hyphae, since glucose concentration at the medium

surface was considered to be constant throughout the simulation and differentiation into reproductive hyphae was not considered. Consequently, after biomass concentration at the surface reached the maximum level, growth ceased at the surface, but continued at higher heights; as time progressed, the profile of biomass concentration behaved as wavefronts of constant shape, moving through space, which does not reflect the experimental data of Nopharatana et al. (2003b) at 16 and 40 h of incubation. According to the authors, the model would fit better to the experimental data if the maximum biomass concentration were calculated as a function of height, although they did not know what would control such a limitation (NOPHARATANA et al., 2003b). However, the real reason for the differences between their predicted profiles and the experimental data may be that growth in their model is only limited by this maximum local biomass concentration, and there is no inactivation related to the event of differentiation or due to the consumption of all the glucose in the medium. This means that only using a maximum concentration threshold is not sufficient to describe the experimental profiles of Nopharatana et al., (2003b) and it is necessary to include another limitation for growth.

4.4.2 Hyphal differentiation should be incorporated into mathematical models

The layer model incorporates the differences between vegetative and reproductive aerial hyphae, using different rules for each type of hypha based on their experimentally observed mode of growth. In addition, a good adjustment of the model parameters to each hyphal type was made possible after the profiles of biomass concentrations of the hyphal types were separated using the half-normal distribution curves. Differentiation of growth is not commonly explored in mathematical models; most models have focused only on one type of hypha, as in Nopharatana et al. (1998). Previous models that incorporated reproductive aerial hyphae are Georgiou and Shuler (1986) and Coradin et al. (2011).

In the first part of the simulation of the model of Coradin et al. (2011), only vegetative hyphae grow. At a predetermined time of differentiation, some active vegetative tips turn into reproductive tips, thus starting the second part of the simulation, in which only reproductive hyphae grow. Different rules were applied for each hyphal type. However, Coradin et al. (2011) used rules for the extension and branching

of reproductive hyphae that do not reflect the growth of *Rhizopus oligospous* on PDA: in their model, reproductive hyphae are formed from the tips of vegetative hyphae instead of being formed from the nodes of the rhizoids; branches are formed every 280 µm, whereas the micrographs show fewer branches; and inactivation occurs only when a prohibited movement occurs (e.g. a hyphal tip encountering another hypha), and not when the formation of sporangia occurs, even though sporangia are visible in the micrographs. Due to these rules, the biomass concentration profile for reproductive hyphae in the simulation by Coradin et al. (2011) is at least two-fold higher than the experimental concentration profile and remains almost constant with height, until 3 mm of height, whereas in the experimental data there is a decrease with height.

Georgiou and Shuler (1986) developed a pseudohomogeneous model for growth of surface and reproductive hyphae extending from a single colony of *Aspergillus nidulans*. Even though their model is not appropriate to describe the data of Nopharatana et al. (2003b), because it does not describe vegetative aerial hyphae or the distribution of biomass over height, biomass growth is described as a function of the radius of the colony, their approach to describe differentiation is interesting. In their model, four types of hyphae are described: undifferentiated, competent (i.e. able to form conidiophores), mature conidiophores and conidia. Differentiation depends on the concentrations of glucose and nitrate and the age of the mycelium: 24 h after a particular area is colonized by undifferentiated mycelium, this mycelium is competent to differentiate; the rate of differentiation of competent to mature conidiophores increases with low concentration of nitrate; the rate of differentiation of mature conidiophores to conidia depends on the concentration of both nitrate and glucose.

Neither the layer model developed in the current work nor the model of Coradin et al. (2011) include nutrient in their description of the system, thus differentiation is set to occur at a certain point in time. In order to use the lack of nutrients as the trigger for differentiation, as done by Georgiou and Shuler (1986), it is necessary to extend these models by, for example, fusing them with the model of Balmant et al. (2015), which describes the growth a single hypha, using equations for mass transfer of intracellular nutrients and vesicles. For this fusion, it would be appropriate to use the rules of growth and branching from the layer model and the three-dimensional description of hyphae from the model of Coradin et al. (2011). In the model of Balmant et al. (2015), the hypha is divided into a series of tanks of the same size as the cubes used by Coradin et al. (2011), which facilitates this fusion.

4.4.3 The layer model may be used in a variety of situations involving the growth of aerial hyphae

The layer model may also be used, as it is, to describe the growth of aerial hyphae in the spaces between adjacent particles; the distribution of the aerial hyphae in these spaces affects the pressure drop through forcefully-aerated beds. Another possible application would be to extend the layer model for both aerial and penetrative hyphae (Sugai-Guérios et al., 2016) to study O_2 transfer through the aerial mycelium and inside the particle, in order to estimate the concentration profile of O_2 inside the solid. This was previously done by Rahardjo et al. (2005a) and Oostra et al. (2001), but in a very simplistic manner: They considered only biofilm hyphae, with a homogeneous biomass concentration through the height of the biofilm; also, they did not describe the growth of penetrative hyphae.

The layer model could also be adapted to describe aerial hyphae of other fungal species, however some parameters and rules would have to be adapted. For example, reproductive hyphae from *A. nidulans* are 100 µm long and they extend from the sides of vegetative aerial hyphae and not from nodes at the surface (FISCHER; KÜES, 2006). Other changes may be guided by comparing experimental biomass profiles obtained for other species with the sensitivity analysis presented in this work.

Finally, this work also shows that the profile of aerial biomass of *R. oligosporus* can be described by a half-normal distribution curve, thus, this curve can be used for future macroscale models to describe aerial biomass, in a simple and easy manner. In macroscale models, it is not advisable to try to describe the growth of each hypha individually, rather mycelial growth should be described as a pseudohomogeneous distribution of biomass in space. In case researchers choose to incorporate a more precise biomass distribution to model fungal growth in a few particles, mimicking a fraction of a fermentation bed, for example, they may use the half-normal distribution curve to describe biomass concentration around particles. This curve may be useful in the estimation of porosity and pressure-drop in the bed.

4.5 CONCLUSIONS

Aerial hyphae had been previously modeled by Nopharatana et al. (1998) and by Coradin et al. (2011), but these models did not reproduce well the profiles of biomass concentration as a function of height obtained

by Nopharatana et al. (2003b). The layer model proposed in this work is the first to describe these profiles accurately, with the advantage of using simple rules for direction of growth and inactivation, namely tips of aerial hyphae extend following random walk movements and stop extending in case of steric impediments.

Another advantage of the layer model, both for aerial and for penetrative hyphae (SUGAI-GUÉRIOS et al., 2016), is that it can be fused with the phenomenological model of Balmant et al. (2015) and the 3D spatial description used by Coradin et al. (2011). This would result in a full mesoscale morphological model for the growth of mycelia on solid particles, which could be used to investigate mesoscale phenomena in SSF systems (SUGAI-GUÉRIOS et al., 2015).

5 REVISITING HYPHAL GROWTH ON SOLID SURFACES: A MICROSCOPIC POINT OF VIEW ON DIFFERENTIATION

5.1 INTRODUCTION

The growth of filamentous fungi on the surfaces of moist solid particles is used for industrial production not only of microbial metabolites, such as enzymes, organic acids and pigments, but also of food products, such as tempeh and soy sauce (THOMAS et al., 2013). This type of industrial process is named solid-state fermentation (SSF) and is characterized by a continuous gas phase around the solid particles, in which water is present mainly as moisture inside the particles, although there may be a thin film of water at the particle surface. The particles used in SSF are commonly agro-industrial wastes, such as citrus pulp, sugar cane bagasse and wheat straw, which undergo thermal and often chemical pretreatment to facilitate access to the nutrients within. Although SSF is an ancient technique for food production, many aspects of growth and morphology of the mycelia of filamentous fungi on solid particles are unclear.

The hyphae formed during growth of filamentous fungi in SSF are classified, based on the environment they occupy, into surface, aerial and penetrative hyphae (RAHARDJO et al., 2006). A fourth type of hypha, named biofilm hyphae, is identified when a network of hyphae grow within a liquid film at the surface of the particle (RAHARDJO et al., 2006). Each environment imposes different chemical and physical conditions for growth, such as limitations of nutrient and water availability or physical barriers. These conditions affect the metabolism

of the hypha and, as a result, each hyphal type may differ with respect to the moment they start and stop growing, when and where branches are formed, and when and where the product of interest of the SSF process is formed, such as enzymes or organic acids. These processes determine the spatial distribution of active tips and the profiles of biomass concentration for each type of hypha, affecting mass transfer phenomena inside the hyphal network, inside the particle and in the inter-particle spaces, and, consequently, the productivity of the SSF process.

While surface hyphae and, to a lower degree, aerial hyphae have been intensively investigated since the 1970s (BULL; TRINCI, 1977; RAHARDJO et al., 2006), penetrative hyphae have not been studied at the same level of detail, probably due to the difficulty in observing and measuring their growth. However, the observations made for surface and aerial hyphae do not necessarily apply to penetrative hyphae, which grow in a very different physical and chemical environment. For example, in the case of *Rhizopus oligosporus* growing on PDA (potato dextrose agar), the growth morphologies of aerial and penetrative hyphae were certainly quite different (NOPHARATANA et al., 2003b): Penetrative hyphae extended downwards in a direction almost perpendicular to the solid surface, while aerial hyphae extended in various directions. In addition, in the profiles of biomass concentration as a function of height and depth at 40 h, the highest density of aerial hyphae was around 35 g L^{-1} and occurred at the surface, while the highest density of penetrative hyphae was only 3 g L^{-1} and occurred 0.45 mm below the surface.

Another study regarding penetrative hyphae used a discrete model, a so-called layer model, to describe the extension of vegetative penetrative hyphae in order to understand the phenomena that influence branching and extension of these hyphae (SUGAI-GUÉRIOS et al., 2016). In this model, the solid particle is divided into symmetrical layers parallel to the surface. The model starts with active hyphal tips at the surface and, over a series of iterations, probability rules are used to determine whether two, one or no hyphal segments are added to a given active tip, simulating apical branching, hyphal extension without branching or tip inactivation, respectively. The adjusted rules indicate that the final length of vegetative penetrative hyphae is determined mainly by two factors: the firmness of the solid particle, which determines the turgor pressure required for the tip to penetrate the solid particle, and the pressure drop inside the hypha, which affects the turgor pressure at the tip. This model was based on micrographs of *R. oligosporus* taken at only two different incubation times (NOPHARATANA et al., 2003a,b), thus many aspects of the model were based on suppositions and were not

confirmed experimentally, for example, the moment when the first penetrative hypha is formed and the rate at which new penetrative tips are formed at the surface during the incubation time.

The objective of the current work is to characterize how the growth of penetrative hyphae differs from that of aerial hyphae and surface hyphae, by determining the timing of their formation, their branching and the expression of extracellular polygalacturonases through confocal microscopy. In addition, we investigated the effect of the type of carbon source available in the medium on the growth and morphology of the penetrative hyphae. *Aspergillus niger* was chosen for the present study because of its potential application for the production of polygalacturonases and other pectinases through SSF (PITOL et al., 2016; NIU et al., 2015) and because it is a well characterized species, since its genome has been sequenced and some transcriptome and secretome studies have been conducted (LEVIN et al., 2007; MARTENS-UZUNOVA, 2008; BRAAKSMA et al., 2010; BENOIT et al., 2015; NIU et al., 2015). Two fluorescent strains were developed for this study: pgaRed, which constitutively expresses both *eGFP*, the product of which remains in the cytosol, and a fusion gene of *mCherry* and endopolygalacturonase B (*pgaB*); and pgxRed, which constitutively expresses *eGFP* and, in the presence of galacturonate or polygalacturonate, expresses a fusion gene of *mCherry* and exopolygalacturonase B (*pgxB*). These polygalacturonases hydrolyze the bonds between galacturonate monomers in polygalacturonate and in pectin.

5.2 MATERIAL AND METHODS

5.2.1 Strains, media and culture conditions

Aspergillus niger ATCC 1015 (CBS 113.46) was used as the parental strain for the construction of the pgaRed and pgxRed strains. Both of these strains express the enhanced green fluorescent protein (EGFP) under the control of the *gpd* promotor from *Aspergillus nidulans*, which is a strong constitutive promoter. In each strain, a native polygalacturonase gene was fused with the gene for the red fluorescent protein variant called mCherry (SHANER et al., 2004), and this fused gene was used to replace that of the original polygalacturonase. The polygalacturonase gene used in the fusion in pgaRed was *pgaB* and the

polygalacturonase used in the fusion in pgxRed was *pgxB*. All plasmids were produced in *E. coli* TOP10 cells.

Luria Broth culture medium supplemented with 50 µg mL^{-1} of kanamycin was used for *E. coli* cultures, with incubation at 37 °C and 250 rpm. *A. niger* conidia were obtained on PDA plates at 30 °C. For *A. niger* transformation, mycelium was obtained by inoculating approximately 10^8 conidia into 125 mL of YP medium (10 g L^{-1} yeast extract, 20 g L^{-1} peptone) supplemented with 30 g L^{-1} gelatin, and incubating at 28 °C and 200 rpm for 48 h. Mycelium was harvested by vacuum filtration and rinsed with sterile water before protoplast transformation.

For microscopy, synthetic complete media (SC) were used: 6.7 g L^{-1} yeast nitrogen base for microbiology (product code 51483; Sigma-Aldrich, Germany), 20 g L^{-1} agar, 120 mM NaH$_2$PO$_4$/Na$_2$HPO$_4$ buffer (pH 6) and supplemented with a carbon source. For most experiments, the SC was supplemented with 20 g L^{-1} of D-glucose (SCD medium). In the experiments with different carbon sources, D-glucose was replaced by starch (SCSta medium), by D-galacturonate (using the sodium salt; SCGal medium) or by polygalacturonate (using the sodium salt; SCPga medium), maintaining the same molar concentration (in Cmols per liter) in all media. Conidia were spread over the solidified medium surface, resulting in 40 conidia mm^{-2}. A small piece of the inoculated medium was excised and gently laid on a glass bottom dish, with the inoculated surface of the medium perpendicular to the glass surface, before being transferred to the microscope (Figure 5.1). Inoculated media were incubated before and during image capture at 30°C.

Figure 5.1 Schematic representation of the procedure used to prepare the medium sample for microscopy.
The surface of the SC plate was inoculated with conidia (A), a small piece of the medium was excised (B) and laid on a glass bottom dish (C). The optical fields captured start at the side of the medium that is closest to the bottom of the dish and include a part of the medium, the medium surface and a part of the gas phase (D).
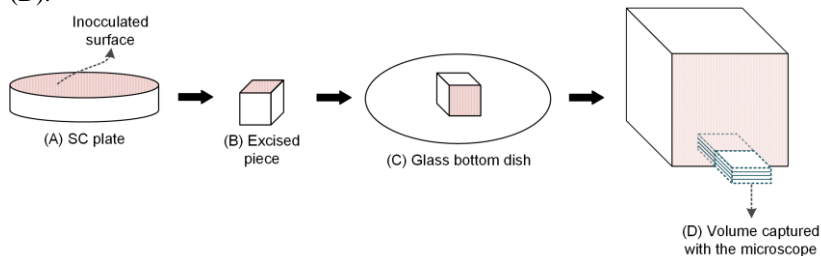
5.2.2 **Transformation of *A. niger* and plasmid construction**

The integration cassette for eGFP was obtained directly from the pSM1 vector, which contains a hygromycin resistance gene (*hph*) as a selection marker (PÖGGELER et al., 2003). The integration cassettes for the fused polygalacturonase genes were constructed in this work.

The integration cassette for pgxB-mCherry consisted of: a homologous 5' flank (2.7 kb), which included the *pgxB* ORF without the stop codon (1.3 kb) and its promoter region; the *mCherry* ORF without the start codon (0.7 kb); and a homologous 3' flank (1.0 kb), containing the *pgxB* terminator. The 5' and 3' flanks were amplified by PCR (KAPA HiFi HotStart, Kapa Biosystems) with primers P1/P2 and P5/P6, respectively (Table 5.1). The *mCherry* gene was amplified from the pRSETB_mCherry plasmid (a kind gift from R.Y. Tsien) by PCR (KAPA HiFi HotStart, Kapa Biosystems) with the primers P3/P4 (Table 5.1). The amplified flanks and the *mCherry* ORF were joined using assembly PCR and the resulting cassette was ligated into the pCR®-Blunt II-TOPO vector (Life Technologies, EUA). Through primers P2/P3, a linker coding for 5 residues of glycine was inserted between the ORFs of *pgxB* and *mCherry*.

Table 5.1 Oligonucleotides used in the study.

Name	Sequence
P1	CGACGGTATCGATAAGCTTGATATCGAATTCCTGCAGCCCGGGCCATCCCCTACCTCCTCTTC
P2	GCTCACTCCACCTCCGCCACCCCGCGTAACACTCTCGTCAC
P3	GTGACGAGAGTGTTACGCGGGGTGGCGGAGGTGGAGTGAGCAAGGGCGAGGAGGA
P4	AAGAACCACCAAGTAGAGCATTACTTGTACAGCTCGTCCATGCC
P5	TGGACGAGCTGTACAAGTAATGCTCTACTTGGTGGTTCTTC
P6	CCACCGCGGTGGCGGCCGCTCTAGAACTAGTGGATCCCCCGGGTCCTCAATAACCTTCCTCTC
P7	AGCTTGCATGCCTGCAGGTCGACTCTAGAGAATGCTGGAAGGAGCTTGCCTTTCG
P8	GCTCACTCCACCTCCGCCACCATCGCTGCAGGAAGCGCCCG
P9	CGGGCGCTTCCTGCAGCGATGGTGGCGGAGGTGGAGTGAGCAAGGGCGAGGAGGA
P10	ACAGCTGGCCAGAGACCCGTTTACTTGTACAGCTCGTCCATGCC
P11	TGGACGAGCTGTACAAGTAAACGGGTCTCTGGCCAGCTGT
P12	CGGCCAGTGAATTCGAGCTCGGTACCCGGGCCTCTCTCTTTCTACGACTCGGC
P13	ACATGAATTGACCGTTGCAGACCA
P14	CCTCCCTTCGAATTCCAGTCACTC

The plasmids containing the pgxB-mCherry cassette and the eGFP cassette were linearized with *SmaI* and *HindIII* (Thermo Scientific, USA), respectively, and co-transformed into *A. niger* ATCC 1015 using a protoplast transformation method. Transformed colonies were selected in hygromycin plates. Correct integration of the pgxB-mCherry cassette into the genome was confirmed with colony PCR using a Phire direct PCR kit (Thermo Scientific) and primers P1/P6.

The same methods were used for the pgaRed strain, with small changes. The 5' and 3' flanks were amplified with primers P7/P8 and P11/P12, respectively (Table 5.1). The *mCherry* ORF was amplified from the pRSETB_mCherry plasmid with primers P9/P10 (Table 5.1). Prior to transformation, the pgaB-mCherry cassette was digested with *EcoRI* (Thermo Scientific, USA). For colony PCR of colonies of transformed *A. niger*, primers P13/P14 were used.

5.2.3 Confocal microscopy

Confocal microscopy was performed with an A1R[+] confocal microscope (NIKON Instruments Inc., Japan), with either a 20× objective or a 40× objective with water immersion, as detailed in Table 5.2. eGFP was excited with the 488 nm laser and detected with a filter interval ("band pass") of 500-550 nm. mCherry was excited with the 561 nm laser and detected with a filter interval ("band pass") of 570-620 nm. Images were acquired as z-series of optical fields using the Nis Elements 4.20 Confocal software package (NIKON Instruments Inc., Japan). Images are presented as maximum intensity projections, created with Fiji ImageJ software (SCHINDELIN et al., 2012). Specific image capture setups, such as resolution, z-depth and optical field size, are detailed for each figure in Table 5.2.

Table 5.2 Microscope settings and image preparations.

Fig.	Strain	Medium	Objective (numerical aperture)	Number of fields captured in the experiment	Pixel dimensions in acquired images (μm/px)	Field dimension in acquired images (μm × μm)	Number of z-sections (for each field)	z-step (μm)	Time interval between captures of the same field	Zoom in acquisition	Number of z-sections used in projection	Crop
						Microscope settings						Image manipulations
2	pgaRed	SCD	20× (0.75)	1	0.62	1171 × 633	121	1	18 min	1×	121	A, B and C are cropped
3	pgaRed	SCD	20× (0.75)	1	0.62	1171 × 633	121	1	18 min	1×	73	Yes
4	pgaRed	SCD	20× (0.75)	1	0.62	1171 × 633	121	1	18 min	1×	51	Yes
5	pgaRed	SCD, SCSta	20× (0.75)	3 fields for each medium	1.24	1203 × 1203	76	2	4 h	1×	64 for SCD, 25 for SCSta	Yes (only the initial hours)
7	pgaRed	SCGal, SCPga	20× (0.75)	3 fields for each medium	1.24	1203 × 1203	76	2	4 h	1×	33 for SCGal, 46 for SCPga	Yes (only the initial hours)
8	pgxRed	SCPga	20× (0.75)	3 fields	1.24	948 × 1383	76	2	2.8 h	1×	54	Yes
9A	pgxRed	SCPga	20× (0.75)	1	0.31	316 × 316	17	1	none	1×	17	Yes
9B	pgxRed	SCPga	40× (1.15), water immersion	1	0.12	250 × 250	17	1	none	2×	17	Yes
9C	pgxRed	SCPga	40× (1.15), water immersion	1	0.12	250 × 250	7	1	none	2×	1	Yes

5.3   RESULTS

The micrographs presented in the following sections correspond to four experiments, each with a different purpose. The strain, media and image capture setups used are described briefly at the beginning of each section and in more detail in Table 5.2. All given incubation times correspond to time after inoculation, unless otherwise specified. Although the same inoculation density was intended in all experiments, the inoculation density in the particular region of the surface that was observed microscopically seems to be higher in the experiment presented in sections 5.3.2, 5.3.3 and 5.3.4. The consequences of the difference in conidia density are discussed in section 5.3.2.

5.3.1   Time-lapse of the colonization of a solid surface by *Aspergillus niger* pgaRed at a low inoculation density

A time-lapse analysis of the growth of *A. niger* pgaRed on SCD (glucose) was conducted in order to determine the moment the first penetrative hypha is formed and how branching occurs in penetrative hyphae. Image capture began 5 h after inoculation and micrographs were taken every 18 min until 24 h. The size of each optical field was 1171 μm by 633 μm and the z-series of optical fields corresponded to 120 μm of field depth (Table 5.2), starting from the side of the medium closest to the bottom of the dish.

In the germination process of *A. niger*, two germ tubes are usually formed from opposite sites on the conidium surface, one after the other. In this experiment, initially, there were 3 conidia in the field captured (Figure 5.2A). The first germ tube was formed at around 6.2 h: for the two conidia on the left, the first germ tube was a penetrative hypha, while the germ tube of the third conidium was a surface hypha (Figure 5.2A). At around 8.8 h, the second germ tube of each conidium was formed: as a surface hypha for the two conidia on the right and as a penetrative hypha for the conidium on the left (Figure 5.2B). This leads to the conclusion that both surface and penetrative hyphae grow in the first few hours after germination and, in fact, for some conidia, the first germ tube may penetrate into the medium rather than extending along the surface. The early development of penetrative hyphae improves the attachment of the mycelium to the solid (SUGAI-GUÉRIOS et al., 2016), which, in the absence of penetrative hyphae, occurs only through the production of an

extracellular matrix, in the case of *A. niger* (VILLENA; GUTIÉRREZ-CORREA, 2007).

In the present experiment, in contrast with penetrative hyphae, vegetative aerial hyphae began to appear only after surface hyphae had already occupied the solid surface, around 13.6 h (Figure 5.2C). The formation of aerial hyphae is triggered by a determined cell density in the medium, which induces the synthesis and secretion of hydrophobin, a protein that lowers the water surface tension and, hence, allows aerial hyphae to grow into the air (KRIJGSHELD et al., 2013).

Branching in penetrative hyphae was mostly subapical and occurred closer to the base of the hypha (i.e. the hyphal region closest to the surface) than to its tip. For example, in one of the first penetrative hyphae formed, two branches were formed between 10.5 h and 10.8 h, when the parental hypha was 282 µm long (Figure 5.2B). The first branch was formed 59 µm from the solid surface, and the second branch was formed 31 µm from the surface. As in surface hyphae of *A. nidulans* (FIDDY and TRINCI, 1976), the order in which branches form is not sequential along the length of the parental hypha, that is, new branches may form between the tip and an older branch, or between two older branches or between the solid surface and the branch furthest from the tip. Figure 5.3 shows 10 subapical branches extending from the same penetrative hypha at various sites, without a clear order.

Figure 5.2 Time-lapse of mycelium formation from 3 conidia of *A. niger* pgaRed growing on SCD.
(A) The first germ tubes formed for each conidium; (B) The second germ tubes formed for each conidium and two subapical branches formed from a penetrative hypha, in which vacuoles are already visible; (C) The moment when the first aerial hypha appears; (D) Morphology before differentiation; (E) Morphology after differentiation; (F) The entire growth area captured at the end of the experiment, with some reproductive hyphae. Dashed lines represent the medium surface. In (A) through (C), P, S and VA indicate penetrative germ tube, surface germ tube and vegetative aerial hyphae, respectively. The arrows in (B) point to the first branches in penetrative hyphae while the arrows in (E) and (F) point to the reproductive hyphae formed from penetrative hyphae deep within the medium. The circle in (E) highlights subapical branches of penetrative hyphae extending upwards. Images are maximum intensity projections of z-series of optical fields corresponding to 120 µm of field depth. All scale bars represent 50 µm.

Cont. Figure 5.2

(A) 8.1 h

(B) 11.1 h

(C) 13.6 h

Cont. Figure 5.2

(D) 17.9 h

(E) 20.0 h

(F) 24.0 h
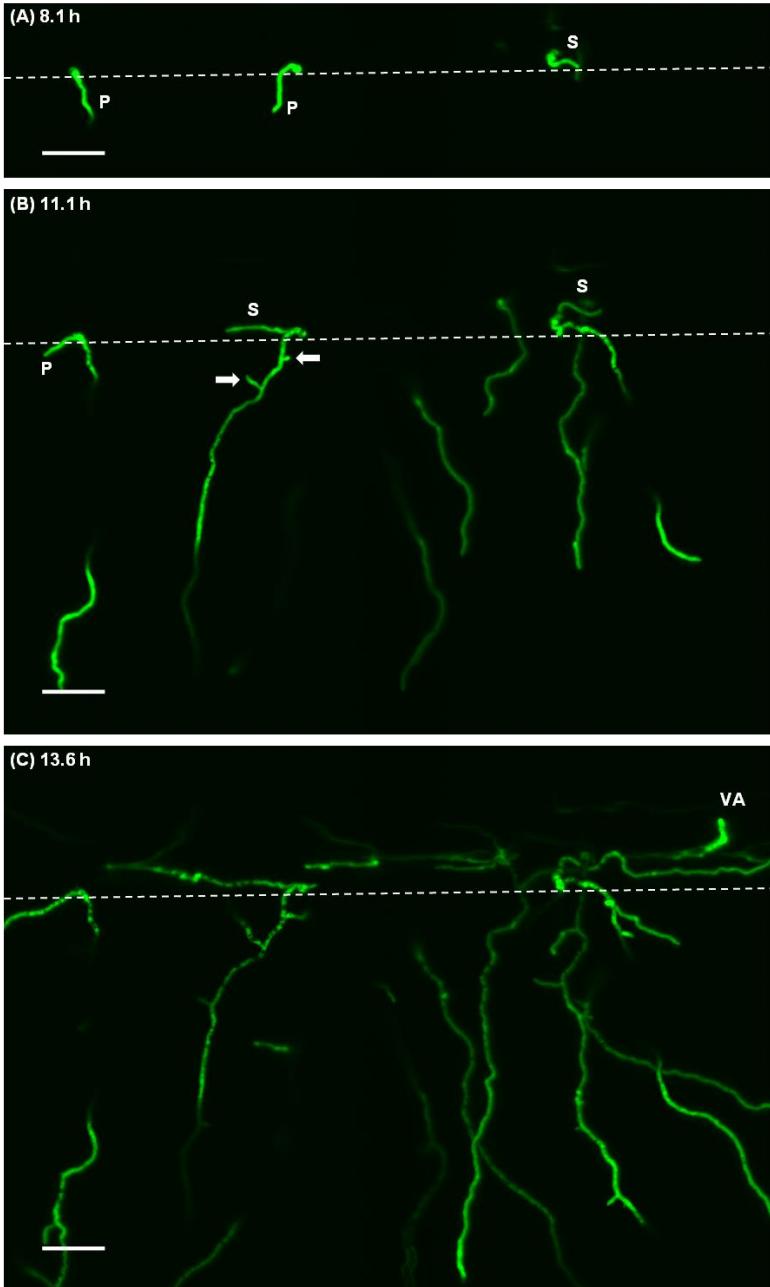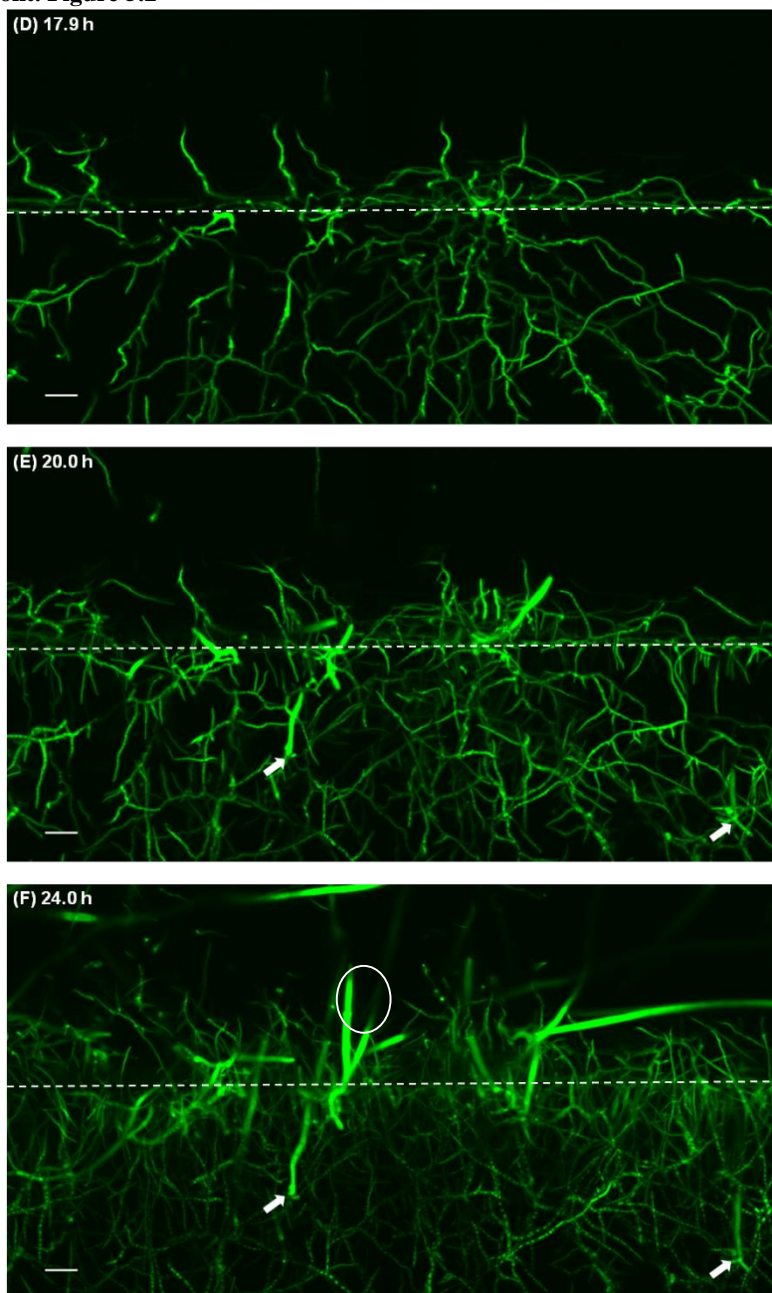
Figure 5.3 Time-lapse of the formation of subapical branches (indicated by arrows) from a single penetrative hypha of *A. niger* pgaRed growing on SCD.
In the first frame (14.5 h), 3 new branches were formed at almost the same time, in different positions. In the following 4.3 h, a total of 7 new branches were formed. Branches formed in daughter hyphae are not highlighted. Images are maximum intensity projections of z-series of optical fields corresponding to 72 µm of field depth. All scale bars represent 50 µm.
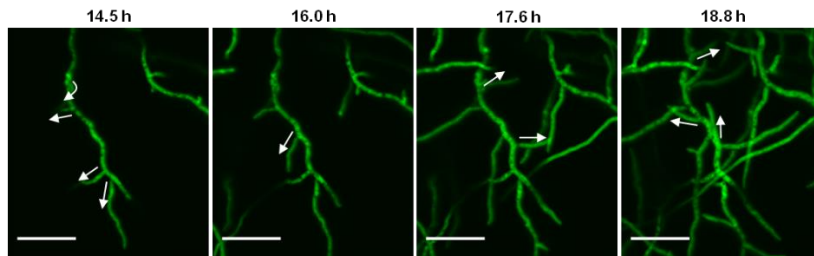
At around 18 h, segments of vegetative hyphae differentiate to foot cells, namely thick-walled hyphal segments, and reproductive hyphae begin to extend from them (Figure 5.2E). The asexual reproductive hyphae of *Aspergillus*, the conidiophores, consist of mainly three structures: stalks, which extend unbranched from the foot cell into the air; the vesicles, which are the swollen tips of fully grown stalks, with a diameter of around 10 µm; and conidia and their supporting structures, namely metulae and philiades, which are attached to the vesicle (KRIJGSHELD et al., 2013; BOYCE; ANDRIANOPOULOS, 2006). The only structures visible at the end of the experiment, at 24 h, were foot cells and stalks (Figure 5.2F), which can be distinguished from vegetative hyphae due to their larger diameter, of 6-7 µm, while the diameter of vegetative aerial hyphae is 2-3 µm (KRIJGSHELD et al., 2013). Foot cells are formed in segments of either surface hyphae or of penetrative hyphae below the surface, but not of vegetative aerial hyphae (Figure 5.2F). The formation of reproductive hyphae in *A. nidulans* occurs only after the mycelium has become competent to respond to developmental signals and may occur as a programmed event, depending only on the age the mycelium, or it may be triggered by stress conditions, such as nutrient deprivation (ADAMS et al., 1998). In the current work, since all hyphal types (surface, aerial and penetrative) continued to grow after the start of the formation of reproductive hyphae, the start of the production of structures for asexual reproduction at 18 h in this experiment probably occurs as a programmed event.

After 18 h, penetrative hyphae started to behave slightly differently, as though they had also undergone differentiation. One of the changes was in the branching pattern for penetrative hyphae. Initially, branches were rare and most of biomass growth was due to the extension of the initial tips (Figure 5.2D). After differentiation, many branches were formed in the same hypha at almost the same time as one another and with short distances between these branches (Figure 5.2E). Consequently, most of biomass growth was due to formation and extension of these new branches. In addition, some branches extended upwards towards the solid surface (Figure 5.2E), which did not happen before differentiation. Nevertheless, during the entire experiment, all growth seemed to follow negative autotropism, with new hyphae extending into previously empty spaces, which resulted in many hyphae growing in diagonal directions and even towards the surface.

Another change was the formation of penetrative hyphae from surface hyphae. Before differentiation, most (but not all) of the penetrative hyphae present had originated from the penetrative germ tubes and their branches. After differentiation, many of the subapical branches that formed on surface hyphae grew into the solid particle as penetrative hyphae (Figure 5.2E). In addition, some branches of penetrative hyphae that extended upwards eventually crossed the solid surface, turning into vegetative or reproductive aerial hyphae (Figure 5.2E,F).

Vacuolization of hyphae began before the differentiation process (Figure 5.2B). In *Aspergillus* species, at least four forms of vacuoles have been reported: small and numerous vacuoles close to the tip; tubular vacuoles, in which nutrients are transported through diffusion; large spherical vacuoles in basal regions of hyphae, with a diameter almost equal to the hyphal diameter; and large vacuoles with varying sizes and shapes that result from fusion of spherical vacuoles (SHOJI et al., 2006, DARRAH et al., 2006). In the present experiment, the resolution used allowed only for the detection of the large vacuoles, which are characterized as intracellular regions without green fluorescence (Figure 5.2). The formation of these vacuoles is related to the age of the hyphal segment, and not to the age of the mycelium, hence they first appear at different times for each hypha (e.g. at 9.3 h in penetrative hyphae, at 12.4 h in surface hyphae and at 16.7 h in aerial hyphae). In the experiments of SHOJI et al. (2006) and KIKUMA et al. (2006) with *Aspergillus oryzae*, large spherical vacuoles were rare in vegetative aerial hyphae and absent in stalks of reproductive hyphae before the formation of the vesicle structure at the end of the conidiophore. However, at the end of the present

experiment (24 h), there were many of these vacuoles in vegetative aerial hyphae, including in extending hyphae, and in both of the reproductive hyphae that originated from penetrative hyphae deep within the solid and that still had not formed the vesicle structure at their tip (Figure 5.4). If Shoji et al. (2006) and Kikuma et al. (2006) had analyzed vegetative aerial hyphae after a longer incubation time, it is probable that they would have seen vacuoles in those hyphae.

The role of these large spherical vacuoles is to, at first, reduce the volume of non-vacuolar cytoplasm, namely every component of the cytoplasm except for the vacuoles, thus reducing the metabolic demands for biosynthesis, since the requirements for synthesizing vacuoles are lower than the requirements for synthesizing other components of the cytoplasm (VESES et al., 2008). Later on, these vacuoles degrade organelles that are no longer necessary in these hyphal segments (SHOJI et al., 2014). The products of this degradation may be stored in these spherical vacuoles or transported through tubular vacuoles to other active regions of the mycelium, where they may be reused as nutrients (SHOJI et al., 2014). This autophagic process intensifies with the age of the hyphal segment, increasing the size of the vacuoles until they occupy almost the entire segment, assuming the geometry of the hyphal segment (SHOJI et al., 2006). In the present work, since the parental hypha already contained large spherical vacuoles when the subapical branches were formed, these vacuoles could be nutrient suppliers for the new subapical tips, especially after differentiation, when the nutrient concentration close to the surface is lower.

These large spherical vacuoles also contribute to maintain a high osmolyte concentration in the cytosol and, consequently, to maintain the turgor pressure (WEBER, 2002), which is necessary to maintain the standing position of aerial hyphae and to improve penetration into the solid. This is of particular importance for the reproductive hyphae that had to penetrate the medium to reach the air space (Figure 5.2). In one of these hyphae, large vacuoles were only visible 2.7 h after the hypha first began to grow, at a high density and limited to the base of the hypha (Figure 5.4). 2.2 h after vacuoles first appeared, the base was again free of vacuoles, although vacuoles were still present in an intermediary segment of the stalk. Since a high density of vacuoles appeared in this hyphal segment in a short period of time, it is more likely that they had been transported from the penetrative hypha at the base to the reproductive hypha than that they were formed within the reproductive hypha itself. Since vacuoles were not seen in the stalks formed directly in the air phase in the present experiment or in any of the stalks analyzed by

Kikuma et al. (2006), the most likely role of the vacuoles seen in Figure 5.4 is to ensure a high turgor pressure for penetration.

Figure 5.4 Time-lapse of the stalk of a reproductive hypha of *A. niger* pgaRed formed from a penetrative hypha 255 μm below the surface of the SCD medium. Dashed lines represent the medium surface and arrows point to the estimated position of the stalk tip. This stalk began to grow at 17.6 h and, until 20.3 h, when the stalk was 90 μm long, it did not have any large vacuole. From 20.3 h to 22.5 h, the base of the stalk was filled with large vacuoles, while there were no vacuoles in the 70-90 μm segment closest to the tip. After 22.5 h, the stalk had two regions free of vacuoles, in the apical and basal compartments, and an intermediary region with large vacuoles. After 22.5 h, it was difficult to visualize the region of the stalk close to tip because of the high hyphal density that blocked the passage of the EGFP fluorescence and because of the low fluorescence in part of this region due to the large vacuoles. Images are maximum intensity projections of z-series of optical fields corresponding to 50 μm of field depth. All scale bars represent 50 μm.
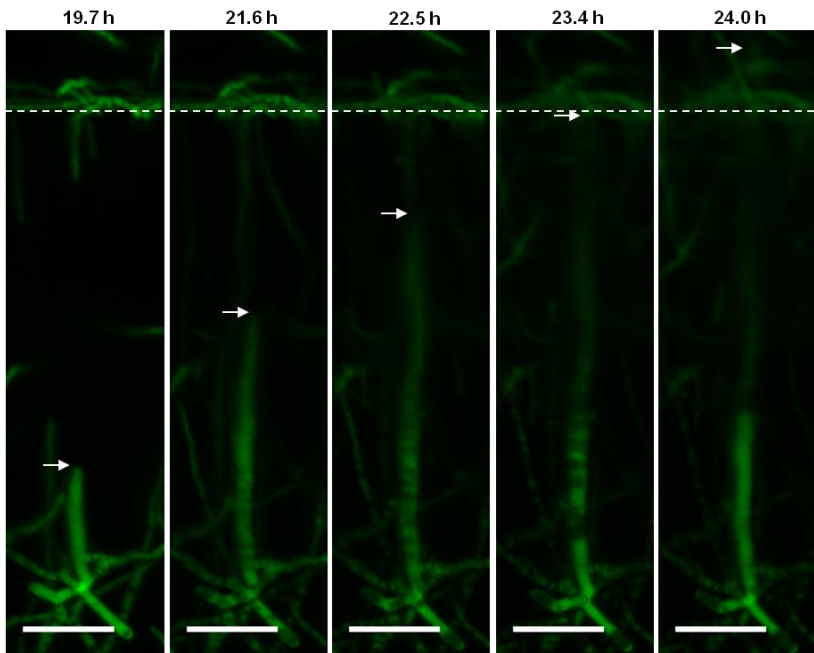
5.3.2 The effect of a higher conidia density on growth and morphology of penetrative hyphae of *Aspergillus niger* pgaRed

A new experiment was conducted in which the *A. niger* pgaRed was grown in media containing different carbon sources, including in glucose (SCD). The mycelial growth on glucose in this new experiment differed in some aspects from that in the experiment described in section 5.3.1 and these differences will be discussed in this section.

In this experiment, three regions of the SCD medium surface were captured, even though only one region is shown in Figure 5.5A, and micrographs were taken every 4 h (Table 5.2). A larger optical field (1203 µm by 1203 µm) was used in order to capture the entire depth of medium occupied by penetrative hyphae. While cutting the medium for this experiment, some conidia were carried to the side of the medium that was laid on the glass plate and germinated there, thus, some hyphae that appear growing deep within the media are not related to the conidia inoculated on the surface, hence these hyphae are not considered in the following analysis. Some of the optical fields containing these hyphae were not included in the construction of the projections shown in Figure 5.5.

Figure 5.5 Time-lapse of growth of *A. niger* pgaRed on (A) SCD and on (B) SCSta.
Dashed lines represent the medium surface and the arrow points to one apical branch. Images are maximum intensity projections of z-series of optical fields corresponding to 126 µm and 48 µm of field depth for SCD and SCSta, respectively. All scale bars represent 100 µm.

Cont. Figure 5.5
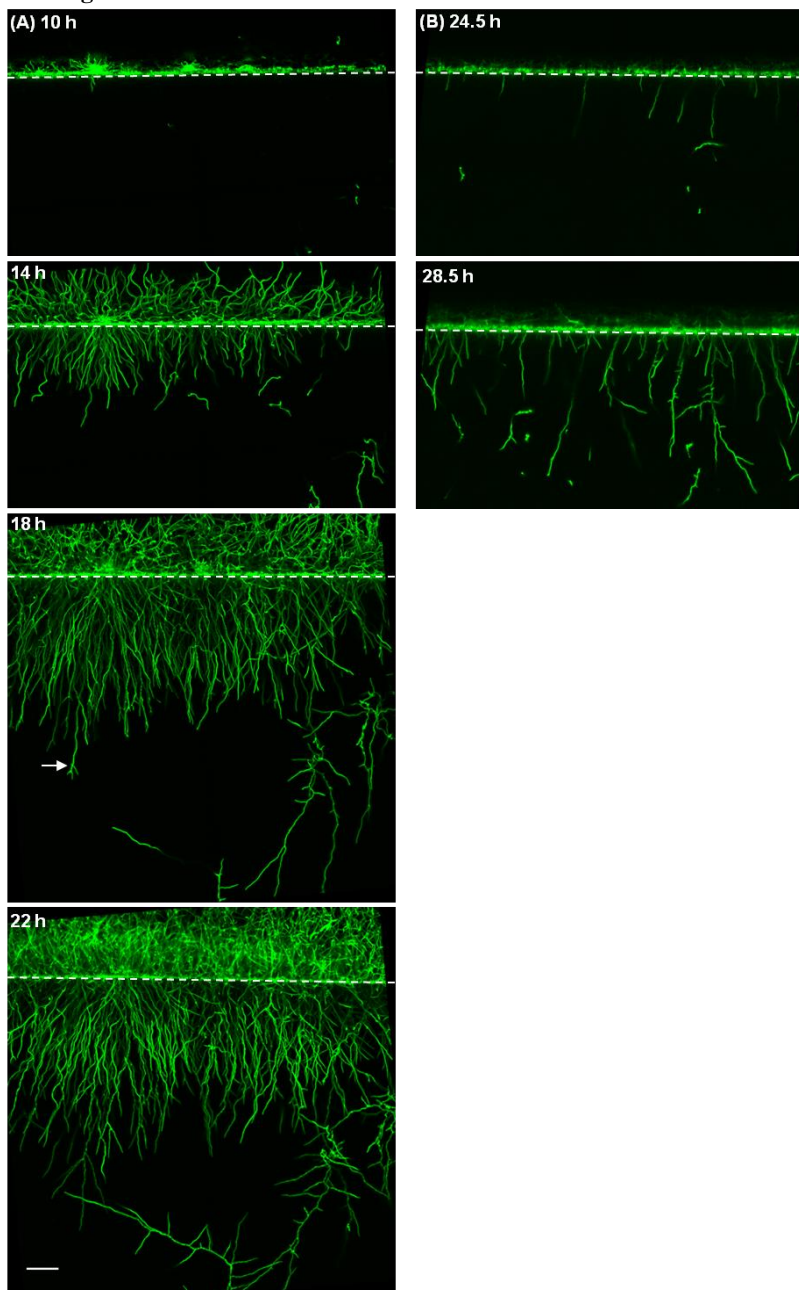
        The germination time was the same as in the previous experiment (approximately 6 h), but most germ tubes formed grew as surface hyphae and not as penetrative hyphae (Figure 5.5A). In fact, the first penetrative hyphae were visible only after most of the surface was occupied by surface hyphae, at 10 h. The probable reason for this different behavior is that, in this experiment, there were some agglomerations of conidia within the conidia suspension used as inoculum, which led to a higher conidia density on the surface, given that each conidia agglomeration was counted as 1 conidium when the conidia suspension was prepared. At the resolution used in this experiment, it is not possible to verify if the conidia remained agglomerated after inoculation. A higher density of conidia, possibly combined with conidia agglomerations, would probably induce the formation of conidial anastomosis tubes (CATs), either directly from the conidia or from germ tubes (READ et al., 2012). Again, these structures were not visible at the resolution used, however, if the formation of CATs was in fact induced, this would probably favor the formation of surface germ tubes over penetrative germ tubes, since anastomosis involving penetrative germ tubes would have the solid medium as a barrier. As a consequence, in this experiment, the surface of the medium was occupied more rapidly than in the previous experiment, which led to an earlier development of aerial hyphae, which were already visible at 10 h.

        There were other differences between growth on SCD in this experiment and growth on SCD in the previous experiment, related to the initial directions of growth of penetrative and aerial hyphae and to the formation of branches in penetrative hyphae. In the experiment with higher conidia density, at first, penetrative and aerial hyphae grew almost perpendicularly to the surface, and diagonal growth only occurred for hyphae at the borders of the mycelium, extending towards empty spaces; whereas, in the previous experiment, there was no predominant direction of growth. Also in this experiment, there were almost no branches in penetrative hyphae before differentiation (at 18 h) and, based on branch angles, most of the branches formed after differentiation seem to be apical, hence, with acute angles between the new tips and the parental hypha, while, in the previous experiment, all branches were subapical and many of them originated far from the tip. These differences are probably due to negative autotropism combined with a higher number of hyphae growing close to the surface at the same time in the early hours of the present experiment, meaning that it was not possible for hyphae to grow in a diagonal direction without encountering other hyphae, except at the borders of the mycelium. In addition, the high density of penetrative

hyphae near the surface probably suppressed the formation of branches in this region before and after differentiation, thus, branches were formed in regions with a lower hyphal density, namely close to the active tips.

As in the previous experiment, penetrative hyphae seem to have differentiated at 18 h. A differentiation process has never been described for penetrative hyphae, but Bull and Trinci (1977) described how surface hyphae differentiated when growing from a single colony. Before differentiation, there is an exponential increase in the number of tips. After a new tip is formed, its extension rate increases until it reaches around the same rate as that of the parental hypha and, thereafter, remains essentially constant. Therefore, with the extension rate of most hyphae being essentially constant, the exponential increase in the number of tips leads to an exponential increase in biomass. Consequently, before differentiation, the hyphal growth unit, which is calculated by dividing total hyphal length by the number of tips, remains constant as branches are formed. This might have happened with penetrative hyphae before their differentiation in the experiment in which the inoculum density was lower, namely that reported in section 5.3.1, although it is not possible to calculate the HGU because penetrative hyphae grew beyond the optical field used. However, this is definitely not the case for the experiment with a high inoculum density, in which branches were rare before differentiation, thus the HGU only increased with time. This indicates that the mode of growth of penetrative hyphae is different from that of surface hyphae before differentiation.

After differentiation of a single colony, most of the growth of surface hyphae occurs at the margin of the colony (BULL; TRINCI, 1977). On the other hand, the tips of leading penetrative hyphae, namely the tips that are deeper in the medium, have almost ceased their extension after differentiation (Figure 5.5A). The leading hyphae probably stopped extending because they reached their maximum length (Figure 5.6). Sugai-Guérios et al. (2016) proposed that this maximum length is not due to the exhaustion of nutrients, rather it is a result of the minimal turgor pressure necessary for penetration of the medium and the pressure drop along the hypha, so that, after penetrating a certain depth, penetrative hyphae are unable to maintain a turgor pressure at the tip that is high enough for further penetration. Growth of the penetrative mycelium after differentiation occurs mostly through formation of branches, which may be formed far from the leading tips (Figure 5.2). Therefore, it is clear that the behavior of penetrative hyphae is quite different from that of surface hyphae, both before and after differentiation. The present work represents

the beginning of the characterization of the growth of penetrative hyphae, while more studies are required.

Figure 5.6 Depth reached by three leading penetrative hyphae during incubation for each carbon source tested.
Values were taken from 3 micrographs for each media (except for galacturonate, for which only 2 micrographs were used). Only hyphae descendent from conidia inoculated on the surface of the agar were considered and tips from apical branches were ignored. The error bars represent the standard error of the mean. Estimated moment of differentiation was 18 h in glucose medium and 23 h in galacturonate and polygalacturonate media. Differentiation was not observed in starch medium until the end of the experiment.
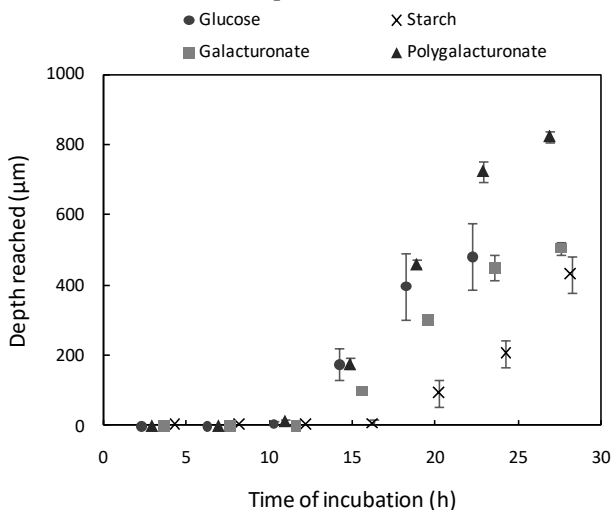
5.3.3 The effect of the type of monosaccharide on growth and morphology of penetrative hyphae of *Aspergillus niger*

In the same experiment as that described in section 5.3.2, the pgaRed strain was also grown on a medium with galacturonate (SCGal), in order to observe if growth or branching vary with different monomeric carbon sources. Galacturonate was chosen because it is the major carbon source when *A. niger* is grown on pectin. Both media were inoculated at the same time but images were captured in sequence, resulting in a difference in the time interval between inoculation and the first image capture for the two media. Again, three regions of the SCGal medium surface were captured and one of them is shown in Figure 5.7A, in which

only a part of the z-series of optical fields was included in the projection in order to minimize the presence of hyphae originating from conidia that germinated on the side the slide, as explained in the previous section. Since Figures 5.5 and 5.7 represent different field depths, it is not possible to compare biomass concentrations in these media based on visual analysis of hyphal density in these figures.

$A.$ *niger* catabolizes galacturonate through the reductive pathway, in which galacturonate is converted to pyruvate and glycerol in four enzymatic steps, with the formation of 2 molecules of $NADP^+$ (HILDITCH et al., 2007). The glycerol may be catabolized, forming dihydroxyacetone-3-phosphate, which can be converted to pyruvate (DAVID et al., 2006). Then, pyruvate can enter the tricarboxylic acid cycle. The theoretical amount of ATP formed per mole of galacturonate is approximately 80% of the amount formed per mole of glucose, which could lead to a lower yield coefficient for conversion of biomass from substrate ($Y_{x/s}$) and, consequently, either a slower growth rate or a similar growth rate combined with a faster rate of substrate uptake. Glycerol may also be used for lipid synthesis or accumulated in order to increase turgor pressure either for penetration (DE JONG et al., 1997) or to prevent loss of water through osmosis (DURAN et al., 2010).

Figure 5.7 Time-lapse of growth of *A. niger* pgaRed on (A) SCGal and on (B) SCPga.
Dashed lines represent the medium surface and arrows indicate stalks formed in SCGal. Green marks inside the SCPga medium are due to auto-fluorescence from the medium. Images are maximum intensity projections of z-series of optical fields corresponding to 64 µm and 90 µm of field depth for SCGal and SCPga, respectively. All scale bars represent 100 µm.

Cont. Figure 5.7
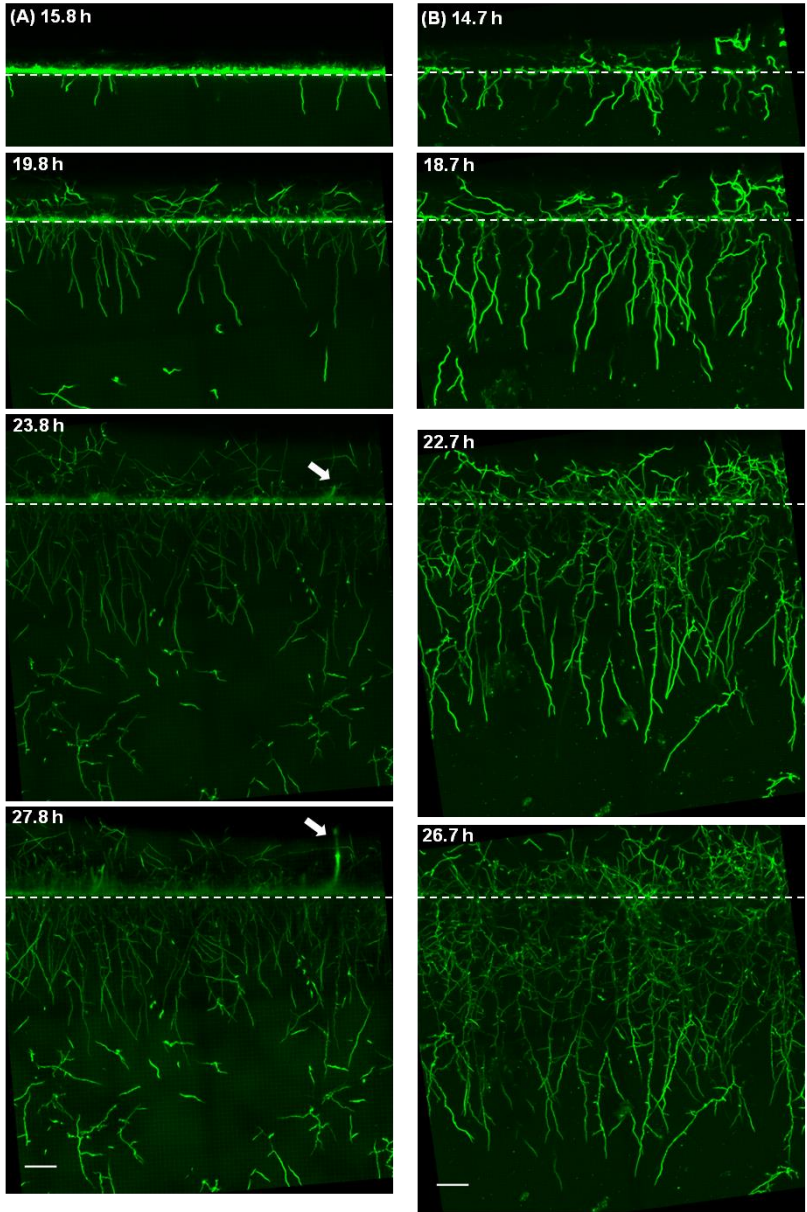
The germination time was around 4 h longer in the medium with galacturonate (Figure 5.7A) than with glucose (Figure 5.5A). This difference occurred because the time required for germination of conidia depends directly on the composition of the medium. For *A. niger*, the carbon and nitrogen sources of the medium are used not only to support growth of the germ tube but also as trigger compounds, which initiate the swelling of the conidia through water uptake (HAYER et al., 2013). Firstly, the type of trigger compound present in the medium affects the rate of consumption of trehalose and mannitol, which are nutrient sources internal to the conidia and are used for the swelling process in the first hours after inoculation (HAYER et al., 2014). Secondly, around 1.3 h after inoculation, the external carbon source begins to be metabolized for the swelling process, thus affecting directly the swelling rate (HAYER et al., 2013; HAYER, 2014). Formation of the germ tube of *A. niger* depends on the swelling rate since there is a minimal conidium size for it to occur (HAYER, 2014). The glucose used in the SCD medium in the present experiment serves both as the carbon source and as the trigger for germination of *A. niger* conidia (HAYER et al., 2013). On the other hand, galacturonate in the SCGal medium probably serves only as the carbon source and not as the trigger, since one of the requirements for a monosaccharide to work as a trigger for *A. niger* is for the position of the hydroxyl group of carbon 4 to be the same as it is in glucose (HAYER et al., 2013) and this is not the case for galacturonate. In SCGal, the probable trigger is L-tryptophan, which results in a slower consumption rate of internal trehalose and mannitol than glucose (Hayer et al., 2014). Therefore, the cause for a longer germination time in SCGal than in SCD is probably a lower the swelling rate in SCGal due to L- tryptophan in its role as a trigger and then galacturonate in its role as a carbon source.

Other differences in the mode of growth of *A. niger* pgaRed on glucose and on galacturonate media are summarized in Table 5.3. The time interval between germination and differentiation was the same in both media (around 13 h). As occurred in the glucose medium, growth after differentiation in the galacturonate medium was also characterized by the formation of reproductive hyphae, intense subapical branching in the penetrative hyphae and almost no growth of the leading penetrative hyphae. The depth reached by three leading hyphae was similar in galacturonate and in glucose media (Figure 5.6). In addition, based on the length that penetrative hyphae extended in each 4-h interval, the extension rate of leading hyphae was of a similar magnitude in both media.

Table 5.3 Summary of the differences in the mode of growth of *A. niger* pgaRed in each carbon source.

Carbon source	Glucose (SCD)	Starch (SCSta)	Galacturonate (SCGal)	Polygalacturonate (SCPga)
Germination time (approximated)	6 h	12 h	10 h	11 h
The moment when the first penetrative hypha is formed (approximated)	10 h	24 h	14 h	11h, but most growth occurs after 15 h
Mode of growth of penetrative hyphae	They grew mainly between 10 h and 18 h	They probably continued to grow after the experiment was interrupted at 28 h	Most of extension occurs from 15 h to 23 h, after 23 h it is mostly extension of new penetrative hyphae at the surface and extension of branches	They grew mainly between 15h and 23h, after 23 h it is mostly branching
Branches in penetrative hyphae	Apical, starting at around 18 h	Subapical (perpendicular direction from parent hypha), starting at around 28 h	Subapical (perpendicular direction from parent hypha), starting at around 19 h; there are many branches per hypha	Subapical (perpendicular direction from parent hypha), starting at around 19 h; there are many branches per hypha
The moment when the first aerial hypha is formed (approximated)	10 h	24 h	19 h	15 h
Mode of growth of aerial hyphae	At first, they extend mostly upwards; then, in any direction, including downwards	These hyphae are difficult to visualize	They extend in any direction, including downwards; reproductive hyphae start forming at 23 h.	They extend in any direction, including downwards; reproductive hyphae were not seen
Branches in AH	Subapical, starting at around 18 h	It is uncertain	Subapical, starting at around 23 h	Subapical, starting at around 19 h

However, there were some morphological differences between penetrative hyphae grown on glucose and on galacturonate (Figure 5.5A and 5.7A): on galacturonate, there were more branches per penetrative hypha and branches were more evenly spaced along the length of the parental hypha. In addition, most branches that formed on penetrative hyphae during growth in the galacturonate medium were perpendicular to their parental hyphae, whereas, in the glucose medium, most branches were apical. These differences were likely caused by a slower biomass growth rate in the galacturonate medium, which leads to lower hyphal density and, consequently, more space being available in the medium for subapical branching in regions closer to the medium surface, resulting in the morphology observed in Figure 5.7A.

Growth of aerial hyphae was similar on both the glucose and the galacturonate media: aerial hyphae began to appear only when the surface was mostly occupied; they extended in various directions, but growth in a diagonal direction was more frequent in galacturonate because of the low density of aerial hyphae; also, most of the branches appeared after differentiation. The main difference between growth in these two media was that here was no visual difference in local biomass concentration between aerial and penetrative hyphae after the differentiation in the galacturonate medium, whereas, at 22 h in the glucose medium, the density of the aerial hyphae within the region from the surface up to a height of 200 μm was greater than that in the region from the surface down to a depth of 200 μm.

5.3.4 The effect of the degree of polymerization of the carbon source on growth and morphology of penetrative hyphae of *Aspergillus niger* pgaRed

In the same experiment as that described in sections 5.3.2 and 5.3.3, *A. niger* pgaRed was grown on media that contained two different polymeric substrates, starch (SCSta) and polygalacturonate (SCPga), in order to compare growth on these polymeric substrates with growth on glucose and galacturonate, respectively. The germination time on the polygalacturonate medium was around 12 h, similar to that on the galacturonate medium, with the germ tubes forming mostly surface hyphae (Table 5.3). Further, on the polygalacturonate medium, penetrative hyphae differentiated at approximately the same time as on the galacturonate medium, around 23 h, with intensified formation of branches in penetrative hyphae and reduced extension of the tips of

leading hyphae. On the other hand, reproductive hyphae were not visible in the mycelium that grew on the medium containing polygalacturonate.

Compared to penetrative hyphae that grew in the medium containing galacturonate, penetrative hyphae formed in the polygalacturonate medium were longer (Figure 5.6) and with more branches per hypha (Figure 5.7). Longer hyphae allow secretion of hydrolytic enzymes deeper into the solid through the tips of leading hyphae. It is possible that, after detecting the composition of the medium, the mycelium may have a way of increasing pressure at the base of penetrative hyphae (e.g. through synthesis of larger vacuoles in this region) or of decreasing internal pressure drop per length, so that hyphae may be longer in polymeric media. The latter could be achieved by increasing the diameter, however, the resolution used in our experiment did not allow an accurate measurement of the diameter of hyphae formed in each medium. Another difference was that there were a few apical branches in penetrative hyphae grown on polygalacturonate medium, whereas there were none in penetrative hyphae grown on galacturonate medium (Figure 5.7).

In the polygalacturonate medium, aerial hyphae extended earlier (before 15 h) than in the galacturonate medium (Table 5.3). After 19 h, most of the biomass in the polygalacturonate medium was comprised of penetrative hyphae, while the amounts of aerial and penetrative hyphae were similar for the biomass formed in galacturonate. This may indicate that, in media with polymeric substrates, the formation of penetrative hyphae is favored over aerial hyphae in order to have a high rate of secretion of hydrolytic enzymes deep within the substrate, thus, increasing the rate of hydrolysis of the polymer and the supply of monomer to the fungus. On the contrary, in a medium containing glucose or galacturonate, there is no need for extracellular hydrolytic enzymes.

A. niger pgaRed grew poorly on the starch medium (Table 5.3). The germination time was around 12 h (6 h longer than in the medium with glucose), with penetrative hyphae being visible only at 24 h, when most of the surface was occupied by hyphae (Figure 5.5B). Even at 28 h, penetrative hyphae were still short and mostly unbranched. Therefore, the growth mode had a greater similarity to that on galacturonate medium (Figure 5.7A) than it did to that on glucose medium (Figure 5.5A), namely the constant formation of new penetrative hyphae from surface hyphae. In addition, at 28 h, as in the polygalacturonate medium, most of the hyphae were surface and penetrative hyphae, thus they were able to contribute to the hydrolysis of the starch by secreting amylases directly into the medium.

5.3.5 Expression of pgxB-mCherry in penetrative hyphae of *Aspergillus niger* pgxRed

It is estimated that the genome of *A. niger* contains 4 genes for exopolygalacturonase and 7 genes for endopolygalacturonase, each with a different expression and secretion profile (MARTENS-UZUNOVA, 2008; MARTENS-UZUNOVA; SCHAAP, 2009; BRAAKSMA et al. 2010). Exopolygalacturonase B (*pgxB*) is expressed in the presence of galacturonate, polygalacturonate and pectin, but not in the presence of glucose as the only carbon source (MARTENS-UZUNOVA, 2008; BRAAKSMA et al. 2010). On the other hand, endopolygalacturonase B (*pgaB*) is expressed in media containing many carbon sources, including glucose and galacturonate (MARTENS-UZUNOVA, 2008; BRAAKSMA et al. 2010). The original objective was to compare the expression of both enzymes during the development of the mycelium, however, the red fluorescence of pgaB-mCherry was not visible in the pgaRed strain grown on any of the carbon sources tested. Therefore, the expression experiments were carried out only with the pgxRed strain, using polygalacturonate media (SCPga). This section presents the results of expression of pgxB-mCherry in penetrative hyphae, while the expression in aerial hyphae is discussed in the next section.

In the first experiment with *A. niger* pgxRed, the moment of expression of pgxB-mCherry was determined. Three regions of the SCPga medium surface were captured, even though only one region is shown in Figure 5.8. Image capture began at 11 h and micrographs were taken every 2.8 h until 24 h; the size of each optical field was 1172 μm by 1709 μm (Table 5.2). In this experiment, penetrative hyphae differentiated between 21 and 24 h, as described in the previous sections, namely with intense subapical branching and interruption of extension of tips of leading hyphae. This differentiation seemed to affect the expression of pgxB-mCherry, for which three different behaviors were visible in penetrative hyphae (Figure 5.8): a few hyphae expressed pgxB-mCherry only before differentiation; most hyphae expressed pgxB-mCherry only after differentiation; and some hyphae did not express pgxB-mCherry until the end of the cultivation (24 h).

Figure 5.8 Time-lapse of growth of *A. niger* pgxRed and expression of pgxB-mCherry on SCPga.
Dashed lines represent the approximate position of the medium surface and arrows indicate the apical expressing hyphae. Red marks inside the medium are due to auto-fluorescence from the medium. Images are maximum intensity projections of z-series of optical fields corresponding to 106 μm. All scale bars represent 100 μm.
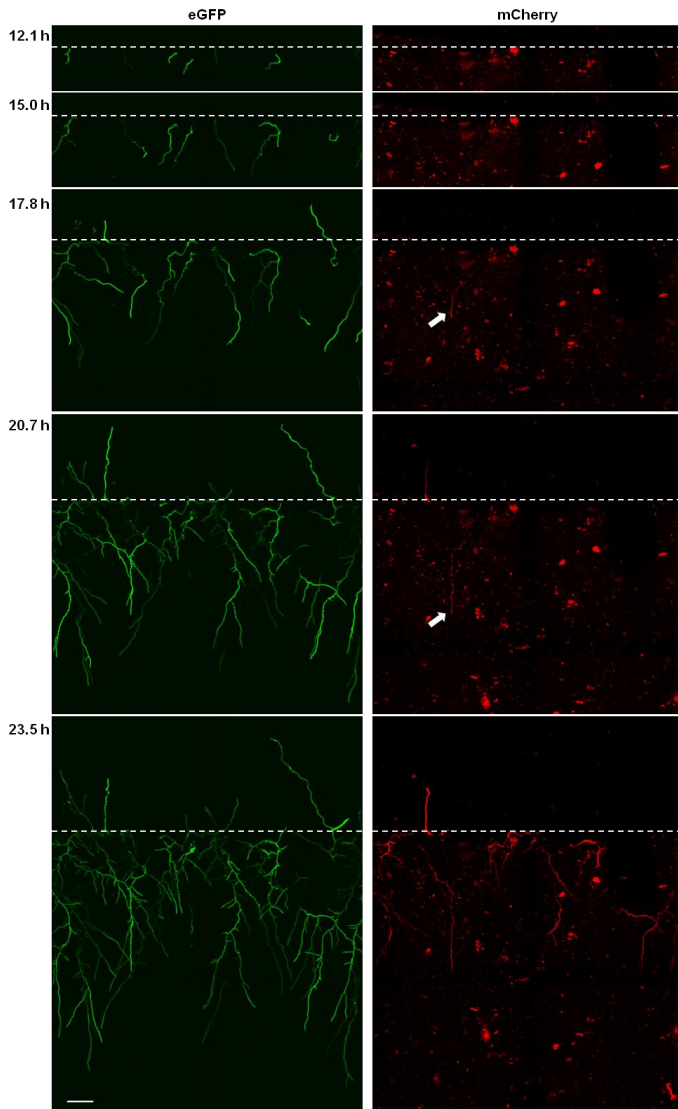
Among the three regions of the medium analyzed, only seven hyphae, among dozens, presented any mCherry fluorescence before differentiation, but all of these seven expressed pgxB-mCherry in the same manner: these hyphae started growing at 12 h, but mCherry fluorescence was detected for the first time at 18 h, when these hyphae had reached at least 270 µm below the surface (Figure 5.8). At 18 and 21 h, mCherry fluorescence was limited to the apical segments of these hyphae, with the highest intensity exactly at the tip. On the other hand, at 24 h, even though the tips continued to extend, there was little or no mCherry fluorescence at the tips and the highest mCherry fluorescence was located in the hyphal segments corresponding to where the tips had been at 21 h. This suggests that, for these hyphae, *pgxB* expression occurs only in the apical compartments and stops with the differentiation that penetrative hyphae undergo. There was no morphological features that was exclusive to apically expressing hyphae and, therefore, it is not possible to identify these hyphae without the mCherry fluorescence.

Most of the penetrative hyphae belong to the second group: hyphae that express pgxB-mCherry only after differentiation and mostly in subapical compartments. At 24 h, more mCherry fluorescence was detected in parental hyphae than in branches, and it was only present in hyphae close to the surface, down to approximately 600 µm below the surface, at a time when penetrative hyphae had reached depths of approximately 1000 µm. mCherry fluorescence in surface hyphae is also only detected at 24 h. Interestingly, some hyphal segments that expressed pgxB-mCherry at 24 h contained large spherical vacuoles, thus the presence of these vacuoles does not indicate absence of metabolic activity.

It is important to note that, even though expression of *pgxB* varies in time and space, the extracellular pectinolytic activity may be more homogeneous due to the other isoenzymes *A. niger* also expresses (BENOIT et al., 2015).

In the second experiment with *A. niger* pgxRed, the localization of the pgxB-mCherry in the cellular structure of penetrative hyphae was determined, with micrographs captured at 30 h at a higher resolution (Table 5.2). In those hyphae that expressed pgxB-mCherry, mCherry fluorescence was absent from the tips (Figure 5.9A) but present in the subapical regions, with the intensity being highest at the border of the hyphae and in septa (Figure 5.9B), which indicates the enzyme is retained either in the cell wall or in the periplasm, which is the compartment between cell wall and cell membrane. For example, in one of the hyphae

in which mCherry fluorescence was absent at the tip, there was
fluorescence in the subapical periplasm 4 µm from this tip (Figure 5.9A).

Figure 5.9 Localization of pgxB-mCherry at 30 h in penetrative hyphae of *A. niger* pgxRed growing on SCPga.
(A) pgxB-mCherry was absent from hyphal tips (Tick arrow points to the position of a tip); (B) In subapical compartments, the intensity of mCherry was higher in the periplasm than in the cytosol; (C) In a few vacuoles, mCherry fluorescence was higher than in the cytosol (Arrows point to the positions of vacuoles). Images are maximum intensity projections of z-series of optical fields corresponding to different field depths (Table 5.2). All scale bars represent 20 µm.
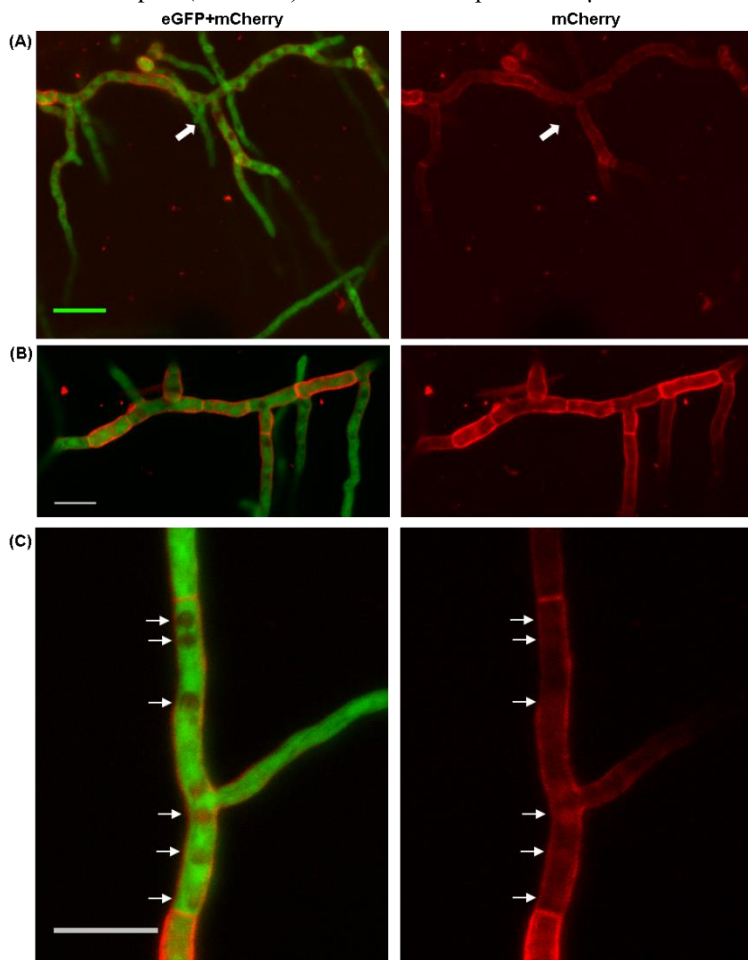
Some large spherical vacuoles also presented mCherry fluorescence with intensity higher than in the cytosol but lower than in cell wall and septa (Figure 5.9C). This could mean that pgxB-mCherry was transported into the vacuole in order to be degraded. However, it is unexpected that mCherry fluorescence was still detected, which could be either because degradation had not started yet or because degradation rate was lower than uptake of the enzyme by the vacuole.

This is not the first time that the presence of secreted enzymes in periplasm, cell wall and septa is reported. For example, Gordon et al. (2000) detected glucoamylase-sGFP (synthetic GFP) in subapical cell walls and septa of *A. niger* at a higher intensity than in the tip; they suggested that the enzymes present in the cell wall had been retained there after being previously secreted at the tip. However, Hayakawa et al. (2011) recently proved that secretion of α-amylase-EGFP occurs at the tip and at subapical septa at the same time and independently in *Aspergillus oryzae*. In addition, they showed that some membrane proteins, for example, a purine/xanthine permease and a general amino acid transporter, are secreted preferentially at the septa. According to the authors, secretion at the septa involves a separate mechanism, with the complex responsible for secretion being comprised of different proteins. Secretion through the lateral membrane in subapical regions is also a probability, since Valkonen et al. (2007) localized proteins of the secretory pathway in lateral membranes of *Trichoderma reesei* that were different from those present at the tip. Hayakawa et al. (2011) also showed that enzymes secreted subapically by *Aspergillus oryzae* are retained in the periplasm and not in the cell wall, as initially proposed by Gordon et al. (2000), therefore, it is likely that the subapically expressed pgxB-mCherry is also localized in the periplasm of *A. niger* (Figure 5.9B).

The absence of mCherry fluorescence in the tips indicates that the enzymes produced after differentiation, by the subapically-expressing hyphae, are secreted directly at septa or even at lateral membrane of these compartments instead of being transported to the tip for apical secretion. Although the cell wall in subapical compartments is of low porosity, some of these enzymes probably diffuse through the cell wall into the medium eventually (HAYAKAWA et al., 2011). An indication for this is that protein secretion has been detected in regions of the surface mycelium that did not have extending tips (LEVIN et al., 2007), thus the porosity of the cell wall of subapical regions is low enough for diffusion of some proteins.

Hayakawa et al. (2011) found that secretion by *A. oryzae* through the septa only occurred at low hyphal density, both in liquid and on solid

media. However, in the present work, secretion *A. niger* at low hyphal density (18 and 21 h) was apical while secretion at high hyphal density (24 h) was subapical, either occurring at septa or at the lateral plasma membrane. In this case, the site of secretion seems to depend on the developmental stage of the mycelium, namely whether it is undifferentiated or differentiated.

5.3.6   Expression of pgxB-mCherry in aerial hyphae of *Aspergillus niger* pgxRed

In the experiment for time-lapse expression of pgxB-mCherry in SCPga, aerial hyphae first appeared at 18 h. At 21 h, only three aerial hyphae had mCherry fluorescence, although at very low intensity and limited to the base of the aerial hyphae (i.e. close to the medium surface) and absent from the tip (Figure 5.8). At the end of the experiment (24 h), half of all aerial hyphae present had mCherry fluorescence, which was still absent from the tip and concentrated at the base of the hypha.

The expression in aerial hyphae seems to be synchronized with the subapical expression in penetrative hyphae. It is unlikely that *pgxB* is being expressed in the hyphae supporting the aerial hyphae and being translocated towards the extending tip, through cytosolic streaming, because the mCherry fluorescence in the hyphae supporting these aerial hyphae is not particularly intense. Since aerial hyphae are not in contact with the medium, the same activator for the expression of *pgxB* that initiates subapical expression in penetrative hyphae is probably being transported from the base of the aerial hypha towards its tip, activating the expression of *pgxB*. This hypothesis can be tested through a FRAP (fluorescence recovery after bleaching) assay as follows: after around 23 h of incubation, the entire aerial hypha should be bleached; if recovery of mCherry fluorescence is faster close to the surface of the medium, it would indicate that pgxB-mCherry is being transported from the base of the aerial hypha towards its tip; otherwise, if, for example, recovery occurs homogeneously in the bleached area, then the activator of expression is being transported towards the tip of the aerial hypha.

5.4   DISCUSSION

The present work is the first to characterize the development of penetrative hyphae over time. Consequently, it is the first to describe their differentiation, how their morphology is affect by the type of carbon

source and conidia density, and the two modes of expression of *pgxB*, namely apical and subapical expression. In terms of enzyme expression throughout the mycelium, this is also the first work to show the heterogeneity in expression between adjacent hyphae develop with time.

The following sections explore the most important aspects resulting from the characterization of penetrativa hyphae and how they will help the development of future mathematical models.

5.4.1   Two populations of penetrative hyphae?

In the present work, two strains of *A. niger* were constructed in order to investigate the two populations of penetrative hyphae that are visible in the micrographs of *A. oryzae* growing on rice grains (MATSUNAGA et al., 2002; ITO et al., 1989) and of *R. oligosporus* growing on artificial media (NOPHARATANA et al., 2003a,b) and in soybeans (JURUS; SUNDBERG, 1976). Sugai-Guérios et al. (2016) proposed that the longer hyphae be named scouting penetrative hyphae and that they are the first to stop extending and their role is to secrete a pool of hydrolytic enzymes in order to determine the type of nutrients present in the solid, so that the rest of the mycelium can secrete the appropriate hydrolytic enzymes. Meanwhile, the shorter hyphae, named vegetative penetrative hyphae, represent most of the biomass inside the particle, being responsible for anchoring the mycelium to the particle and secreting the appropriate hydrolytic enzymes (SUGAI-GUÉRIOS et al., 2016). This hypothesis predicts that most of the polygalacturonases secreted by scouting penetrative hyphae would be those that are under constitutive promoters, such as *pgaB*, with expression starting at the moment these hyphae first appear until they reach their final length, so that scouting enzymes could be distributed through the entire depth of the medium, which typically has a variable composition in space in real SSF systems. Meanwhile, most of the polygalacturonases secreted by vegetative penetrative hyphae would be those that are under promoters induced by galacturonate, such as *pgxB*.

With the strains constructed in this work, however, it was not possible to distinguish scouting and vegetative hyphae in any of the experiments, for two reasons. First, in the micrographs obtained (Figures 5.2, 5.5, 5.7 and 5.8), there was no clear difference of length amongst the penetrative hyphae. Nor was there any clear difference in other morphological features, such as branching mode or extension rate. Second, the expression of pgaB-mCherry was not detected in any of the

media tested. On the other hand, the expression of pgxB-mCherry proved the existence of at least two populations of penetrative hyphae, which differ in the time and the site of *pgxB* expression, but do not differ in morphology: apically-expressing and subapically-expressing penetrative hyphae (Figure 5.8). Therefore, hereon, we will limit the discussion to the two populations detected in the present experiments.

This temporal shift between apical secretion and subapical secretion (i.e. either through septa or lateral membranes) can be explained by the change in the composition of the medium. During the first hours of growth, when the concentration of polymeric nutrients is high throughout the medium, secretion of hydrolytic enzymes through the tip is preferable compared to subapical secretion because tips will pass through various depths of the medium in the first hours and because of the higher porosity of the apical cell wall compared to the subapical cell wall. On the other hand, after differentiation, the polymer concentration in the region close to the surface is lower (MITCHELL et al., 1990), but oligosaccharides may still be present. At this stage, secretion of more exopolygalacturonases through subapical compartments has the advantage of requiring less extracellular nutrients for the synthesis of the enzymes, since the large vacuoles are probably already present in these subapical compartments and may supply a large amount of aminoacids that were generated from autophagy of unused proteins and organelles.

Previous studies on gene expression for *A. niger* on solid media were conducted only for the growth of colonies of surface hyphae, with membranes being used to prevent growth of penetrative and aerial hyphae. Significantly different levels of protein expression were detected along the radius of the colony, based on mRNA analysis (LEVIN et al., 2007; BENOIT et al., 2015), and in adjacent surface hyphae in the periphery of the colony, using GFP fused with extracellular enzymes (VINCK et al., 2005/2011). Vinck et al. (2005/2011) suggested that there are two subpopulations of hyphae within the leading hyphae of *A. niger*: 50% of the hyphae expressed large amounts of extracellular enzymes and 50% expressed low amounts. However, they captured fluorescence at a single time of incubation, therefore, it was not clear how this heterogeneity was formed. One possibility is that the low-expressing hyphae did not express the GFP-fused enzyme, but rather their fluorescence was the result of expression in the high-expressing hyphae, with later diffusion of the fluorescent construct through the mycelial network.

On the other hand, through the time-lapse study undertaken in the present work, it was possible to visualize the development over time of

the heterogeneity in expression of *pgxB* in penetrative hyphae. Basically, there are two or three groups of hyphae: some hyphae express *pgxB* at their tips only before differentiation, some express it subapically only after differentiation and, possibly, some do not express it at all (Figure 5.8). This results in different temporal and spatial expression levels, with differences not only among adjacent hyphae and with depth within the medium, but also with time. In this case, in the early hours of growth, there is no expression of *pgxB*, followed by expression in some tips of penetrative hyphae that are extending closely behind the leading penetrative hyphae, but not in the actual leading hyphae, and only until differentiation occurs. Then, *pgxB* is expressed only in the segments of penetrative hyphae that are close to the surface. Therefore, throughout the experiment, *pgxB* was never expressed in the tips of leading penetrative hyphae. This confirms the suggestion made by Niu et al. (2015) that *A. niger* probably does not use PGXB for scouting nutrients in the medium. Their suggestion was based on the fact that *pgxB* requires a minimal amount of galacturonate in the medium in order to be expressed, while genes for scouting enzymes should be under constitutive promoters.

The only previous work to analyze spatial expression specifically of *pgxB* in *A. niger* was for surface hyphae on solid medium with sugar beet pulp, which is rich in pectin (BENOIT et al., 2015). They inoculated conidia into a single position of the medium and analyzed mRNA levels in 5 concentric areas around the inoculation site, after 5 days of incubation, using membranes to prevent the formation of aerial and penetrative hyphae. Although endo- and exopolygalacturonases were expressed in all regions, some of these enzymes had a higher level of expression in the center of the colony, others in the periphery and others had almost the same level of expression along the radius. Based on these results, the authors suggested that the transcription levels of some genes were determined by the age of the mycelium. For example, *pgxB*, which was more expressed in the center of the colony, is preferably expressed in old hyphae. This is somewhat similar to the fluorescence level of pgxB-mCherry in the current work after differentiation, which was higher in older hyphae than in extending tips, but it is not what happens before differentiation.

The studies on radial heterogeneity of surface hyphae from the literature showed that, when nutrient is depleted from the center of the colony, protein secretion occurs mainly at the periphery of the colony, whereas, when nutrient is not depleted, protein secretion occurs throughout the entire colony (LEVIN et al., 2007; BENOIT et al., 2015). If this is also true for penetrative hyphae, it means that nutrient was not

depleted close to the surface at the moment of differentiation, since there was expression of *pgxB* in hyphae close to the surface. In this case, expression of *pgxB* after differentiation could be an attempt to improve hydrolysis of the oligosaccharides remaining in the medium in order to utilize the medium's nutrients fully.

The mechanism of regulation of the *pgxB* gene has not been fully elucidated and, therefore, it is difficult to understand how the mycelium controls different manners of expression in the apically and subapically-expressing hyphae. It has been confirmed that the promoter for *pgxB* is induced in the presence of galacturonate, through a transcriptional activator called GaaR, and repressed in the presence of glucose, through the transcription factor CreA (NIU et al., 2015; ALAZI et al., 2016). Now that the gene for GaaR has been identified, it will be interesting to see how its expression varies across the mycelium and with incubation time. Vinck et al. (2011) showed that, for surface hyphae, the radial heterogeneity of the expression of genes for some amylolytic and some xylanolytic enzymes is caused by the radial heterogeneity of the expression of their transcriptional activators, AmyR and XlnR, respectively. For *pgxB*, it remains unclear as to how the mycelium would create these different expression behaviors in penetrative hyphae, but it is clear that there are at least two metabolic distinct populations of penetrative hyphae.

5.4.2 An overview of the differentiation process of penetrative hyphae

At around the same time that asexual reproduction starts, marked by the extension of stalks, penetrative hyphae also undergo differentiation, which affects growth and *pgxB* expression (Table 5.4). This differentiation occurred in all media and inoculum densities tested, except for the starch medium, in which the germination time was much longer and, consequently, the experiment ended before the time of differentiation was reached. This differentiation process is very different from the differentiation process for that occurs for surface hyphae of a single colony, which, for example, continue their growth at the periphery of the colony after differentiation (BULL; TRINCI, 1977), whereas penetrative hyphae stop growing at the periphery.

Table 5.4 Changes that occur in penetrative hyphae with the differentiation.

	Before differentiation	After differentiation
Branching	Rare	Intense
Maximum depth reached by the mycelium	Increasing with time	Constant
Hyphal extension towards the surface	Rare	Common if there is space for extension, including some penetrative hyphae turning into vegetative and reproductive aerial hyphae
pgxB expression: location related to the hypha	Tips of few hyphae	Subapical compartments of most hyphae that were not expressing before differentiation
pgxB expression: location related to the surface of the solid	At the borders of the mycelium	Close to the surface

The trigger for the differentiation of penetrative hyphae is unclear, but the most likely possibility is that it is connected to asexual reproduction, even though stalks of reproductive hyphae were not visible until the end of some experiments in which penetrative hyphae differentiated (Figure 5.5A and 5.7B). The same trigger that initiates asexual reproduction might also initiate intense branching in penetrative hyphae, which, in turn, would generate a high pressure drop inside these hyphae. Sugai-Guérios et al. (2016) proposed that leading penetrative hyphae extended as long as the turgor pressure at the tip was above a minimal threshold, while the turgor pressure at the tip depended on the pressure at the base of the hypha and on the intracellular pressure drop. Therefore, the intense formation of branches at the moment of differentiation would cause a significant reduction of the turgor pressure at the tips of parental hyphae (which are also the leading hyphae in Figures 5.5 and 5.7), so that they are unable to continue penetrating the medium. This is likely the cause of the decreasing rate of extension of leading penetrative hyphae, which is indirectly represented in Figure 5.6.

Before differentiation, hyphal growth is mainly through extension of leading hyphae into the medium, increasing the depth reached by the mycelium, and, after differentiation, subapical branches increase the density of penetrative hyphae within already occupied regions of the medium. The branches formed after differentiation do not serve the purpose of increasing the number of tips for enzymatic secretion, since these newly formed tips do not express *pgxB*. On the other hand, subapical branching indirectly improves enzymatic secretion because it increases the biomass in the basal region of the mycelia where expression and

secretion of PGXB occurred. These branches also serve to increase nutrient uptake at a moment when the concentration of extracellular nutrients is low.

5.4.3 Insights into how to develop a 3D model for penetrative hyphae of *Aspergillus niger*

The layer model developed by Sugai-Guérios et al. (2016) for penetrative hyphae is a 1D discrete model, in which the medium depth is divided into layers and hyphal growth is simulated by the addition of hyphal segments to each layer. The layer model was developed based on micrographs of penetrative hyphae of *Rhizopus oligosporus*, therefore, branching was modeled as subapical for vegetative penetrative and as apical for short penetrative hyphae. However, the rule used to determine hyphal extension was the same for both hyphal types. Although the layer model itself does not include a nutrient mass balance or angles between branches, it could be modified into a 3D phenomenological model by fusing it with previous models (SUGAI-GUÉRIOS et al., 2015/2016), specifically, by incorporating the 3D spatial description developed for aerial hyphae by Coradin et al. (2011) and the intracellular mass balance of nutrients and biomass-generating vesicles developed by Balmant et al. (2015). This fused model could be used to investigate the mechanisms involved in growth of penetrative hyphae, as suggested by Sugai-Guérios et al. (2015/2016). However, before fusing these models, more information on how penetrative hyphae grow would be necessary in order improve the rules of the layer model. The original rules of the layer model were based on micrographs of *R. oligosporus* growing in PDA at 16 and 40 h of incubation (NOPHARATANA et al., 2003b). Although biomass density profiles for each incubation time were extracted from those micrographs, allowing the calibration of the model, only 2 incubation times is not enough to understand how the morphology of the mycelium develops. It would still be necessary to determine, for example, the germination time, the rate of formation of new tips at the surface, the angle between branches and how the model parameters are affected by the nutrient type.

In order to obtain these data, the fluorescent strains were constructed in the present work. Although previous experimental data was for *R. oligosporus*, the present work focus on *A. niger*, which is a potential producer of pectinases through SSF (PITOL et al., 2016; NIU et al., 2015) and because it is a well characterized species, through genome,

transcriptome and secretome studies (LEVIN et al., 2007; MARTENS-UZUNOVA, 2008; BRAAKSMA et al., 2010; BENOIT et al., 2015; NIU et al., 2015). The micrographs obtained in the present work can be used to understand how morphology of penetrative mycelium is formed and also how to adapt the rules originally developed for *R. oligosporus* to describe the growth of *A. niger*. Table 5.5 shows some of the changes required, some of which will depend on the inoculation density. The growth direction of leading hyphae would be downwards, as in the original layer model.

Table 5.5 Suggestions for improvement of the layer model and the development of 3D model for penetrative hyphae.

	Low inoculation density	High inoculation density
The moment when the first penetrative hypha is formed	It should be the time necessary for germination of the conidia, to be determined experimentally	It should be the time necessary for surface hyphae to reach a certain hyphal density, to be determined by simulation growth of surface hyphae
Formation of new penetrative tips at the surface	Before differentiation: almost all penetrative hyphae are formed from the spore as germ tubes. After differentiation: penetrative hyphae are formed from surface hyphae at a rate that may be obtained from Figure 5.2	All penetrative hyphae are formed from surface hyphae at a rate that probably varies with time and as a function of hyphal density immediately below the surface, and which may be obtained from Figures 5.5 and 5.7
Formation of branches	An approach similar to the one used in the layer model for scouting penetrative hyphae, which is for subapical branching (more details in the text)	
Direction of growth of new branches	Equal probability in every direction, as in the layer model for aerial hyphae, based on random walk	
How to describe differentiation	After differentiation, the maximum probability of penetrative hyphae extending (of the layer model) should change to a lower value and the maximum probability of branching should change to a higher value (see the text)	

Although branching is different in Figure 5.2 and Figure 5.5, the same rules could be used to describe both processes. Firstly, branching should be allowed only after a hypha has reached a certain length. Secondly, since it is possible that more than one branch is formed at the same time, we suggest that the length of a parental hypha be divided into a few segments and that the formation of a branch be tested for each segment individually instead of the entire hypha, as done in the layer model for scouting penetrative hyphae. Thirdly, the probability of

branching in a given hyphal segment should be calculated by multiplying a constant, named "maximum probability of branching", by the percentage of vacant space around this segment. The maximum probability of branching would have a low value before differentiation and a high value after differentiation. This would allow the production of subapical branches close to the tip, mimicking the apical branches in Figure 5.5A, and also the production of branches well distributed along the whole length of the hypha (Figure 5.7).

The time between germination and differentiation seems to be unaffected by the carbon source. The type of carbon source would affect the time of germination and the parameters used to calculate the probability of a hypha extending and the maximum probability of branching, but the rules of growth and the equations would likely be the same. The exact effect of the carbon source on these parameters will be better understood when trying to calibrate the model parameters.

5.5 CONCLUSIONS

Penetrative hyphae are the least studied hyphal type among those formed during SSF, however, they are important for the anchoring of the mycelium into the solid particle and for the hydrolysis and uptake of extracellular nutrients (MITCHELL et al., 1989; VARZAKAS, 1998). The current study provides a better understanding about how penetrative hyphae of *A. niger* grow and how this is affected by the inoculation density and by the type of carbon source, including the new finding that germ tubes may form penetrative hyphae directly when the inoculation density is low. In addition, it became clear that these hyphae undergo differentiation, with morphological and metabolic consequences.

Although there have been a few works showing heterogeneous expression of enzymes in mycelia growing on solid surfaces, this is the first to show the development of this heterogeneity over time. The intense expression of *pgxB* in subapical compartments and the presence of *pgxB* in the lateral and septal periplasms contributes with evidence to the recent concept that secretion of extracellular enzymes is not limited to the tips of hyphae (READ, 2011).

6   GENERAL DISCUSSION

The main contributions of the present thesis are: a critical review of previous mathematical models and how they may contribute to the development of a new and larger 3D phenomenological model describing hyphal growth on solid media (chapter 2); a better understanding of the growth of aerial and penetrative hyphae through the layer model, namely how to describe in simple rules branching and tip inactivation (chapters 3 and 4); the construction of a fluorescent strain of *Aspergillus niger* that can be used in future studies to investigate growth of this fungus in different conditions and to obtain data for calibration of future mathematical models (chapter 5); the microscopic characterization of the differentiation of penetrative hyphae of *Aspergillus niger* (chapter 5). The changes made in the present work for the development of the layer model, compared to the work of Balmant (2013), are presented in section 6.1.

In addition, this is the first work to show the growth of penetrative hyphae in time-lapse, including the early hours of extension of these hyphae. Based on these results, it is clear that penetrative hyphae have a growth pattern that is very different from the growth patterns of surface hyphae and aerial hyphae. Also for the first time, the development over time of the heterogeneity in expression of *pgxB* was shown; previously, expression of this gene had only been reported for surface hyphae and at a specific incubation time (BENOIT et al., 2015). The main findings resulting from the experiments with the fluorescent strain are highlighted in section 6.2.

The micrographs obtained in the present work indicate the changes necessary to adapt the layer model to describe penetrative growth of *A. niger*, before fusion with other models to create a 3D phenomenological model. Sections 6.3 and 6.4 give suggestions for future steps in the development of such a model.

6.1 FROM THE PROBABILITY DISTRIBUTION MODEL TO THE LAYER MODEL

The layer models for penetrative and aerial hyphae, presented in chapters 3 and 4, respectively, are modified versions of the "probability distribution model" developed in the doctoral thesis of Wellington Balmant (BALMANT, 2013). The structure of the probability distribution model was maintained in the layer model, namely the division of space into layers and the description of hyphal growth as the addition of hyphal segments of a fixed length to each layer. In addition, both models describe

four populations of hyphae: vegetative and scouting penetrative hyphae, vegetative and reproductive aerial hyphae. However, many of the rules that describe growth and branching were changed in the layer model (Tables 6.1 and 6.2).

Table 6.1 Differences between the probability distribution model of Balmant (2013) and the new layer model for penetrative hyphae presented in chapter 3.

Characteristic	Probability distribution model	Layer model
Experimental data described	*Rhizopus oligosporus* growing on PDA (NOPHARATANA et al., 2003b)	*Rhizopus oligosporus* growing on PDA and on starch medium (NOPHARATANA et al., 2003a,b) and *Aspergillus oryzae* growing on rice grains (ITO et al., 1989)
When new tips of vegetative penetrative hyphae were formed at the surface	At 0 h and 16 h	In every iteration
The length of each segment of penetrative hyphae	70 µm	140 µm
When penetrative hyphae stopped extending	Based on the probability of vegetative penetrative hyphae inactivating: $$P_I = \left(\frac{d}{d_{\lim}} \right)^k$$	Based on the probability of vegetative penetrative hyphae extending: $$P_E = P_{E,\max} \left(1 - \frac{d}{d_{\lim}} \right)^k$$
Initial site of growth of scouting penetrative hyphae	Tips of vegetative penetrative hyphae throughout the medium	Nodes of stolons at the surface (Figure 1.3)
When scouting penetrative hyphae grow	As long as there were active tips of vegetative penetrative hyphae	Only in the beginning of the incubation, stopping before 16 h.
How the profile of biomass concentration of scouting penetrative hyphae was obtained from the experimental data	Adjusting the sum of two normal distribution curves to the experimental data, as done for aerial hyphae	Subtracting the average concentration of scouting penetrative hyphae from the total biomass concentration of penetrative hyphae (for PDA data)
Sensitivity analysis	No	Yes

Most of the changes were made in the model for penetrative hyphae (Table 6.1). An important change was with respect to the rule for determining whether vegetative penetrative hyphae continued or stopped extending at a certain depth: in the probability distribution model, extension depended only on the depth of the extending tip (d) and a limiting depth ($d_{\lim}$); in the layer model, it also depended on an additional

parameter, $P_{E,max}$, which accounts for the firmness of the medium, so that there is a limitation for the penetration of tips throughout the entire solid that does not depend on the depth of the tip. The concept of the limiting depth is also different in each model. Balmant (2013) explained the limiting depth as a consequence of zero oxygen concentration beyond 2.45 mm from the surface, however, as explained in section 3.4.3, it is unlikely that penetrative hyphae stop extending only because of lack of oxygen in the medium, especially since there is evidence that filamentous fungi may use fermentative metabolic pathways (DE ASSIS et al., 2015; ANDERSEN et al., 2011). In the layer model, the limiting depth was proposed to be related to pressure drop inside the hypha and turgor pressure at the extending tip. This hypothesis is an important aspect of the layer model and seems to be coherent with the micrographs obtained in the present work with *A. niger* (section 5.4.2).

Another example is how scouting hyphae were described in each model (Table 6.1). Balmant (2013) divided the profiles of biomass concentration of the experimental data using the sum of two normal distribution curves, each with a peak in concentration below the surface of the medium. For the layer model, this approach was not used because there was no clear indication of the depth in which the peak in concentration of scouting penetrative hyphae occurred, which is necessary in order to determine whether a half-normal or a normal distribution curve should be used. Therefore, a simpler approach was used, with linearization of the biomass concentration in the region that was exclusive for scouting penetrative hyphae and extrapolation to all depths. In addition, the rules used to describe scouting penetrative hyphae were very different for both models.

For aerial hyphae, most of the changes were related to reproductive hyphae (Table 6.2). For example, it is known that reproductive aerial hyphae of *Rhizopus* start extending from nodes at the surface (Figure 1.3), such that they were treated as extending from the surface in the layer model, whereas Balmant (2013) treated them as forming from active tips of vegetative aerial hyphae. In addition, since branches are rare in these hyphae (SHURTLEFF; AOYAGI, 1979), in the layer model, it was considered that the peak in biomass concentration of these hyphae was at the surface, therefore, a half-normal distribution curve was used instead of the normal distribution curve used by Balmant (2013). This resulted in a different set of parameters for the half-normal distribution curves at 40 h.

Table 6.2 Differences between the probability distribution model of Balmant (2013) and the new layer model for aerial hyphae presented in chapter 4.

Characteristic	Probability distribution model	Layer model
Value of exponent m_e of Eq. (4.4)	2	1
Initial site of growth of reproductive aerial hyphae	Some of the active tips of vegetative aerial hyphae	Nodes of stolons at the surface
Position of the peak in biomass concentration of reproductive aerial hyphae for the normal distribution curve	1.8 mm above the surface	At the surface (0 mm)
When reproductive hyphae stop growing	A fixed percentage of them stops extending every iteration	Through a probability test, in which the probability of stopping is proportional to the height from the surface
Sensitivity analysis	No	Yes

Due to the differences between the layer model and the probability distribution model of Balmant (2013), different sets of parameters were obtained in the calibration of the model with the data of Nopharatana et al. (2003b). The fitted profiles obtained were similar for both models, except for aerial hyphae at 40 h. In the profile generated with the probability distribution model, the biomass concentration of vegetative aerial hyphae was almost constant in the first layers, but then decreased sharply between 0.42 mm and 1.12 mm above the surface (BALMANT, 2013), thus it did not resemble a half-normal distribution curve, which the experimental data follow. Therefore, the layer model resulted in a better reproduction of the experimental data.

Other two improvements were made with the layer model. First a sensitivity analysis was conducted with the layer model and it indicated that the parameters with the greatest influence on the biomass concentration profiles were the parameters related to limitation of growth: $P_{E,\max}$, $d_{\lim}$ and k for penetrative hyphae and $X_{\max}$ and m_e for vegetative aerial hyphae. Second, the layer model was used to reproduce two additional sets of experimental data for penetrative hyphae, for *Rhizopus oligosporus* growing on starch medium (NOPHARATANA et al., 2003a) and for *Aspergillus oryzae* growing on rice grains (ITO et al., 1989). By describing the data of Ito et al. (1989), the layer model became the first model to reproduce data of a real SSF system at the mesoscale.

Most of the changes made for the layer model were based on observations of the micrographs of Nopharatana et al. (2003a,b) and literature descriptions of growth of *Rhizopus* (SHURTLEFF; AOYAGI,

1979), therefore the new rules have a better biological fundament than do the rules of the model of Balmant (2013), for example, the rules used for reproductive aerial hyphae.

6.2 NEW INSIGHTS AS TO HOW PENETRATIVE HYPHAE OF *Aspergillus niger* GROW WITHIN SOLID MEDIA

The present work is not the first to show the morphology of penetrative hyphae, but it is the first to show how this morphology is formed over time, since it is the first time-lapse analysis of penetrative hyphae and the first to show the early hours of growth of these hyphae. This allowed important conclusions as to how penetrative hyphae grow: their differentiation process, the influence of the type of carbon source on their mode of growth and how they grow differently from aerial and surface hyphae.

Penetrative hyphae differentiate at around the same time as the formation of structures of asexual reproduction. It is not clear whether these events are related or not, but it is possible that they are initiated by the same trigger and resulting transcription factor. Differentiation of penetrative hyphae is characterized by interruption of the extension of leading hyphae, intense branching and a shift between apical expression of *pgxB* in some hyphae to subapical expression of *pgxB* in other hyphae; although it is unknown why and how these specific phenomena are triggered during differentiation. Based on the hypothesis proposed by the layer model that the length of penetrative hyphae is controlled by the internal pressure drop, it is possible that intense branching is the cause for the interruption of extension, since intense branching causes an increase in pressure drop inside the hypha and consequent reduction in the turgor pressure at the tip, which causes the leading hyphae to stop extending. As for the shift in the mode of expression of *pgxB*, it is probably related to a shift in the expression of its transcription activator, *GaaR*. Since this activator was identified only recently, there are no studies on its expression throughout the mycelium; such studies would be necessary to confirm whether it is the cause of the spatial heterogeneity in the expression of *pgxB* or not.

In the present work, four types of carbon sources were tested: glucose, starch, galacturonate and polygalacturonate. The type of carbon source affected the final length of leading hyphae and the frequency of branches per hypha, both of which were higher in the polygalacturonate medium than in the galacturonate medium. The germination time was affected more by the type of monomer present in the medium than it was

by the carbon source being a monosaccharide or a polysaccharide. The positions of branches in penetrative hyphae were not influenced directly by the type of carbon source, but rather by the hyphal density: subapical branches were the default choice (Figure 5.2), but, when hyphal density was high, branches were formed close to the tip, as either apical or subapical branches (Figure 5.5).

In the schematic representation of the development of mycelia on solid media presented in Chapter 2 (Figure 2.4), aerial and penetrative hyphae start growing at the same time. This representation was based on literature micrographs, which are either for the plan view of growth of surface hyphae at different incubation intervals or a side view towards the end of the cultivation (MITCHELL et al., 1990; NOPHARATANA et al., 2003a,b). The micrographs obtained in the present work show that this representation is only accurate for *A. niger* when conidia are agglomerated in the inoculum suspension, which may have triggered conidial anastomosis and the formation of surface germ tubes rather than penetrative germ tubes. In this case, penetrative hyphae are formed only after surface hyphae have reached a certain hyphal density (Figure 5.5A), at the same time as aerial hyphae, as represented in Figure 2.4. On the other hand, when conidia are well separated on the surface, both surface and penetrative germ tubes are formed (Figure 5.2). Penetrative germ tubes will continue to grow as penetrative hyphae, thus, penetrative mycelium will develop at the same time as surface mycelium.

Before this work, there were some indications that penetrative hyphae grew similarly to surface hyphae: both hyphal types are in contact with the solid, and the morphology of penetrative hyphae (NOPHARATANA et al., 2003a,b) seemed similar to that of surface hyphae at the periphery of a single colony. However, it is now clear that they grow in very different manners. The main difference is that penetrative hyphae have a limiting length, while surface hyphae do not, therefore, after differentiation, the growth of penetrative hyphae occurs mainly through subapical branches close to the surface, whereas at the edge of the colony surface hyphae can continue extending outwards, even if the surface hyphae in the middle of the colony have differentiated.

The micrographs also contributed evidence to a better understanding of intracellular mechanisms, namely the secretion of extracellular enzymes and vacuolization. Secretion of extracellular enzymes was initially suggested to be limited to the tips of extending hyphae, but recent studies indicate secretion at septa and at the lateral membrane (READ, 2011). The present study confirms this: after differentiation, there was intense subapical expression of *pgxB*, followed

by the presence of pgxB-mCherry at septa and lateral periplasms of subapical compartments and the absence of pgxB-mCherry at tips. As for vacuolization, there were two new findings. The first finding is that vegetative aerial hyphae may eventually form large spherical vacuoles in old hyphal segments. This has not been reported in the literature, possibly because these hyphae are formed in the later stages of growth and previous experiments may have been interrupted before these hyphae reached the age for formation of vacuoles. The second finding is that large vacuoles may, in fact, be formed in stalks before their tips swell to form the vesicle-structure, however this seems to occur only when these stalks originate from foot cells below the surface and, therefore, require a certain turgor pressure to penetrate through the solid towards the surface.

Unfortunately, it was not possible to visualize the formation of scouting hyphae in the experiments with *A. niger*. Consequently, it was not possible to verify the hypothesis made in the layer model, namely that scouting hyphae stop extending first and that they express scouting enzymes. With a new set of micrographs without germinated conidia on the side of the medium, it would be possible to obtain profiles of biomass concentration and to try to adjust the sum of two normal distribution curves to these profiles in order to infer the existence of 2 populations. Nevertheless, it is necessary to verify if the formation of scouting hyphae depends on the fungal species, the medium firmness or other aspects of the medium. Therefore, it would be interesting to investigate growth of *A. niger* in other media, for example, PDA, in which *Rhizopus oligosporus* produces scouting hyphae

6.3 TOWARDS A 3D PHENOMENOLOGICAL MODEL

In the review presented in chapter 2, a fusion of mathematical models is suggested in order to create a three-dimensional phenomenological model, which could be used to investigate mesoscale phenomena in SSF systems, such as particle shrinkage and the agglomeration of substrate particles. The present work makes contributions towards the development of such a model: it gives insights as to how each phenomenon should be described in the fused model (Chapter 2); the rules that limit the length of penetrative hyphae (chapter 3), the rules for generating apical branches that are either homogeneously spaced (chapter 4) or not (chapter 3), the rules concerning the direction of growth of aerial hyphae (chapter 4), how the rules should be adapted to the different mode of growth of penetrative hyphae of *Aspergillus niger* (chapter 5); how the type of carbon source may affect the model (chapter

5) and how hyphal density affects growth (chapter 4 and 5). The next step would be to start the fusion itself.

Much work is still required to conclude the 3D phenomenological model. Even though most of the important phenomena have been characterized, it is necessary to define the appropriate ranges of values for kinetic parameters, preferably based on experimental results, including from the literature, and to try to decipher how the fungus grows, based on time-lapse micrographs. The best approach to achieve the 3D phenomenological model is in steps. The first step would be to develop a 3D phenomenological model for growth of one surface germ tube (Figure 6.1). The basis of this model would be the tanks-in-series model of Balmant et al. (2015), with the addition of an equation for the rate of nutrient uptake across the membrane (section 2.4.3.2). The solid particle could be divided into cubes as done for the air phase in the model of Coradin et al. (2011), the difference being that the status of each cube would be the concentration of nutrient at that position, which, in turn, would be calculated by mass balance equations similar to those used by Balmant et al. (2015), but only with diffusion terms. Initially, this model could be calibrated with the data obtained by Larralde-Corona et al. (1997), which consists of the length of a surface germ tube of *Aspergillus niger* over time, measured in media with different concentrations of glucose.

The second step would be to adapt the germ tube model to describe the extension of a penetrative germ tube, as observed in Figure 5.2. In this case, it would be necessary to include the change of status of cubes in the solid from "medium" to "hypha" and, when this occurred, the mass of extracellular in the nutrient before the change in status would have to be transferred to the adjacent cubes of medium. In a third step, the formation of the second germ tube and the formation of the first branch could be included. For this version of the model, it would be necessary to determine how intracellular flow is divided at branch points.

The fourth step would be to adapt the 3D phenomenological model to describe the growth of hyphae on glucose or on galacturonate medium with a high density inoculum (Figures 5.5 and 5.7). In this case, it would be easier to describe penetrative and aerial hyphae separately, as done in the layer model, since the rules of growth are different. In this model, the rules of growth would be based on the layer models, with the modifications proposed in Chapter 5 and septation based on the model of Prosser and Trinci (1979), as suggested in chapter 2. In the case of penetrative hyphae, the equations of Balmant et al. (2015) would probably result in leading hyphae extending until the bottom of the medium, since

the equations only consider limitation by nutrient availability. This can be solved either by modeling turgor pressure directly and limiting the extension of penetrative hyphae to a minimal value of turgor pressure or by using an equation similar to the equation for the probability of extension of the layer model, equation (3.1), to calculate the parameter for extension of the tip k_c as a function of depth.

Figure 6.1 Schematic representation of the phenomena that should be included in the 3D phenomenological model for one surface germ tube (front view).
(1) Diffusion of monomeric nutrient in the solid; (2) absorption of the nutrient across the membrane; (3) Diffusive and convective transport of intracellular nutrient; (4) Consumption of the nutrient for the production of intracellular vesicles; (5) transport of vesicles towards the tip; (6) Fusion of vesicles at the apical membrane, resulting in apical extension.
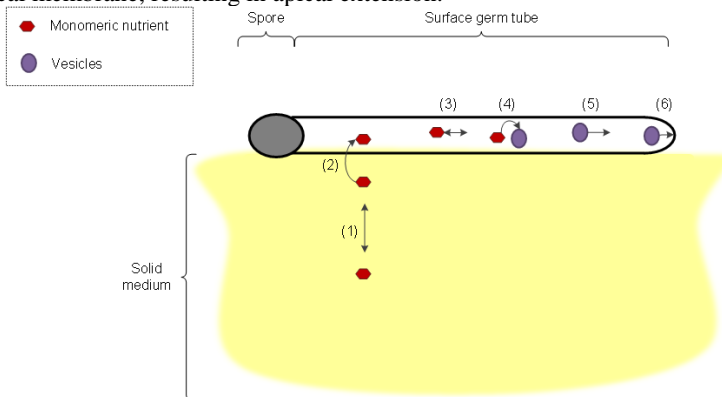
6.4 FUTURE PROSPECTS

The present work has addressed many questions regarding how filamentous fungi grow on solid media and how to model this growth. In the process, new questions have been raised, which may guide future work. Below are suggestions for future work that might help addressing the main questions raised:

- Use *A. niger* pgxRed to investigate expression of *pgxB* in a medium with galacturonate and to investigate how growth is affected by the concentration of the carbon source, inoculum density (with non-agglomerated conidia) and firmness of the medium (varying agar concentration); try different media and conditions in order to induce the formation of scouting penetrative hyphae

(starting with PDA), and test to see if the green fluorescence is strong enough to visualize the mycelium in real SSF systems, such as wheat bran;

- Use the micrographs obtained in the present work to obtain numerical data for biomass and tip densities as functions of distance from the surface, for the distances between branches and for the frequency of branches per hypha, with these analyses being done at several times during development of the mycelium;

- Fuse the models as suggested in section 6.3 and update the layer model for *A. niger* as suggested in section 5.4.3;

- Adapt the layer model to describe the growth of aerial hyphae across the space between particles.

- Analyze the expression of *GaaR* throughout the mycelium with time, perhaps by modifying *A. niger* pgxRed by adding a copy of *GaaR* fused with a third fluorescent protein, in order to detect the expression and transport of this transcription factor and relate it to the expression of pgxB;

- Study fermentative metabolism in penetrative hyphae. It would be necessary to, first, determine the culture conditions (e.g. inoculum density and media composition) that are necessary for production of ethanol by *Aspergillus niger* during growth on solid media and the moment of production, and, second, construct a strain that expresses GFP in the cytosol and alcohol dehydrogenase fused with a fluorescent protein such as mCherry in order to see the spatial and temporal distribution of this enzyme;

- Analyze expression of *pgaB* simultaneously with pgxB, by modifying *A. niger* pgxRed by adding a copy of *pgaB* fused with a third fluorescent protein, in order to determine whether these genes are expressed by the same hyphae or at the same time.

7 CONCLUDING REMARKS

The main objective of this study was to understand how the network of aerial and penetrative hyphae is formed when filamentous fungi grow on solid media and how pectinases are produced in these hyphae. This was achieved, firstly, by a review of previous mathematical models and identification of the best approaches to be incorporated in a 3D phenomenological model to study the development of the mycelium on solid media. On the basis of this review, it is recommended that the discretization of the space and hyphae be done using cubes, such as was done by Coradin et al. (2011), and that the formulation of the intracellular mass balance equations be done in the manner of the model of Balmant et al. (2015).

Secondly, a simple model, called a layer model, was developed in order to explore the mechanisms that determine when hyphae branch, how they choose the direction in which to grow and when they stop extending. This model was developed for penetrative and aerial hyphae, with different mechanisms for each hyphal type: penetrative hyphae extend mainly downwards with irregularly spaced branches and they stop extending when the turgor pressure at their tip is not enough to penetrate the solid medium, this being related to the firmness of the solid and the internal pressure drop; while aerial hyphae choose their direction of growth as though their tips moved in a random walk, with regularly spaced branches, and they stop extending due to steric impediment. During the development of the model for penetrative hyphae, different roles were suggested for each type of hypha formed: scouting penetrative hyphae and vegetative penetrative hyphae.

Thirdly, a fluorescent strain of *Aspergillus niger* was developed and used to investigate how penetrative hyphae grow and branch in media containing different types of carbon source. During this investigation, a differentiation process for penetrative hyphae was identified, with this differentiation being characterized by interruption of the extension of leading hyphae, intense branching in regions of low hyphal density and a change in the mode of expression of *pgxB*. Analysis of the expression of *pgxB* indicates that there are at least two types of hyphae: hyphae that express it apically and before differentiation and hyphae that express it subapically and after differentiation. Both hyphae continue to grow after differentiation. This fluorescent strain can be used to generate experimental data for the development and calibration of future mathematical models. It has already been used to suggest new rules for

growth of penetrative hyphae for future incorporation into the 3D phenomenological model.

REFERENCES

ADAMS, T. H.; WIESER, J. K.; YU, J. H. **Asexual sporulation in** *Aspergillus nidulans*. Microbiology and Molecular Biology Reviews, v. 62, n. 1, p. 35-54, 1998.

ALAZI, E. et al. **The transcriptional activator GaaR of** *Aspergillus niger* **is required for release and utilization of D-galacturonic acid from pectin**. FEBS Letters, v. 590, p. 1804-1815, 2016.

ALEXOPOULOS, C.J.; MIMS, C.W.; BLACKWELL, M. **Introductory Mycology**. John Wiley & Sons, New York, 1996.

AMORE, A.; GIACOBBE, S.; FARACO, V. **Regulation of cellulase and hemicellulase gene expression in fungi**. Current Genomics, v. 14, p. 230-249, 2013.

ANDERSEN et al. **Comparative genomics of citric-acid-producing Aspergillus niger ATCC 1015 versus enzyme-producing CBS 513.88**. Genome Res., v. 21, n. 6, p. 885-897, 2011.

AURIA, R.; ORTIZ, I.; VILLEGAS, E.; REVAH, S. **Influence of growth and high mould concentration on the pressure drop in solid state fermentations**. Process Biochemistry, v. 30, p. 751–756, 1995.

BALMANT, W. **Modelagem matemática do crescimento microscópico de fungos filamentosos em superfícies sólidas**. PhD Thesis, Federal University of Paraná, 2013.

BALMANT, W.; SUGAI-GUÉRIOS, M. H.; CORADIN, J. H.; KRIEGER, N.; FURIGO Jr, A.; MITCHELL, D. A. **A model for growth of a single fungal hypha based on well-mixed tanks in series:** simulation of nutrient and vesicle transport in aerial reproductive hyphae. PLoS ONE, v. 10, e0120307, 2015.

BARRY, D. J.; WILLIAMS, G. A. **Microscopic characterisation of filamentous microbes:** towards fully automated morphological quantification through image analysis. J. Microscopy, v. 244, n.1, 1-20, 2011.

BENOIT, I. et al. **Degradation of different pectins by fungi:** correlations and contrasts between the pectinolytic enzyme sets identified in genomes and the growth on pectins of different origin. BMC Genomics, v. 13:321, 2012.

BENOIT, I. et al. **Spatial differentiation of gene expression in Aspergillus niger colony grown for sugar beet pulp utilization**. Sci. Rep., v. 5, article 13592, 2015.

BEREPIKI, A.; LICHIUS, A.; READ, N. D. **Actin organization and dynamics in filamentous fungi**. Nature Reviews Microbiology, v. 9, p. 876-887, 2011.

BIZ, A. **Soluções para biorrefinarias de polpa cítrica**. PhD Thesis, Federal University of Paraná, 2015.

BLEICHRODT, R. et al. **Cytosolic streaming in vegetative mycelium and aerial structures of *Aspergillus niger*.** Studies in Mycology, v. 74, p. 31–46, 2013.

BOSWELL, G. P.; DAVIDSON, F. A. **Modelling hyphal networks.** Fungal Biology Reviews, v. 26, p. 30-38, 2012.

BOSWELL, G. P.; JACOBS, H.; RITZ, K.; GADD, G. M.; DAVIDSON, F. A. **The development of fungal networks in complex environments**. Bull Math Biol, v. 69, p. 605–634, 2007.

BOYCE, K. J.; ANDRIANOPOULOS, A. Morphogenesis: control of cell types and shape. In: ESSER, K. (Ed.) **The mycota.** 2. ed. Springer, v. 1, cap. 1, 2006.

BRAAKSMA, M.; MARTENS-UZUNOVA, E. S.; PUNT, P. J.; SCHAAP, P. J. **An inventory of the *Aspergillus niger* secretome by combining in silico predictions with shotgun proteomics data**. BMC Genomics, v. 11, p. 584-595, 2010.

BULL, A. T.; TRINCI, A. P. J. **The physiology and metabolic control of fungal growth**. Advances in Microbial Physiology, v. 15, p. 1-84, 1977.

CHAHAL, D. S.; MOO-YOUNG, M.; VLACH, D. **Protein production and growth characteristics of *Chaetomium cellulolyticum* during solid state fermentation of corn stover**. Mycologia, v. 75, p. 597-603, 1983.

CODLING, E. A.; PLANK, M. J.; BENHAMOU, S. **Random walk models in biology.** J. R. Soc. Interface, v. 5, p. 813-834, 2008.

COLLINGE, A. J.; TRINCI, A. P. J. **Hyphal tips of wild-type and spreading colonial mutants of *Neurospora crassa*.** Arch. Microbiol., v. 99, p.353-368, 1974.

CORADIN, J. H. et al. **A three-dimensional discrete *lattice*-based system for modeling the growth of aerial hyphae of filamentous fungi on solid surfaces:** A tool for investigating micro-scale phenomena in solid-state fermentation. Biochem. Eng. J., v. 54, p. 164–171, 2011.

CZYMMEK, K. J.; BOURETT, T. M.; HOWARD, R. J. **Fluorescent protein probes in fungi.** Methods in Microbiology, v. 34, p. 27-62, 2004.

DARRAH, P. R.; TLALKA, M.; ASHFORD, A.; WATKINSON, S. C.; FRICKER, M. D. **The Vacuole System Is a Significant Intracellular Pathway for Longitudinal Solute Transport in Basidiomycete Fungi**. Eukaryotic Cell, v. 5, n. 7, p. 1111-1125, 2006.

DAVID, H.; HOFMANN, G.; OLIVEIRA, A. P.; JARMER, H.; NIELSEN, J. **Metabolic network driven analysis of genome-wide transcription data from *Aspergillus nidulans***. Genome Biology, v. 7, n. 11, ref. 108, 2006.

DAVIDSON, F. A. **Mathematical modelling of mycelia**: a question of scale. Fungal Biology Reviews, v. 21, p. 30-41, 2007.

DE ASSIS, L. J.; RIES, L. N. A.; SAVOLDI, M.; DINAMARCO, T. M.; GOLDMAN, G. H.; BROWN, N. A. **Multiple Phosphatases Regulate Carbon Source-Dependent Germination and Primary Metabolism in *Aspergillus nidulans***. G3: Genes| Genomes| Genetics, v. 5(5), p. 857-872, 2015.

DE BEKKER, C.; BRUNING, O.; JONKER, M. J.; BREIT, T. M.; WÖSTEN, H. A. B. **Single cell transcriptomics of neighboring hyphae of *Aspergillus niger***. Genome Biol., v. 12, R71, 2011.

DE JONG, J. C.; McCORMACK, B. J.; SMIRNOFF, N.; TALBOT, N. J. **Glycerol generates turgor in rice blast.** Nature, v. 389, p. 244-245, 1997.

DE VRIES, R. P.; VISSER, J. *Aspergillus* **enzymes involved in degradation of plant cell wall polysaccharides.** Microbiology and Molecular Biology Reviews, v. 65, n. 4, p. 497–522, 2001.

DELMAS, S.; PULLAN, S. T.; GADDIPATI, S.; KOKOLSKI, M.; MALLA, S. et al. **Uncovering the genome-wide transcriptional responses of the filamentous fungus Aspergillus niger to lignocellulose using RNA sequencing**. PLoS Genet, v. 8, e1002875, 2012.

DU, C.; LIN, S. K. C.; KOUTINAS, A.; WANG, R.; DORADO, P.; WEBB, C. **A wheat biorefining strategy based on solid-state fermentation for fermentative production of succinic acid**. Bioresource Technology, v. 99, p 8310–8315, 2008.

DURAN, R.; CARY, J. W.; CALVO, A. M. **Role of the osmotic stress regulatory pathway in morphogenesis and secondary metabolism in filamentous fungi**. Toxins, v. 2, p. 367-381, 2010.

EDELSTEIN, L.; HADAR, Y.; CHET, I.; HENIS, Y.; SEGEL, L. A. **A model for fungal colony growth applied to** *Sclerotium rolfsii*. Journal of General Microbiology, v. 129, p 1873-1881, 1983.

EDELSTEIN, L.; SEGEL, L.A. **Growth and metabolism in mycelial fungi.** J. Theor. Biol., v. 104, p. 187-210, 1983.

FERRER, J.; PRATS, C.; LÓPEZ, D. **Individual-based modelling: An essential tool for microbiology**. Journal of Biological Physics, v. 34, p. 19–37, 2008.

FIDDY, C.; TRINCI, A. P. J. **Mitosis, septation, branching and the duplication cycle in** *Aspergillus nidulans*. J. Gen. Microbiol., v.97, p. 169-184, 1976.

FISCHER, R.; KÜES, U. Asexual sporulation in mycelial fungi. In: ESSER, K. (Ed.) **The mycota.** 2. ed. Springer, v. 1, cap. 14, 2006.

FUHR, M. J.; SCHUBERT, M.; SCHWARZE, F. W. M. R.; HERRMANN, H. J. **Modelling the hyphal growth of the wood-decay fungus *Physisporinus vitreus***. Fungal Biology, v. 115, p. 919-932, 2011.

GEORGIEV, Y. et al. **Isolation, characterization and modification of citrus pectins.** J. BioSci. Biotech., v. 1, n. 3, p.223-233, 2012.

GEORGIOU, G.; SHULER, M. L. **A computer model for the growth and differentiation of a fungal colony on solid substrate**. Biotechnology and Bioengineering, v. 28, p. 405-416, 1986.

GLASS, N. L.; RASMUSSEN, C.; ROCA, M. G.; READ, N. D. **Hyphal homing, fusion and mycelial interconnectedness**. Trends in Microbiology, v. 12, p. 135-141, 2004.

GOODAY, G. W. **An autoradiographic study of hyphal growth of some fungi.** J. Gen. Microbiol., v. 67, p.125-133, 1971.

GORDON, C. L. et al. **Glucoamylase: green fluorescent protein fusions to monitor protein secretion in *Aspergillus niger*.** Microbiology, v. 146, p. 415-426, 2000.

GORIELY, A.; TABOR, M. **Mathematical modeling of hyphal tip growth.** Br. Mycol. Soc., v. 22, p. 77-83, 2008.

GRIMM, L. H.; KELLY, S.; KRULL, R.; HEMPEL, D. C. **Morphology and productivity of filamentous fungi**. Applied Microbiology and Biotechnology, v. 69, p. 375–384, 2005.

HARRIS, S. D. **Branching of fungal hyphae**: regulation, mechanisms and comparison with other branching systems. Mycologia, v. 100, p. 823–832, 2008.

HAYAKAWA, Y.; ISHIKAWA, E.; SHOJI, J.; NAKANO, H.; KITAMOTO, K. **Septum-directed secretion in the filamentous fungus *Aspergillus oryzae*.** Mol Microbiol.; v. 81, n. 1, p. 40-55, 2011.

HAYER, K. **Germination of *Aspergillus Niger* conidia.** PhD Thesis, The University of Nottingham, 2014.

HAYER, K.; STRATFORD, M.; ARCHER, D. B. **Germination of** *Aspergillus Niger* **conidia is triggered by nitrogen compounds related to L-amino acids**. Applied and Environmental Microbiology, v. 80, n. 19, p. 6046-6053, 2014.

HAYER, K.; STRATFORD, M.; ARCHER, D. B. **Structural features of sugars that trigger or support conidial germination in the filamentous fungus** *Aspergillus Niger*. Applied and Environmental Microbiology, v. 79, n. 22, p. 6924-6931, 2013.

HEATON, L. L. M.; LÓPEZ, E.; MAINI, P. K.; FRICKER, M. D.; JONES, N. S. **Growth-induced mass flows in fungal networks**. Proc R Soc B, v. 277, p. 3265-3274, 2010.

HICKEY, P. C. et al. **Live-cell imaging of filamentous fungi using vital fluorescent dyes and confocal microscopy.** Methods in Microbiology, v. 34, p. 63-87, 2004.

HILDITCH, S.; BERGHÄLL, S.; KALKKINEN, N.; PENTTILÄ, M.; RICHARD, P. **The missing link in the fungal D-galacturonate pathway:** identification of the L-threo-3-deoxy-hexulosonate aldolase. The Journal of Biological Chemistry, v. 282, n. 36, p. 26195-26201, 2007.

HOPKINS, S.; BOSWELL, G. P. **Mycelial response to spatiotemporal nutrient heterogeneity:** A velocity-jump mathematical model. Fungal Ecology, v. 5, p. 124-136, 2012.

HUTCHINSON, S.A. et al. **Control of hyphal orientation in colonies of** *Mucor hiemalis***.** Trans. Br. Mycol. Soc., v. 75, p. 177-191, 1980.

IKASARI, L.; MITCHELL, D. A. **Two-phase model of the kinetics of growth of** *Rhizopus oligosporus* **in membrane culture.** Biotech. Bioeng., v. 68, p. 619-627, 2000.

INDERMITTE, C.; LIEBLING, T. M. **Culture analysis and external interaction models of mycelial growth**. Bulletin of Mathematical Biology, v. 56, n. 4, p. 633-669, 1994.

ITO, K. et al. **Mycelial distribution in rice koji.** J. Ferment. Bioeng., v. 68, p. 7-13, 1989.

JURUS, A. M.; SUNDBERG, W. J. **Penetration of *Rhizopus oligosporus* into soybeans in tempeh.** Appl. Environ. Microbiol., v. 32, p. 284-287, 1976.

KIKUMA, T.; OHNEDA, M.; ARIOKA, M.; KITAMOTO, K. **Functional analysis of the *atg8* homologue *aoatg8* and role of autophagy in differentiation and germination in *Aspergillus oryzae*.** Eukaryotic Cell, v. 5, n. 8, p. 1328-1336, 2006.

KRIJGSHELD, P.; BLEICHRODT, R.; VAN VELUW, G. J.; WANG, F.; MÜLLER, W. H.; DIJKSTERHUIS, J.; WÖSTEN, H. A. B. **Development in *Aspergillus*.** Studies in Mycology, v. 74, p. 1-29, 2013.

LARRALDE-CORONA, C. P., LÓPEZ-ISUNZA, F., VINIEGRA-GONZÁLEZ, G. **Morphometric evaluation of the specific growth rate of *Aspergillus niger* grown in agar plates at high glucose levels.** Biotechnol. Bioeng., v. 56, p.287-294, 1997.

LAUKEVICS, J. J.; APSITE, A. F.; VIESTURS, U. S.; TENGERDY, R. P. **Steric hindrance of growth of filamentous fungi in solid substrate fermentation of wheat straw.** Biotechnology and Bioengineering, v. 27, n. 12, p. 1687-1691, 1985.

LEVIN, A. M. et al. **Spatial differentiation in the vegetative mycelium of *Aspergillus niger*.** Eukaryotic Cell, v. 6, n. 12, p. 2311-2322, 2007.

LEW, R. R. **How does a hypha grow?** The biophysics of pressurized growth in fungi. Nature Reviews Microbiology, v. 9, p. 509-518, 2011.

LÓPEZ-ISUNZA, F.; LARRALDE-CORONA, C. P.; VINIEGRA-GONZÁLEZ, G. **Mass transfer and growth kinetics in filamentous fungi**. Chemical Engineering Science, v. 52, p. 2629–2639, 1997.

MARKHAM, P. Organelles of filamentous fungi. In: GOW, N. A. R.; GADD, G. M. (Ed.) **The growing fungus.** Chapman and Hall, 1995, cap. 5.

MARKHAM, P.; COLLINGE, A. J. **Woronin bodies of filamentous fungi**. FEMS Microbiology Letters, v. 46, p. 1–11, 1987.

MARTENS-UZUNOVA, E. S. **Assessment of the pectinolytic network of aspergillus niger by functional genomics** - insights from the transcriptome. PhD Thesis, Wageningen University, 2008.

MARTENS-UZUNOVA, E. S.; SCHAAP, P. J. **Assessment of the pectin degrading enzyme network of Aspergillus niger by functional genomics**. Fungal Genetics and Biology, v. 46, p. 170-179, 2009.

MATSUNAGA, K.; FURUKAWA, K.; HARA, S. **Effects of enzyme activity on the mycelial penetration of rice koji**. J. Brew. Soc. Japan., v. 97, p. 721-726, 2002.

MEEUWSE, P.; KLOK, A. J.; HAEMERS, S.; TRAMPER, J.; RINZEMA, A. **Growth and lipid production of *Umbelopsis isabellina* on a solid substrate - mechanistic modeling and validation**. Process Biochemistry 47: 1228–1242, 2012.

MITCHELL, D. A. et al. **A semimechanistic mathematical model for growth of *Rhizopus oligosporus* in a model solid-state fermentation system.** Biotech. Bioeng., v. 38, p.353-362, 1991.

MITCHELL, D. A.; BEROVIC, M.; KRIEGER, N. **Biochemical engineering aspects of solid state bioprocessing**. Advances in Biochemical Engineering/Biotechnology, v. 68, p. 61-138, 2000.

MITCHELL, D. A.; DOELLE, H. W., GREENFIELD, P. F. **Suppression of penetrative hyphae of *Rhizopus oligosporus* by membrane filters in a model solid-state fermentation system.** Biotechnology Techniques, v. 3, p. 45-50, 1989.

MITCHELL, D. A.; GREENFIELD, P. F.; DOELLE, H. W. **Mode of growth of *Rhizopus oligosporus* on a model substrate in solid-state fermentation.** World J. Mircobiol. Biotechnol., v.6, p.201-208, 1990.

MITCHELL, D. A.; KRIEGER, N.; BEROVIČ, M. **Solid state fermentation bioreactors**: Fundamentals of design and operation. Springer, Heidelberg, 2006.

MITCHELL, D. A.; VON MEIEN, O. F.; KRIEGER, N. **Recent developments in modeling of solid-state fermentation**: heat and mass

transfer in bioreactors. Biochemical Engineering Journal, v. 13, p. 137–147, 2003.

MITCHELL, D. A.; VON MEIEN, O. F.; KRIEGER, N.; DALSENTER, F. D. H. **A review of recent developments in modeling of microbial growth kinetics and intraparticle phenomena in solid-state fermentation**. Biochemical Engineering Journal, v. 17, p. 15-26, 2004.

MONEY, N. P. **Insights on the mechanics of hyphal growth**. Fungal Biol. Rev., v. 22, p. 71-76, 2008.

MONEY, N. P. **Turgor pressure and the mechanics of fungal penetration**. Canadian Journal of Botany, v. 73 (S1), p. 96-102, 1995.

MOORE, D.; McNULTY, L. J.; MESKAUSKAS, A. Branching in fungal hyphae and fungal tissues - growing mycelia in a desktop computer. In: DAVIES, J. **Branching morphogenesis.** Landes Bioscience / Eurekah.com e Springer Science+Business Media, 2004, cap. 4, 2005.

MÜLLER, C.; MCINTYRE, M.; HANSEN, K.; NIELSEN, J. **Metabolic engineering of the morphology of *Aspergillus oryzae* by altering chitin synthesis**. Appl. Environ. Microbiol., v. 68, p. 1827-1836, 2002.

MUSSATTO, S. I.; BALLESTEROS, L. F.; MARTINS, S.; TEIXEIRA, J. A. **Use of agro-industrial wastes in solid-state fermentation processes**. In Show K-Y, Industrial Waste, InTech, Rijeka, Croatia, 2012.

NIU, J.; HOMAN, T. G.; ARENTSHORST, M.; DE VRIES, R. P.; VISSER, J.; RAM, A. F. J. **The interaction of induction and repression mechanisms in the regulation of galacturonic acid-induced genes in *Aspergillus niger***. Fungal Genetics and Biology, v. 82, p. 32-42, 2015.

NOPHARATANA, M. **Microscale studies of fungal growth in solid state fermentation.** PhD Thesis, The University of Queensland, 1999.

NOPHARATANA, M.; HOWES, T.; MITCHELL, D. **Modelling fungal growth on surfaces**. Biotechnology Techniques, v. 12, p. 313–318, 1998.

NOPHARATANA, M.; MITCHELL, D.A.; HOWES, T. **Use of confocal microscopy to follow the development of penetrative hyphae during**

growth of *Rhizopus oligosporus* in an artificial solid-state fermentation system. Biotech. Bioeng., v. 81, n.4, p. 438-447, 2003a.

NOPHARATANA, M.; MITCHELL, D.A.; HOWES, T. **Use of confocal scanning laser microscopy to measure the concentrations of aerial and penetrative hyphae during growth of *Rhizopus oligosporus* on a solid surface.** Biotech. Bioeng., v. 84, n.1, p. 71-77, 2003b.

OOSTRA, J. et al. **Intra-particle oxygen diffusion limitation in solid-state fermentation**. Biotechnol. Bioeng., v. 75, p. 13–24, 2001.

PANDEY, A.; SOCCOL, C. R.; MITCHELL, D. **New developments in solid-state fermentation**: I – Bioprocesses and products. Process Biochemistry, v. 35, p. 1153-1169, 2000.

PAPAGIANNI, M. **Fungal morphology and metabolite production in submerged mycelial processes**. Biotechnology advances, v. 22, p. 189–259, 2004.

PARENICOVÁ, L.; BENEN, J. A.; KESTER, H. C.; VISSER, J. **pgaa and pgab encode two constitutively expressed endopolygalacturonases of *Aspergillus Niger*.** Biochem. J., v. 345, p. 637-644, 2000.

PEÑALVA, M. A. **Endocytosis in filamentous fungi**: Cinderella gets her reward. Current Opinion in Microbiology, v. 13, p. 684–692, 2010.

PITOL, L. O.; BIZ, A.; MALLMANN, E.; KRIEGER, N.; MITCHELL, D. A. **Production of pectinases by solid-state fermentation in a pilot-scale pecked-bed bioreactor.** Chemical Engineering Journal, v. 283, p. 1009-1018, 2016.

PÖGGELER, S.; MASLOFF, S.; HOFF, B.; MAYRHOFER, S.; KÜCK, U. **Versatile EGFP reporter plasmids for cellular localization of recombinant gene products in filamentous fungi**. Curr. Genet., v. 43, p. 54-61, 2003.

PROSSER, J. I. Kinetics of filamentous growth and branching. In: GOW N. A. R.; GADD, G. M. **The Growing Fungus**. Chapman Hall, London, 1995.

PROSSER, J. I.; TRINCI, A. P. J. **A model for hyphal growth and branching.** J. Gen. Microbiol., v. 111, p.153–164, 1979.

RAHARDJO, Y. S. P. et al. **Contribution of aerial hyphae of** *Aspergillus oryzae* **to respiration in a model solid-state fermentation system.** Biotech. Bioeng., v.78, p.539-544, 2002.

RAHARDJO, Y. S. P.; SIE, S.; WEBER, F. J.; TRAMPER, J.; RINZEMA, A. **Effect of low oxigen concentrations on growth and α-amylase production of** *Aspergillus oryzae* **in model solid-state fermentation systems.** Biomolecular Engineering, v. 21, p. 163-172, 2005a.

RAHARDJO, Y.S.P et al. **Aerial mycelia of** *Aspergillus oryzae* **accelerate α-amylase production in a model solid-state fermentation system.** Enz. Microbiol. Technol., v. 36, n.7, p. 900-902, 2005b.

RAHARDJO, Y.S.P.; TRAMPER, J.; RINZEMA, A. **Modeling conversion and transport phenomena in solid-state fermentation:** a review and perspectives. Biotechnol. Adv., v. 24, n.2, p. 161-179, 2006.

RAJAGOPALAN, S.; MODAK, J.M. **Evaluation of relative growth limitation due to depletion of glucose and oxygen during fungal growth on a spherical solid particle.** Chem. Eng. Sci., v. 50, p. 803-811, 1995.

READ, N. D. **Exocytosis and growth do not occur only at hyphal tips**. Molecular Microbiology, v. 81, p. 4-7, 2011.

READ, N. D.; GORYACHEV, A. B.; LICHIUS, A. **The mechanistic basis of self-fusion between conidial anastomosis tubes during fungal colony initiation**. Fungal Biology Reviews, v. 26, p. 1-11, 2012.

RICHARD, P.; HILDITCH, S. **D-Galacturonic acid catabolism in microorganisms and its biotechnological relevance.** Appl. Microbiol. Biotech., 82, 597-604, 2009.

RIQUELME, M. et al. **Architecture and development of the** *Neurospora crassa* **hypha - a model cell for polarized growth**. Fungal Biology, v. 115, p. 446-474, 2011.

RIQUELME, M.; BARTNICKI-GARCÍA, S. **Advances in understanding hyphal morphogenesis: Ontogeny, phylogeny and cellular localization of chitin synthases.** Fungal Biol. Rev., v. 22, p.56-70, 2008.

SCHINDELIN, J.; ARGANDA-CARRERAS, I.; FRISE, E. et al. **Fiji**: an open-source platform for biological-image analysis. Nature methods, v. 9(7), p. 676-682, PMID 22743772, 2012.

SCHUTYSER, M. A. I.; DE PAGTER, P.; WEBER, F. J.; BRIELS, W. J.; BOOM, R. M.; RINZEMA, A. **Substrate aggregation due to aerial hyphae during discontinuously mixed solid-state fermentation with** *Aspergillus oryzae*: Experiments and modeling. Biotechnology and Bioengineering, v. 83, p. 503–513, 2003.

SHANER, N. C.; CAMPBELL, R. E.; STEINBACH, P. A.; GIEPMANS, B. N.; PALMER, A. E.; TSIEN, R. Y. **Improved monomeric red, orange and yellow fluorescent proteins derived from Discosoma sp. red fluorescent protein**. Nat. Biotechnol, v. 12, p. 1524-1534, 2004.

SHOJI, J.; ARIOKA, M.; KITAMOTO, K.**Vacuolar membrane dynamics in the filamentous fungus** *Aspergillus oryzae*. Eukaryotic Cell, v. 5, n. 2, p. 411-421, 2006.

SHOJI, J.; KIKUMA, T.; KITAMOTO, K. **Vesicle trafficking, organelle functions, and unconventional secretion in fungal physiology and pathogenicity.** Current Opinion in Microbiology, v. 20, p. 1-9, 2014.

SHURTLEFF, W.; AOYAGI, A. **The Book of Tempeh**. Soyinfo Center, 1979.

SIGMA. **Product specification:** P9135 Pectin from Citrus Peel. Accessed on August 8th 2016 at: http://www.sigmaaldrich.com/catalog/product/sigma/p9135?lang=pt&region=BR

SMITS, J. P.; VAN SONSBEEK, H. M.; TRAMPER, J.; KNOL, W.; GEELHOED, W.; PEETERS, M.; RINZEMA, A. **Modelling fungal solid-state fermentation**: the role of inactivation kinetics. Bioprocess Engineering, v. 20, p. 391–404, 1999.

STEINBERG, G. **Hyphal growth**: a tale of motors, lipids, and the *Spitzenkörper*. Eukaryotic Cell, v. 6, p. 351–360, 2007.

SUDO, S.; KOBAYASHI, S.; KANEKO, A.; SATO, K.; OBA, T. **Growth of submerged mycelia of *Aspergillus kawachii* in solid-state culture.** J. Ferment. Bioeng., v. 79 , p. 252-256, 1995.

SUGAI-GUÉRIOS, M. H.; BALMANT, W.; FURIGO JR, A.; KRIEGER, N.; MITCHELL, D. A. **Modeling the growth of filamentous fungi at the particle scale in solid-state fermentation systems**. Adv. Biochem. Eng. Biotechnol., v. 149, p. 171-221, 2015.

SUGAI-GUÉRIOS, M. H.; BALMANT, W.; KRIEGER, N.; FURIGO, A.; MITCHELL, D. A. **Colonization of solid particles by *Rhizopus oligosporus* and *Aspergillus oryzae* in solid-state fermentation involves two types of penetrative hyphae: A model-based study on how these hyphae grow**. Biochem. Eng. Journal, v. 114, p. 173-182, 2016.

SUGDEN, K. E. P.; EVANS, M. R.; POON, W. C. K.; READ, N. D. **A model of hyphal tip growth involving microtubule-based transport**. Physical Review E, v. 75, ref. 031909, 2007.

TAHERI-TALESH, N.; HORIO, T.; ARAUJO-BAZÁN, L.; DOU, X.; ESPESO, E. A.; PEÑALVA, M. A.; OSMANI, S. A.; OAKLEY, B. R. **The tip growth apparatus of *Aspergillus nidulans***. Molecular Biology of the Cell, v. 19, p. 1439–1449, 2008.

TE BIESEBEKE, R. et al. **Branching mutants of *Aspergillus oryzae* with improved amylase and protease production on solid substrates.** Appl. Genet. Mol. Biotech., v.69, p.44-50, 2005.

TE BIESEBEKE, R.; BOUSSIER, A.; VAN BIEZEN, N.; BRAAKSMA, M.; VAN DEN HONDEL, C. A. M. J. J.; DE VOS, W. M.; PUNT, P. J. **Expression of *Aspergillus* hemoglobin domain activities in *Aspergillus oryzae* grown on solid substrates improves growth rate and enzyme production**. Biotechnology Journal, v. 1, p. 822–827, 2006.

TE BIESEBEKE, R.; LEVASSEUR, A.; BOUSSIER, A.; RECORD, E.; VAN DEN HONDEL, C. A. M. J. J.; PUNT, P. J. **Phylogeny of fungal hemoglobins and expression analysis of the *Aspergillus oryzae***

flavohemoglobin gene *fhbA* **during hyphal growth**. Fungal Biol., v. 114, p. 135-143, 2010.

THOMAS, L. **Current developments in solid-state fermentation**. Christian Larroche, Ashok Pandey. Biochemical Engineering Journal, v. 81, p. 146–161, 2013.

TINDEMANS, S. H.; KERN, N.; MULDER, B. M. **The diffusive vesicle supply center model for tip growth in fungal hyphae.** J. Theor. Biol., v. 238, p. 937-948, 2006.

TRINCI, A. P. J. **A study of the kinetics of hyphae extension and branch initiation of fungal mycelia.** J. Gen. Microbiol., v. 81, p. 225-236, 1974.

TRINCI, A. P. J. **Influence of the width of the peripheral growth zone on the radial growth rate of fungal colonies on solid media.** J. Gen. Microbiol., v. 67, p.325-344, 1971.

TUNBRIDGE, A.; JONES, H. **An L-systems approach to the modelling of fungal growth.** J. Visual. Comp. Animat., v.6, p.91-107, 1995.

VALKONEN, M.; KALKMAN, E. R.; SALOHEIMO, M.; PENTTILÄ, M.; READ, N. D.; DUNCAN, R. R. **Spatially segregated snare protein interactions in living fungal cells**. The Journal of Biological Chemistry, v. 282, n. 31, p. 22775-22785, 2007.

VARZAKAS, T. *Rhizopus oligosporus* **mycelial penetration and enzyme diffusion in soya bean tempe**. Process Biochemistry, v. 33, p. 741-747, 1998.

VESES, V.; RICHARDS, A.; GOW, N. A. R. **Vacuoles and fungal biology**. Current Opinion in Microbiology, v. 11, p. 503-510, 2008.

VICCINI, G.; MITCHELL, D. A.; BOIT, S. D.; GERN, J. C.; DA ROSA, A. S.; COSTA, R. M.; DALSENTER, F. D. H.; VON MEIEN, O. F.; KRIEGER, N. **Analysis of growth kinetic profiles in solid-state fermentation**. Food Technology and Biotechnology, v. 39, p. 271-294, 2001.

VILLENA, G. K.; GUTIÉRREZ-CORREA, M. **Morphological patterns of *Aspergillus niger* biofilms and pellets related to lignocellulolytic enzyme productivities**. Letters in Applied Microbiology, v. 45, p. 231-237, 2007.

VINCK, A. et al. **Heterogenic expression of genes encoding secreted proteins at the periphery of *Aspergillus niger* colonies.** Environ. Microbiol., v. 13, p. 216-225, 2011.

VINCK, A.; TERLOU, M.; PESTMAN, W. R.; MARTENS, E. P.; RAM, A. F.; VAN DEN HONDEL, C. A. M. J. J.; WÖSTEN, H. A. B. **Hyphal differentiation in the exploring mycelium of Aspergillus niger**. Mol. Microbiol., v. 58, p. 693-699, 2005.

WEBER, R. W. S. **Vacuoles and the fungal lifestyle.** Mycologyst, v. 16, n. 1, p. 10-20, 2002.

WÖSTEN, H. A. B. et al. **Localization of growth and secretion of proteins in *Aspergillus niger***. J. Gen. Microbiol., v. 137, p. 2017-2023, 1991.

YANG, H. et al. **Mathematical model for apical growth, septation, and branching of mycelial microorganisms.** Biotech. Bioeng., v. 39, n. 1, p. 49-58, 1992b.

YANG, H. et al. **Measurement and simulation of the morphological development of filamentous microorganisms**. Biotech. Bioeng., v. 39, n. 1, p. 44-48, 1992a.